

ISSN 1881-7831 Online ISSN 1881-784X

DD & T

Drug Discoveries & Therapeutics

Volume 7, Number 5
October, 2013



www.ddtjournal.com

DD & T

Drug Discoveries & Therapeutics



ISSN: 1881-7831
Online ISSN: 1881-784X
CODEN: DDTRBX
Issues/Year: 6
Language: English
Publisher: IACMHR Co., Ltd.

Drug Discoveries & Therapeutics is one of a series of peer-reviewed journals of the International Research and Cooperation Association for Bio & Socio-Sciences Advancement (IRCA-BSSA) Group and is published bimonthly by the International Advancement Center for Medicine & Health Research Co., Ltd. (IACMHR Co., Ltd.) and supported by the IRCA-BSSA and Shandong University China-Japan Cooperation Center for Drug Discovery & Screening (SDU-DDSC).

Drug Discoveries & Therapeutics publishes contributions in all fields of pharmaceutical and therapeutic research such as medicinal chemistry, pharmacology, pharmaceutical analysis, pharmaceuticals, pharmaceutical administration, and experimental and clinical studies of effects, mechanisms, or uses of various treatments. Studies in drug-related fields such as biology, biochemistry, physiology, microbiology, and immunology are also within the scope of this journal.

Drug Discoveries & Therapeutics publishes Original Articles, Brief Reports, Reviews, Policy Forum articles, Case Reports, News, and Letters on all aspects of the field of pharmaceutical research. All contributions should seek to promote international collaboration in pharmaceutical science.

Editorial Board

Editor-in-Chief:

Kazuhisa SEKIMIZU
The University of Tokyo, Tokyo, Japan

Co-Editors-in-Chief:

Xishan HAO
Tianjin Medical University, Tianjin, China

Norihiro KOKUDO
The University of Tokyo, Tokyo, Japan

Hongxiang LOU
Shandong University, Ji'nan, China

Yun YEN
City of Hope National Medical Center, Duarte, CA, USA

Chief Director & Executive Editor:

Wei TANG
The University of Tokyo, Tokyo, Japan

Managing Editor:

Hiroshi HAMAMOTO
The University of Tokyo, Tokyo, Japan
Munehiro NAKATA
Tokai University, Hiratsuka, Japan

Senior Editors:

Guanhua DU
Chinese Academy of Medical Science and Peking Union Medical College, Beijing, China

Xiao-Kang LI
National Research Institute for Child Health and Development, Tokyo, Japan

Masahiro MURAKAMI
Osaka Ohtani University, Osaka, Japan

Yutaka ORIHARA
The University of Tokyo, Tokyo, Japan

Tomofumi SANTA
The University of Tokyo, Tokyo, Japan

Wenfang XU
Shandong University, Ji'nan, China

Web Editor:

Yu CHEN
The University of Tokyo, Tokyo, Japan

Proofreaders:

Curtis BENTLEY
Roswell, GA, USA

Thomas R. LEBON
Los Angeles, CA, USA

Editorial and Head Office:

Pearl City Koishikawa 603,
2-4-5 Kasuga, Bunkyo-ku,
Tokyo 112-0003, Japan
Tel.: +81-3-5840-9697
Fax: +81-3-5840-9698
E-mail: office@ddtjournal.com

Drug Discoveries & Therapeutics

Editorial and Head Office

Pearl City Koishikawa 603, 2-4-5 Kasuga, Bunkyo-ku,
Tokyo 112-0003, Japan

Tel: +81-3-5840-9697, Fax: +81-3-5840-9698

E-mail: office@ddtjournal.com

URL: www.ddtjournal.com

Editorial Board Members

Alex ALMASAN (Cleveland, OH)	Yongzhou HU (Hangzhou, Zhejiang)	Yoshinobu NAKANISHI (Kanazawa, Ishikawa)	Yasuko YOKOTA (Tokyo)
John K. BUOLAMWINI (Memphis, TN)	Yu HUANG (Hong Kong)	Xiao-Ming OU (Jackson, MS)	Takako YOKOZAWA (Toyama, Toyama)
Shousong CAO (Buffalo, NY)	Hans E. JUNGINGER (Marburg, Hesse)	Weisan PAN (Shenyang, Liaoning)	Rongmin YU (Guangzhou, Guangdong)
Jang-Yang CHANG (Tainan)	Amrit B. KARMARKAR (Karad, Maharashtra)	Rakesh P. PATEL (Mehsana, Gujarat)	Guangxi ZHAI (Ji'nan, Shandong)
Fen-Er CHEN (Shanghai)	Toshiaki KATADA (Tokyo)	Shivanand P. PUTHLI (Mumbai, Maharashtra)	Liangren ZHANG (Beijing)
Zhe-Sheng CHEN (Queens, NY)	Gagan KAUSHAL (Charleston, WV)	Shafiqur RAHMAN (Brookings, SD)	Lining ZHANG (Ji'nan, Shandong)
Zilin CHEN (Wuhan, Hubei)	Ibrahim S. KHATTAB (Kuwait)	Adel SAKR (Cairo)	Na ZHANG (Ji'nan, Shandong)
Shaofeng DUAN (Lawrence, KS)	Shiroh KISHIOKA (Wakayama, Wakayama)	Gary K. SCHWARTZ (New York, NY)	Ruiwen ZHANG (Amarillo, TX)
Chandradhar DWIVEDI (Brookings, SD)	Robert Kam-Ming KO (Hong Kong)	Yuemao SHEN (Ji'nan, Shandong)	Xiu-Mei ZHANG (Ji'nan, Shandong)
Mohamed F. EL-MILIGI (6th of October City)	Nobuyuki KOBAYASHI (Nagasaki, Nagasaki)	Brahma N. SINGH (New York, NY)	Yongxiang ZHANG (Beijing)
Hao FANG (Ji'nan, Shandong)	Toshiro KONISHI (Tokyo)	Tianqiang SONG (Tianjin)	(As of October 2013)
Marcus L. FORREST (Lawrence, KS)	Chun-Guang LI (Melbourne)	Sanjay K. SRIVASTAVA (Amarillo, TX)	
Takeshi FUKUSHIMA (Funabashi, Chiba)	Minyong LI (Ji'nan, Shandong)	Hongbin SUN (Nanjing, Jiangsu)	
Harald HAMACHER (Tübingen, Baden-Württemberg)	Jikai LIU (Kunming, Yunnan)	Chandan M. THOMAS (Bradenton, FL)	
Kenji HAMASE (Fukuoka, Fukuoka)	Xinyong LIU (Ji'nan, Shandong)	Murat TURKOGLU (Istanbul)	
Xiaojiang HAO (Kunming, Yunnan)	Yuxiu LIU (Nanjing, Jiangsu)	Fengshan WANG (Ji'nan, Shandong)	
Kiyoshi HASEGAWA (Tokyo)	Xingyuan MA (Shanghai)	Hui WANG (Shanghai)	
Waseem HASSAN (Rio de Janeiro)	Ken-ichi MAFUNE (Tokyo)	Quanxing WANG (Shanghai)	
Langchong HE (Xi'an, Shaanxi)	Sridhar MANI (Bronx, NY)	Stephen G. WARD (Bath)	
Rodney J. Y. HO (Seattle, WA)	Tohru MIZUSHIMA (Tokyo)	Yuhong XU (Shanghai)	
Hsing-Pang HSIEH (Zhunan, Miaoli)	Abdulla M. MOLOKHIA (Alexandria)	Bing YAN (Ji'nan, Shandong)	

Reviews

- 172 - 177 **Recent advances in analysis of glutathione in biological samples by high-performance liquid chromatography: a brief overview.**
Tomofumi Santa
- 178 - 184 **Monoclonal antibody-related drugs for cancer therapy.**
Guoning Li, Siping Wang, Xia Xue, Xianjun Qu, Huiping Liu

Brief Report

- 185 - 188 **16,17-dihydroxycyclooctatin, a new diterpene from *Streptomyces* sp. LZ35.**
Guishi Zhao, Shanren Li, Yuanyuan Wang, Huilin Hao, Yuemao Shen, Chunhua Lu

Original Articles

- 189 - 195 **Anti-influenza activity of *Alchemilla mollis* extract: Possible virucidal activity against influenza virus particles.**
Juliann Nzembi Makau, Ken Watanabe, Nobuyuki Kobayashi
- 196 - 200 **Effect of Celergen, a marine derivative, on *in vitro* hepatocarcinogenesis.**
R. Catanzaro, N. Zerbinati, U. Solimene, G. Celep, F. Marotta, A. Kushugulova, M. Milazzo, C. Tomella, G. Bertuccelli, Z. Zhumadilov
- 201 - 208 **Preclinical anticancer effects and toxicologic assessment of hepatic artery infusion of fine-powder cisplatin with lipiodol *in vivo*.**
Toshiya Yamaguchi, Naoko Nakajima, Iwao Nakamura, Hiroko Mashiba, Takashi Kawashiro, Keiko Ebara, Eiji Ichimura, Chihiro Nishimura, Kazuya Okamoto, Yuh-ichiro Ichikawa, Takafumi Ichida

Commentary

- 209 - 211 **Standardized clinical pathways may potentially help to reduce the opacity of medical treatment in China – Reflections on the murder of a doctor in Wenling, Zhejiang.**
Lin Mei, Lingzhong Xu

CONTENTS

(Continued)

Guide for Authors

Copyright

Recent advances in analysis of glutathione in biological samples by high-performance liquid chromatography: a brief overview

Tomofumi Santa*

Graduate School of Pharmaceutical Sciences, The University of Tokyo, Tokyo, Japan.

ABSTRACT: Glutathione (GSH) is a tri-peptide that plays an important role in protecting cells and tissues against oxidative stress. So far a lot of analytical methods of glutathione have been reported. This brief review presents an overview of the analysis of glutathione in biological samples by high-performance liquid chromatography (HPLC) in recent five years, focusing on the sample pretreatment, derivatization and mass spectrometric detection.

Keywords: High-performance liquid chromatography, mass spectrometry, derivatization, glutathione

1. Introduction

Glutathione (GSH, γ -L-glutamyl-L-cysteinyl-glycine) is a tri-peptide that plays an important role in protecting cells and tissues against oxidative stress. Oxidative stress is to be involved in aging, and in various diseases such as cardiovascular diseases, diabetes mellitus, rheumatoid arthritis, Alzheimer's diseases, Parkinson's disease, and carcinogenesis (1-5). Under these conditions GSH is converted to glutathione disulfide (GSSG), the oxidized form of GSH, resulting in a decrease in GSH/GSSG ratio. Therefore, GSH/GSSG ratio is considered to be an indicator of redox status and disease risks, and it is important to measure GSH and GSSG level in the biological samples.

There are several difficulties to measure GSH and GSSG level accurately. GSH can be easily non-enzymatically oxidized to GSSG by molecular oxygen. Furthermore GSH reacts with disulfides and thiol-disulfide exchange can take place. Under normal conditions, GSH is known to be present in mammalian cells in the concentration range 1-10 mM, and the molar ratio of GSH/GSSG is maintained at about 100:1 to

1,000:1 (6). Therefore, oxidation of the small amount of GSH to GSSG or thiol-disulfide exchange greatly changes the GSH/GSSG ratio. To measure GSH level in plasma, the following point should be also considered. GSH level in erythrocytes is about 500-fold higher than that in plasma, thus, hemolysis can cause overestimation of GSH in plasma samples. These facts suggest that the sample pre-treatment is crucial for the exact measurement of GSH and GSSG level.

GSH and GSSG have been measured by several analytical methods (7). In particular, high-performance liquid chromatography (HPLC) with various detection methods such as ultraviolet absorbance (UV), fluorescence detection (FL), electrochemical detection (ECD), is widely used because of its convenience, sensitivity, and selectivity (8-11). Recently, liquid chromatography-mass spectrometry (LC-MS) is sometimes used for the analysis of glutathione and its related compounds (12). This brief review presents an overview of the analysis of glutathione in biological samples in recent five years (2009-2013), focusing on the sample pretreatment, derivatization and LC-MS.

2. Analysis of GSH by HPLC

2.1. Sample pretreatment

Pretreatment of GSH analysis by HPLC usually involves the following procedure, *i.e.*, sample collection, reduction of GSSG, deproteinization, and derivatization of GSH. Samples must be carefully treated for the accurate quantification of GSH and GSSG, since non-enzymatic oxidation of GSH, thiol-disulfide exchange, other side reactions, and hemolysis can occur during the pretreatment. These reactions disturb GSH/GSSG ratios in the samples. Oxidation reaction and thiol-disulfide exchange reaction (13) are dependent on pH and temperature, therefore lower pH and lower temperature is recommended during sample pretreatment and storage. Tubes for sampling are recommended to contain chelating agent such as ethylenediaminetetraacetic acid (EDTA) to suppress oxidation reactions. Addition of the derivatization reagent such as *N*-ethylmaleimide (NEM) to the sample was effective to protect thiol group

*Address correspondence to:

Dr. Tomofumi Santa, Graduate School of Pharmaceutical Sciences, The University of Tokyo, 7-3-1 Hongo, Bunkyo-ku, Tokyo 113-0033, Japan.

E-mail: santa@mof.f.u-tokyo.ac.jp

from oxidation and thiol-disulfide exchange reactions. Reagents, reactions, and practical considerations for the sample pretreatment of GSH and GSSG analysis were described and discussed in detail in the previous reviews (14,15).

2.2. Determination of GSH by HPLC-UV, ECD, FL

HPLC-UV, ECD, FL methods were summarized in Table 1. During acid-induced denaturation of blood samples, oxyhemoglobin elicits the production of several oxidants, which induce a strong artifactual increase in both GSSG and PSSG (S-glutathionylated proteins) concentration. This phenomenon can be prevented by blocking the –SH groups with alkylating agents such as NEM before acidification (16-18). Taking into these considerations, Rossi *et al.* reported the measurement of GSH, GSSG, and PSSG in human red blood cells (19). Blood samples were drawn in the presence of EDTA, and red blood cells (RBCs) were prepared by centrifugation. RBCs samples were washed with phosphate buffered saline (pH 7.4) containing 6 mM glucose (PBSG) and 10 mM NEM, and acidified with 10% (w/v) trichloroacetic acid (TCA). After deproteinization by centrifugation, the excess of NEM in the supernatants was extracted by dichloromethane. The samples were reacted with 2,4-dinitrofluorobenzene (FDNB) for 3 h at room temperature and aliquots were subjected to HPLC analysis. They examined the role of ketone bodies (β -hydroxybutyrate, acetone, acetoacetate) in generation of oxidative stress in human erythrocytes. A simple and rapid determination method of the reduced form of GSH in whole blood was reported (20). Blood samples collected in the tubes containing of a solution of K_3EDTA and were let to react with NEM for 1 min. The samples were acidified by TCA (12%, w/v) and proteins were spun by centrifugation, and aliquots of supernatants were loaded onto an HPLC. Though this method detects only GSH and not its oxidized form, GSSG, it can be used for large-scale clinical studies. HPLC-UV method requires a simple instrument, and can be easily applied to the routine analysis.

HPLC-ECD is a simple and sensitive detection method for thiol compounds such as GSH. In HPLC-ECD, GSH

was usually analyzed without derivatization. Park *et al.* reported the determination of GSH and GSSG using LC-ECD with boron-doped diamond electrode (21). Liver was homogenized in ice-cold PBS containing 1,3-diamino-2-hydroxypropanetetraacetic acid (DPTA) in ice bath. The homogenate was mixed with ice-cold 10% perchloric acid (PCA) containing DTPA. The acidified supernatant was stored at $-80^\circ C$ and subjected to HPLC. This method was applied to the evaluation of hepatic glutathione redox status. Khan *et al.* reported simultaneous determination of ascorbic acid and aminothiols in plasma and erythrocyte using HPLC-ECD (22). Blood samples were collected in EDTA tube, centrifuged, and stored at $-80^\circ C$. The plasma and 10% meta-phosphoric acid solution were mixed and vortexed. After addition of mobile phase and centrifugation at $4^\circ C$, the supernatant was injected to HPLC. Lysed erythrocytes were similarly analyzed. HPLC-FL is widely used method for the analysis of glutathione, since it is highly sensitive and selective. Derivatization reagents such as ortho-phthalaldehyde (OPA), monobromobimane (MBB), ammonium 7-fluorobenzo-2-oxa-1,3-diazole-4-sulphonate (SBD-F), and fluorescent maleimide were often used for this purpose. Conlan *et al.* reported the determination of intracellular glutathione and cysteine using MMB (23). After deproteinization by methanesulfonic acid, the samples were reacted with MMB in 4-(2-hydroxyethyl)-1-piperazineethanesulfonic acid (HEPES) buffer (pH 8.5) in the dark for 30 min in the presence of diethylenetriaminopentaacetic acid (DTPA). GSSG and cysteine (CysSS) were reduced to GSH and Cys by dithiothreitol (DTT) in 1 M HEPES buffer (pH 8.5) at $37^\circ C$ for 30 min followed by the derivatization with MMB. The increase in GSSG content and the higher GSSG/GSH ratio in myofibers compared with myoblasts were reported.

2.3. Determination of total glutathione by HPLC

Assay methods of total glutathione or GSSG in biological samples were summarized in Table 2. In these methods, GSSG and protein bound GSH were reduced to GSH, and the total GSH (total of reduced and oxidized forms

Table 1. Determination of GSH and GSSG by HPLC-UV, FL, ECD

Detection	Analytes	Derivatization	Separation (Column)	GSH (LOQ)	GSSG (LOQ)	Matrix	Ref.
UV (355 nm)	GSH, GSSG, PSSG	NEM, FDNB	C18	NR	NR	Erythrocyte	19
UV (265 nm)	GSH	NEM	NH2	0.05 mM	NR	Human blood	20
ECD (1,475 mV)	GSH, GSSG	None	C18	62.5 pmol (S/N 139.6)	1.6 pmol (S/N 4.4)	Mouse liver	21
ECD (900 mV)	GSH, Cys, Hcy, Nac, Met, GSSG	None	C18	30 ng/mL	96 ng/mL	Human plasma	22
FL (360/455 nm)	CysSS, Vitamin C GSH, GSSG Cys, CysSS	MBB	C18 monolithic	0.03 μM (LOD, S/N = 3)	NR	Human muscle cell	23

NR, not reported; LOQ, limit of quantification; LOD, limit of detection; Hcy, homocysteine; Nac, N-acetylcysteine; Met, methionine. Other abbreviations are described in the text. The detection wavelength or electrode voltage was described in the parentheses of "Detection" column. The excitation and emission wavelengths were described in case of FL.

of GSH) was analyzed. DTT (24,25), tributylphosphine (TBP) (26,27) and tris-(2-carboxyethyl)phosphine (TCEP) (28,29) were used as a reducing agent. The generated GSH was derivatized with OPA (24), SBD-F (26,29), 5-bromo-7-fluorobenzo-2-oxa-1,3-diazole-4-sulphonate (SBD-BF) (28), *N*-1-(pyrenyl)maleimide (NPM) (25), 1,3,5,7-tetramethyl-8-phenyl-(4-iodoacetamido)difluoroboradiaza-s-indane (TMPAB-I) (30), 1,3,5,7-tetramethyl-8-bromomethyl-difluoroboradiaza-s-indacene (TMMB-Br) (31). GSH, GSSG and their derivatives are usually separated on the reversed-phase column. Hydrophilic interaction chromatography (HILIC) is also useful for the separation of these highly polar compounds. Isokawa *et al.* reported the improvement of the sensitivities of SBD-thiol compounds using HILIC column. The content of organic solvent in HILIC is rather

high and the fluorescence intensities of SBD-thiols are greatly increased in the solution containing high percentage of organic solvent (29). Yoshitake *et al.* reported a sensitive analysis of aminothiols using intramolecular fluorescence resonance energy transfer (FRET) between the amine-derivatized and thiol-derivatized fluorophores (27).

2.4. Determination of GSH by LC-MS

Recently, LC-MS has been widely used for the determination of biological compounds, because of its sensitivity and selectivity. This method is also applied to the analysis of GSH, GSSG, and related compounds (Table 3). Iwasaki *et al.* used *N*-benzylmaleimide (NBenzM) and *N*-cyclohexylmaleimide (NCycloM) for

Table 2. Determination of total GSH by HPLC

Detection	Analytes	Derivatization	Separation (Column)	GSH (LOQ)	GSSG (LOQ)	Matrix	Ref.
FL (350/420 nm)	GSSG, GSH	OPA	C18	1.0 µM	0.2 µM	Human blood, plasma	24
FL (330/376 nm)	GSH	NPM	C18	10 nM	NR	Rat brain, liver, lung	25
FL (385/515 nm)	GSH, Cys, Hcy, CysGly,	SBD-F	C18	0.5 µM	NR	Human plasma	26
FL (390/540 nm)	GSH, Cys, Hcy	DCIA, NBD-F	C18	150 fmol	NR	Human plasma	27
FL (385/515 nm)	GSH, Cys, Hcy, CysGly	SBD-BF	C18	0.05 µM	NR	Human plasma	28
FL (375/510 nm)	GSH, Cys, Hcy, CysGly, γ-GluCys, Nac, CA	SBD-F	HILIC	2.7 nM	NR	Human plasma	29
FL (500/510 nm)	CoA, GSH, Nac, Cys, Hcy, 6-MP	TMPAB-I	C18	0.3 nM (LOD S/N = 3)	NR	Human plasma	30
FL (505/525 nm)	GSH, Cys, Hcy, Nac	TMMB-Br	C8	0.2 nM (LOD S/N = 3)	NR	Human blood	31

NR, not reported; LOQ, limit of quantification; LOD, limit of detection; Hcy, homocysteine; Nac, *N*-acetylcysteine; Met, methionine; CA: cysteamine, 6-MP: 6-mercaptopurine; DCIA, 7-diethylamino-3-[(4-(iodoacetyl)amino)phenyl]-4-methylcoumarin; NBD-F, 4-fluoro-7-nitro-2,1,3-benzoxadiazole. Other abbreviations are described in the text. The excitation and emission wavelengths were described in the parentheses of "Detection" column.

Table 3. Determination of GSH and GSSG by LC-MS

Detection	Analytes	Derivatization	Separation (Column)	GSH (LOQ)	GSSG (LOQ)	Matrix	Ref.
MS	GSH, Cys, Hcy	NBenzM,	HILIC	10 µM	10 µM	Mouse serum	32
MS/MS	GSSG, CysSS, HcySS	NCycloM					
MS/MS	GSH, Cys, Hcy, CysGly, and their disulfides	IAM, IPCF	C18	10 nM	5 nM	Human blood	35
MS/MS	GSH, GSSG	NEM	Porous graphitic carbon	1.5 µM	0.1 µM	Human blood	36
MS/MS	GSH, GSSG, GSA	NEM	Porous graphitic carbon	0.1 pmol	0.1 pmol	Human erythrocyte <i>et al.</i>	37
MS/MS	GSH, Cys, Hcy, Nac and their disulfides	BQB	HILIC	3.27 nmol/L (LOD S/N = 3)	NR	Human urine	34
MS/MS	GSH, GSSG	none	Pentafluorophenyl	0.5 µM	0.0625 µM	Human blood	38
MS/MS	GSH	none	C18	1.8 µM (LOD S/N = 3)	NR	Human blood	39
MS	GSH, GSSG	none	C18	0.4 ng/mL	0.5 ng/mL	Microdialysate	40
MS/MS	GSH, GSSG	none	C18 high strength silica	0.40 µM	0.80 µM	Rat and mouse bile	41
MS/MS	22 reduced thiols and 7 disulfides	cICAT	C18	NR	NR	Endothelial cells	42

NR, not reported; LOQ, limit of quantification; LOD, limit of detection; Hcy, homocysteine; CysSS, cystine; HcySS, homocysteine; GSA, glutathione sulfoneamide; Nac, *N*-acetylcysteine; Met, methionine; CA, cysteamine; cICAT, cleavable isotope coded affinity tag. Other abbreviations are described in the text.

the determination of GSH and GSSG (32). At first blood samples were collected into plastic tubes containing NBenzM (10 mM) to react with reduced form of GSH in the presence of deferoxamine mesylate. After reduction of GSSG with DTT, the samples were reacted with NCycloM (50 mM) in the presence of deferoxamine mesylate. After deproteinization using 5-sulfosalicylic acid (5-SSA), the samples were subjected to LC-MS equipped with column-switching system (on-line solid phase extraction and separation). HILIC column was used for separation. The content of organic solvent in HILIC was rather high and it was suitable for electrospray ionization (ESI)-MS (32-34). This method was applied to the investigation of the roles of thiol compounds in lipopolysaccharide (LPS)-induced acute inflammation. Serum glutathione disulfide and cysteine levels were significantly decreased after LPS treatment. Suh *et al.* used iodoacetamide (IAM) for the quenching of GSH and reduced form of thiols (35). The collected blood samples in the tubes containing EDTA were immediately mixed with IAM in Tris-HCl (pH 8) buffer. After deproteinization and solid phase extraction, samples were reacted with isopropyl chloroformate (IPCF) for the derivatization of amino and carboxylic groups, and analyzed with LC-MS/MS. The method was used to assess thiol redox states in plasma and erythrocytes isolated from healthy subjects and thalassemia patients. Moore *et al.* reported LC-MS/MS method for the clinical determination of reduced and oxidized glutathione from whole blood (36). Blood was collected in heparin or EDTA containing tube. The blood samples were mixed with solution containing NEM, 5-SSA and EDTA in 15% methanol. After deproteinization, GSSG and GSH-NEM were analyzed by LC-MS/MS. Harwood *et al.* used NEM to quench GSH (37). An excess of NEM (10 mM) was added, and the samples were left for 20 min at room temperature. Cold ethanol was added to lyse cells and precipitate proteins. After centrifugation the supernatant was removed. Samples were reconstituted in water and subjected to LC-MS/MS. GSH-NEM, GSSG and glutathione sulfonamide in cells were analyzed. Huang *et al.* synthesized ω -bromoacetylquinolinium bromide (BQB) for derivatization of thiol group and applied to the determination of aminothiols and their oxidized forms in urine (34). Urine samples were divided into two parts equally in the presence of EDTA. One part was mixed with Gly-HCl buffer solution (pH 3.5) containing d7-BQB. The labeling was completed within 3 min with the aid of microwave. The other part was treated with TCEP to reduce the oxidized forms of thiols, and reacted similarly with BQB. Finally two solutions were mixed and subjected to LC-MS/MS.

LC-MS/MS methods without derivatization were reported. Blood sample was drawn into tubes containing EDTA and kept on ice to minimize the GSH oxidation and enzymatic degradation, and whole blood was immediately mixed with 10% TCA containing EDTA.

The comparison between LC-MS/MS and HPLC-ECD was discussed (38). Norris *et al.* reported that the combination of stable isotope with methanolic precipitation at sample collection provided superior storage stability of whole blood samples in LC-MS/MS analysis (39). Robin *et al.* reported GSH and GSSG in the microdialysis samples from human dermis (40). Samples were analyzed without any pretreatment. To improve the sensitivity, silver nitrate (100 μ M) was introduced into LC effluent after column separation. Cao *et al.* reported GSH and GSSG analysis in bile samples. After acidification, dilution, and centrifugation, the samples were subjected to LC-MS/MS analysis (41). Drug-induced changes in the biliary GSSG/GSH ratios were observed.

3. Conclusion

In this brief review, determination methods of GSH by HPLC in recent years are summarized. In these methods, separation and detectability were considerably improved compared with the previous papers, and the adoption of mass spectrometric detection greatly improved the selectivity. For the accurate quantification of GSH and GSSG, oxidation, thiol-disulfide exchange, and other side reactions of GSH must be suppressed during the sample pretreatment and storage. The simple and appropriate sample pretreatment methods are still required for determination of GSH.

Acknowledgements

This study was supported in part by Grants-in-Aid for Scientific Research (C) (24590047) from Ministry of Education, Culture, Sports, Science, and Technology of Japan. The author thanks Dr Chang-Kee Lim, King's College Hospital, for his kind suggestions and valuable discussion.

References

1. Ballatori N, Krance SM, Notenboom S, Shi SJ, Tieu K, Hammond CL. Glutathione dysregulation and the etiology and progression of human diseases. *Biol Chem.* 2009; 390:191-214.
2. Sohal RS, Orr W. The redox stress hypothesis of aging. *Free Radical Biol Med.* 2012; 52:539-555.
3. Smeyne M, Smeyne RJ. Glutathione metabolism and Parkinson's disease. *Free Radical Biol Med.* 2013; 63:13-25.
4. Johnson WM, Wilson-Delfosse AL, Mieyal JJ. Dysregulation of glutathione homeostasis in neurodegenerative diseases. *Nutrients.* 2012; 4:1399-1440.
5. Kryston TB, Georgiev AB, Pissis P, Georgakilas AG. Role of oxidative stress and DNA damage in human carcinogenesis. *Mut Res Fundam Mol Mech Mutag.* 2011; 711:193-201.
6. Dalle-Donne I, Rossi R, Colombo G, Giustarini D, Milzani A. Protein S-glutathionylation: A regulatory device from bacteria to humans. *Trends Biochem Sci.* 2009; 34:85-96.

7. Pastore A, Federici G, Bertini E, Piemonte F. Analysis of glutathione: Implication in redox and detoxification. *Clin Chim Acta*. 2003; 333:19-39.
8. Toyooka T. Recent advances in separation and detection methods for thiol compounds in biological samples. *J Chromatogr B Anal Technol Biomed Life Sci*. 2009; 877:3318-3330.
9. McMenamin ME, Himmelfarb J, Nolin TD. Simultaneous analysis of multiple aminothiols in human plasma by high performance liquid chromatography with fluorescence detection. *J Chromatogr B Anal Technol Biomed Life Sci*. 2009; 877:3274-3281.
10. Kusmirek K, Chwatko G, Glowacki R, Kubalczyk P, Bald E. Ultraviolet derivatization of low-molecular-mass thiols for high performance liquid chromatography and capillary electrophoresis analysis. *J Chromatogr B Anal Technol Biomed Life Sci*. 2009; 879:1290-1307.
11. Harfield JC, Batchelor-McAuley C, Compton RG. Electrochemical determination of glutathione: A review. *Analyst*. 2012; 137:2285-2296.
12. Iwasaki Y, Saito Y, Nakano Y, Mochizuki K, Sakata O, Ito R, Saito K, Nakazawa H. Chromatographic and mass spectrometric analysis of glutathione in biological samples. *J Chromatogr B Anal Technol Biomed Life Sci*. 2009; 877:3309-3317.
13. Santa T, Aoyama C, Fukushima T, Imai K, Funatsu T. Suppression of thiol exchange reaction in determination of reduced form thiols by high-performance liquid chromatography with fluorescence detection after derivatization with fluorogenic benzofurazan reagent, 7-fluoro-2,1,3-benzoxadiazole-4-sulfonate (SBD-F) and 4-aminosulfonyl-7-fluoro-2,1,3-benzoxadiazole (ABD-F). *Biomed Chromatogr*. 2006; 20:656-661.
14. Hansen R, Winther JR. An introduction to methods for analyzing thiols and disulfides: Reactions, reagents, and practical considerations. *Anal Biochem*. 2009; 394:147-158.
15. Monostori P, Wittmann G, Karg E, Turi S. Determination of glutathione and glutathione disulfide in biological samples: An in-depth review. *J Chromatogr B Anal Technol Biomed Life Sci*. 2009; 877:3331-3346.
16. Rossi R, Milzani A, Dalle-Donne I, Giustarini D, Lusini L, Colombo R, Simplicio PD. Blood glutathione disulfide: *in vivo* factor or *in vitro* artifact. *Clin Chem*. 2002; 48:742-753.
17. Rossi R, Dalle-Donne I, Milzani A, Giustarini D. Oxidized forms of glutathione in peripheral blood as biomarkers of oxidative stress. *Clin Chem*. 2006; 52:1406-1414.
18. Giustarini D, Dalle-Donne I, Colombo R, Milzani A, Rossi R. An improved HPLC measurement for GSH and GSSG in human blood. *Free Radical Biol Med*. 2003; 35:1365-1372.
19. Rossi R, Giustarini D, Colombo G, Milzani A, Dalle-Donne I. Evidence against a role of ketone bodies in the generation of oxidative stress in human erythrocytes by the application of reliable methods for thiol redox form detection. *J Chromatogr B Anal Technol Biomed Life Sci*. 2009; 877:3467-3474.
20. Giustarini D, Dalle-Donne I, Milzani A, Rossi R. Detection of glutathione in whole blood after stabilization with *N*-ethylmaleimide. *Anal Biochem*. 2011; 415:81-83.
21. Park JH, Mah E, Bruno RS. Validation of high-performance liquid chromatography-boron-doped diamond detection for accessing hepatic glutathione redox status. *Anal Biochem*. 2010; 407:151-159.
22. Khan A, Khan MI, Iqbal Z, Shah Y, Ahmad L, Nazir S, Watson DG, Khan JA, Nasir F, Khan, A, Ismail. A new HPLC method for the simultaneous determination of ascorbic acid and aminothiols in human plasma and erythrocytes using electrochemical detection. *Talanta*. 2011; 84:789-801.
23. Conlan XA, Stupka N, McDermott GP, Francis PS, Barnett NW. Determination of intracellular glutathione and cysteine using HPLC with a monolithic column after derivatization with monobromobimane. *Biomed Chromatogr*. 2010; 24:455-457.
24. Kandar R, VrBova M, Candova J. An assay of total glutathione and glutathione disulfide in human whole blood and plasma using a high-performance liquid chromatography with fluorescence detection. *J Liquid Chromatogr Rel Technol*. 2013; 36:2013-2028.
25. Ates B, Ercal BC, Manda K, Abraham L, Ercal N. Determination of glutathione disulfide levels in biological samples using thiol-disulfide exchanging agent, dithiothreitol. *Biomed Chromatogr*. 2009; 23:119-123.
26. Ferin R, Pavao ML, Baptista J. Methodology for a rapid and simultaneous determination of total cysteine, homocysteine, cysteinylglycine and glutathione in plasma by isocratic RP-HPLC. *J Chromatogr B Anal Technol Biomed Life Sci*. 2012; 911:15-20.
27. Yoshitake M, Nohta H, Sejima N, Todoroki K, Yoshida H, Yamaguchi M. Selective determination of cysteines through precolumn double-labeling and liquid chromatography followed by detection of intramolecular FRET. *Anal Bioanal Chem*. 2011; 399:1665-1675.
28. Cevasco G, Piatek AM, Scapolla C, Thea S. An improved method for simultaneous analysis of amino thiols in human plasma by high-performance liquid chromatography with fluorescence detection. *J Chromatogr A*. 2010; 1217:2158-2162.
29. Isokawa M, Funatsu T, Tsunoda M. Fast and simultaneous analysis of biothiols by high-performance liquid chromatography with fluorescence detection under hydrophilic interaction chromatography. *Analyst*. 2013; 138:3802-3808.
30. Guo XF, Wang H, Guo YH, Zhang ZX, Zhang HS. Simultaneous analysis of plasma thiols by high-performance liquid chromatography with fluorescence detection using a new probe, 1,3,5,7-tetramethyl-8-phenyl-(4-iodoacetamido)difluoroboradiaza-s-indane. *J Chromatogr A*. 2009; 1216:3874-3880.
31. Guo XF, Zhu H, Wang H, Zhang HS. Determination of thiol compounds by HPLC and fluorescence detection with 1,3,5,7-tetramethyl-8-bromomethyl-difluoroboradiaza-s-indacene. *J Sep Sci*. 2013; 36:658-664.
32. Iwasaki Y, Nakano Y, Mochizuki K, Ogawa T, Oda M, Ito R, Saito K, Nakazawa H. Quantification of reduced and oxidized thiols in mouse serum by column-switching hydrophilic interaction chromatography coupled with mass spectrometry. *J Pharm Biomed Anal*. 2011; 56:103-113.
33. Haberhauer-Troyer C, Delic M, Gasser B, Mattanovich D, Hann S, Koellensperger G. Accurate quantification of the redox-sensitive GSH/GSSG ratios in the yeast *Pichia pastoris* by HILIC-MS/MS. *Anal Bioanal Chem*. 2013; 405:2031-2039.
34. Huang Y-Q, Ruan G-D, Liu J-Q, Gao Q, Feng Y-Q. Use of isotope differential derivatization for simultaneous determination of thiols and oxidized thiols by liquid chromatography tandem mass spectrometry. *Anal Biochem*. 2011; 416:159-166.

35. Suh J, Kim R, Yavuz B, Lee D, Lal A, Ames BN, Shigenaga MK. Clinical assay of four thiol amino acid redox coupled by LC-MS/MS: Utility in thalassemia. *J Chromatogr B Anal Technol Biomed Life Sci.* 2009; 877:3418-3427.
36. Moore T, Le A, Niemi A-K, Kwan T, Cusumano-Ozog K, Enns GM, Cowan TM. A new LC-MS/MS method for the clinical determination of reduced and oxidized glutathione from whole blood. *J Chromatogr B.* 2013; 929:51-55.
37. Harwood DT, Kettle AJ, Brennan S, Winterbourn CC. Simultaneous determination of reduced glutathione, glutathione disulfide and glutathione sulphoneamide in cells and physiological fluids by isotope dilution lipid chromatography-tandem mass spectrometry. *J Chromatogr B Anal Technol Biomed Life Sci.* 2009; 877:3393-3399.
38. Squellerio I, Caruso D, Porro B, Veglia F, Tremoli E, Cavalca V. Direct glutathione quantification in human blood by LC-MS/MS: Comparison with HPLC with electrochemical detection. *J Pharm Biomed Anal.* 2012; 71:111-118.
39. Norris RLG, Paul M, George R, Moore A, Pinkerton R, Haywood A, Charles B. A stable-isotope HPLC-MS/MS method to simplify storage of human whole blood samples for glutathione assay. *J Chromatogr B Anal Technol Biomed Life Sci.* 2012; 898:136-140.
40. Robin S, Leveque N, Courderot-Masuyer, Humbert P. LC-MS determination of oxidized and reduced glutathione in human dermis: A microdialysis study. *J Chromatogr B Anal Technol Biomed Life Sci.* 2011; 879:3599-3606.
41. Cao L, Waldon D, Teffera Y, Roberts J, Wells M, Langley M, Zhao Z. Ratios of biliary glutathione disulfide (GSSG) to glutathione (GSH): A potential index to screen drug-induced hepatic oxidative stress in rats and mice. *Anal Bioanal Chem.* 2013; 405:2635-2642.
42. Yuan W, Edward JL. Thiol metabolomics of endothelial cells using capillary liquid chromatography mass spectrometry with isotope coded affinity tags. *J Chromatogr A.* 2011; 1218:2561-2568.

(Received October 18, 2013; Accepted October 26, 2013)

Monoclonal antibody-related drugs for cancer therapy

Guoning Li¹, Siping Wang², Xia Xue³, Xianjun Qu⁴, Huiping Liu^{1,*}

¹ Shandong Luye Pharmaceutical Group Co., Ltd., Yantai, Shandong, China;

² Department of Emergency, Yantaishan Hospital, Yantai, Shandong, China;

³ Department of Pharmacy, The Second Hospital of Shandong University, Ji'nan, Shandong, China;

⁴ Department of Pharmacology, College of Chemical biology and Pharmacy, Capital Medical University, Beijing, China.

ABSTRACT: Much progress has been made during the last few decades in the treatment of malignancies. Many types of cancer cells comprising the tumor mass carry molecular markers that are not expressed or are expressed at much lower levels in normal cells. These findings provide new leads to drug design and development of therapeutic strategies involving monoclonal antibodies (mAbs) or related antibody drugs to treat malignancies. This article reviews recent advances in this targeting approach with a focus on the evolution and current use of prospective antibody drugs as effective ways to treat cancer. Additionally, the development of prospective antibody-drug conjugates will also be briefly described.

Keywords: Antibody, targeted therapy, cancer, antibody-drug conjugate

1. Introduction

In 1986, the US Food and Drug Administration (FDA) approved the first monoclonal antibody drug, muromonab (a murine IgG1 specific for CD3), as a therapy for transplant patients experiencing rejection (1). Since then, the pharmaceutical industry has entered a new era of targeted therapy. Dozens of monoclonal antibodies (mAbs), including murine, chimeric, and humanized antibodies, have been developed for use against multiple diseases, including (but not limited to) autoimmune disorders and cancer, in humans (2). Early in 2008, engineered antibodies were predicted to account for over 30% of all revenue in the biotechnology market (3). The latest global forecast is that the protein engineering market could reach \$168 billion by 2017, and the market's growth is primarily attributed to mAbs, which account for more than 50% of revenue (4).

Cancer remains one of the leading causes of mortality worldwide, affecting over 10 million new patients every year. Currently, the clinical treatment options mainly include surgical resection, radiation, and chemotherapy. Although over 90 chemotherapeutic drugs have been approved for clinical use by the FDA, their efficacy has been severely hindered by dose-limiting toxicity and patient morbidity (5). The story of targeted therapy for malignant cancer is quite a long one. Targeted cancer therapies can be defined as drugs developed against a specific target based on its important biological function in cancer (6,7). Drugs developed for targeted therapy including some small molecules, such as tyrosine kinase inhibitors, and antibody-related drugs. With dramatically improved antitumor action and a substantial reduction in toxicity, mAbs represent a major advance in targeted therapy.

Increased understanding of the molecular events involved in cancer development has led to the identification of a large number of novel targets and, in parallel, to the development of multiple approaches to anticancer therapy (8). Given the urgent need for clinical options and the need for a better prognosis for patients with malignant tumors, new therapeutic strategies must be developed with new drugs (9). The ability of antibodies to exploit antigenic differences between normal and malignant tissue and to induce a variety of antitumor responses while having minimal effect on normal cells offers significant advantages to conventional forms of therapy (10). As a result, pharmacological research on molecular agents, including antibody-related drugs, is making greater progress than ever before. Research on antibody-drug conjugates has also appeared and made significant progress thanks to careful optimization of several parameters, including mAb specificity, drug potency, linker technology, and the stoichiometry and placement of conjugated drugs (11).

2. Stages of antibody development

The concept of targeted therapy using mAbs has been put into practice and revised for several years. Recent studies have used tumor-specific antigens that facilitate

*Address correspondence to:

Dr. Huiping Liu, Shandong Luye Pharmaceutical Group Co., Ltd., Yantai, Shandong, China.
E-mail: huiping_ra@hotmail.com

targeted oncologic therapy. Targeted therapy focuses on specific signal transduction molecules in malignant cells, including crucial molecules involved in cell invasion, metastasis, apoptosis, cell-cycle control, and tumor-related angiogenesis (12). mAbs are developed with a high specificity for antigens expressed on tumor cells; thanks to their specific affinity for a selected target, antibody drugs can affect proximal events in signaling pathways that drive abnormal growth and have relatively low toxicity (10). Unlike many small molecules, mAbs offer unique target specificity, offering better efficiency and fewer side effects (13). The high specificity and affinity of mAbs suggest a bright future for their development and clinical use.

First-generation mAbs were murine antibodies. Second-generation mAbs include chimeric antibodies, humanized antibodies, and fully humanized antibodies. The main objective of modifying antibodies is to reduce their immunogenicity (14). As was just mentioned, the first generation of mAbs typically consisted entirely of mouse cells, so they were viewed as foreign by the human immune system. The human immune system can generate unique and highly specific antibodies to all foreign antigens. This ability is unmatched since the immune system can also vary individual antibody isotypes in order to optimize the body's antibody response. The second generation of mAbs involves "humanized antibodies". This term refers to modifying the protein sequences of antibodies from non-human species to increase their similarity to antibody variants produced naturally in humans (15,16).

3. Mechanisms of mAbs in cancer therapy

The mechanisms underlying the therapeutic efficacy of mAb-based immunotherapy have often been investigated (Figure 1). First, mAbs can induce signal arrest and lead to apoptosis in targeted tumor cells by binding with their specific receptor, inducing modulation of the receptor or interfering with ligand binding and/or dimerization of the receptor (17). mAbs can display action through Fc-based mechanisms such as antibody-dependent cell-mediated cytotoxicity (ADCC) and complement-dependent cytotoxicity (CDC), which can be influenced by the nature of glycosylation of the antibodies (13,18-21).

In ADCC, mAb binds to the tumor antigen. The Fc region of the mAb is exposed and interacts with the Fc gamma receptors (FcγR) on the surface of effector cells, such as natural killer cells, macrophages, monocytes, and eosinophils. Stimulatory effects are mediated through FcγRI on macrophages, dendritic cells (DCs), and neutrophils and through FcγRIIIa on NK cells, DCs, and macrophages (22). The FcγR immunoreceptor tyrosine-based activation motif (ITAM) is then phosphorylated, triggering the activation of effector cells and the secretion of various substances such as cytokines, lytic enzymes, perforin, granzymes, and TNF that mediate the destruction of target cells. In murine models, the cytotoxicity resulting from FcR activation of a NK cell, γδ T cell, or macrophage is responsible for antitumor activity (23). Previous studies have found that ADCC plays a key role in the effectiveness

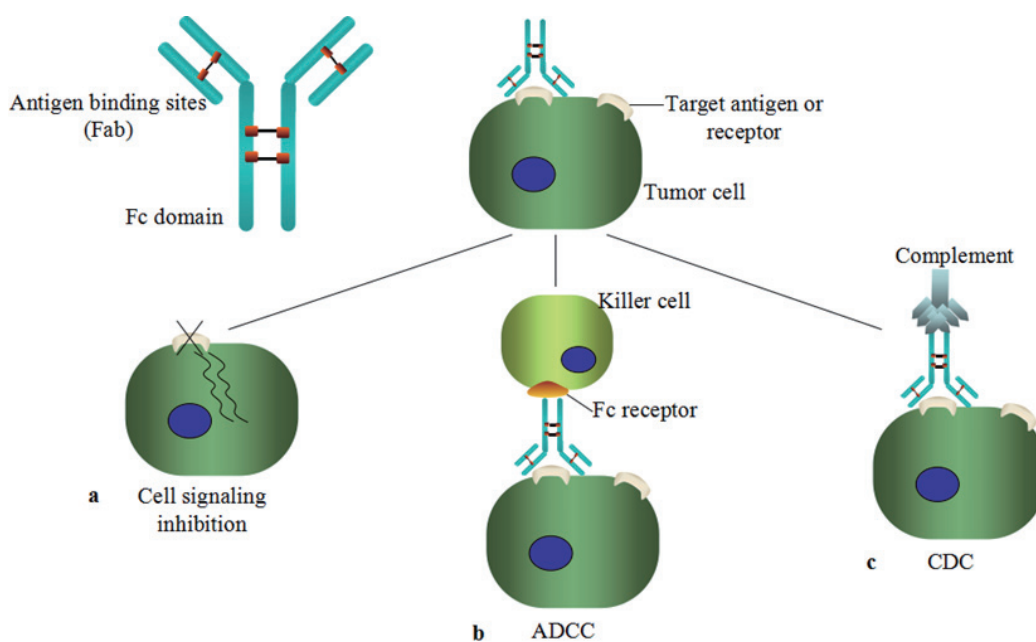


Figure 1. Mechanisms underlying the therapeutic efficacy of mAb-based immunotherapy. (a) mAbs can induce signaling inhibition and lead to apoptosis in targeted tumor cells by binding with their specific receptor, inducing modulation of the receptor or interfering with ligand binding and/or dimerization of the receptor. (b) The Fc region of an antibody recognizes the Fc gamma receptors (FcγR) on the surface of immune effector cells, while the Fab domain specifically binds to a target cell. The FcγR ITAM is then phosphorylated, triggering the activation of the effector cell. (c) C1q binds to the antibody, triggering the complement cascade that leads to the formation of the membrane attack complex (MAC) (C5b to C9) on the surface of the target cell as a result of classic pathway complement activation.

of therapeutic antibodies, which require antibodies, antigen-coated target cells, and FcγR-bearing effectors (24-27).

In contrast, CDC involves C1q, a bundle of six heterotrimeric subunits consisting of globular heads and collagen-like tails. C1q binds the antibody that triggers the complement cascade, leading to the formation of membrane attack complex (MAC) (C5b to C9) on the surface of the target cell as a result of classic pathway complement activation (28).

There are five classes of immunoglobulins – IgA, IgD, IgE, IgG and IgM – that are classified on the basis of the constant region of the heavy chain. Most therapeutic antibodies developed for clinical use are of the human IgG1 isotype, which can induce a stronger ADCC or CDC in comparison to other heavy-chain isotypes of human antibodies (21). In addition to its effector mechanisms, IgG1 has a long half-life in blood that is as long as 21 days or so (29,30). Previous studies found that $IgG1 \geq IgG3 \gg IgG4 \geq IgG2$ in terms of the strength of their ADCC effector action and that $IgG3 \geq IgG1 \gg IgG2 \approx IgG4$ in terms of their level of CDC effector action (20,31).

4. Targets and typical mAb drugs

About 50% of mAbs in the commercial clinical pipeline have been studied as cancer agents (32). MABs for cancer therapy have greatly helped cancer patients. For researchers, the first challenge in developing an effective mAb-based therapeutic strategy is the identification of the right antigen to attack the surface of target cells (10). In order for an antigen to be of use

in targeted antibody therapy, the targeted molecule must be expressed at sufficiently elevated levels on tumor cells relative to normal cells. For example, about 20% of breast cancers have increased amounts of the HER2 protein, so HER2 can serve as a target for development of an antibody drug to treat breast cancer patients with elevated HER2 (33,34).

There are several existing targets of mAb development that have been successfully used in antibody development, and several mAbs have been approved by the US FDA for treatment of cancer (Table 1). Many more mAbs are still in the clinical or preclinical stages of research. According to sales figures for 2012, Rituximab, which is commonly used to treat a variety of human lymphomas and chronic lymphocytic leukemia, has become the largest-selling biologic drug in clinical oncology.

5. Development of antibody-drug conjugates

Antibodies are modified *via* attachment to protein toxins or highly potent, low-molecular-weight drugs to enable antibodies to function as cytotoxic anticancer agents, and the toxins delivered to the interior of cancer cells act as bullets to cancer cells (48). The magic bullet concept put forth by Paul Ehrlich is over 100 years old, while the first credible experiments linking chemotherapeutic agents to antibodies were performed almost 55 years ago (49-51). Antibody-drug conjugates, or ADCs, are a new class of highly potent biopharmaceutical drugs designed as a targeted therapy for the treatment of cancer. These conjugates consist of an antibody with high specificity (a whole

Table 1. Representative target antigens and monoclonal antibodies for the treatment of cancer in clinical use

Target	mAbs	Trade name	Molecular type	Main indication	Company	Year	Ref.
CD20	Rituximab	Rituxan	Chimeric human/mouse antibody	B-cell lymphoma	Roche	1997	34
	Ibritumomab*	Zevalin	Murine IgG1	B-cell lymphoma	Spectrum pharms	2002	35
	Tositumomab	Baxxar	Murine IgG2a	B-cell lymphoma	Smithkline Beecham	2003	36
	Ofatumumab	Arzerra	Human IgG1k	Chronic lymphocytic leukemia	Glaxo Grp Ltd	2009	37,38
CD52	Alemtuzumab	Campath	Humanized IgG1	B-cell chronic lymphocytic leukaemia	Illex pharmaceuticals	2001	39
EGFR	Cetuximab	Erbitux	Humanized IgG1	Colon, lung cancer	Imclone/Bristol-MyersSquibb	2004	40
	Panitumumab	Vectibix	Fully human IgG2	Colon cancer	Amgen	2006	41
HER2	Trastuzumab	Herceptin	Humanized IgG1	Breast cancer	Roche	1998	33
	Pertuzumab	Perjeta	Humanized IgG1	Metastatic breast cancer	Genentech	2012	42,43
VEGF	Bevacizumab	Avastin	Recombinant humanize IgG	Colon, lung, breast and renal cancer	Roche	2004	44
RANKL	Denosumab	Xgeva	Human IgG2	Breast and prostate carcinoma	Amgen	2010	45
CTLA-4	Ipilimumab	Yervoy	Human IgG1k	Melanoma	Bristol-Myers Squibb	2011	46

* Coupled with ⁹⁰Y or ¹¹¹In.

mAb or an antibody fragment) linked *via* a stable chemical linker with labile bonds to a "small" (300 to 1,000 Da) biologically active toxin or drug with manageable toxicity (Figure 2) (52,53). Conjugated mAbs are also referred to as tagged, labeled, or loaded antibodies and are divided into three groups: mAbs with radioactive particles attached, mAbs with chemotherapy drugs attached, and mAbs attached to cell toxins. Thus, ibritumomab tiuxetan (Zevalin[®]) and tositumomab (Bexxar[®]) are, strictly speaking, examples of radiolabeled mAbs that fall under ADC drugs.

Denileukin difitox (trade name: Ontak) is the first ADC drug that was approved in 1999 by the US FDA for the treatment of diffuse large B-cell lymphoma. Although it is not an mAb, IL-2 normally attaches to certain cells that contain the CD25 antigen, which makes it useful for delivering the toxin to these cells. Gemtuzumab ozogamicin (trade name: Mylotarg) was later approved for the treatment of acute myelogenous leukemia in 2000 (54). However, Pfizer/Wyeth withdrew the drug from the market in June 2010 (55,56). Another ADC that was approved in 2011 was Brentuximab vedotin (SGN-35, trade name: Adcetris, marketed by Seattle Genetics and Millennium/Takeda), which is clinically used to treatment relapsed and/or refractory Hodgkin's lymphoma and systemic anaplastic large-cell lymphoma.

With the FDA approval of trastuzumab emtansine (T-DM1, trade name: Kadcyla, marketed by Genentech and Roche) on February 22, 2013, the development of antibody-drug conjugates based on antibodies ushered in a new era of personalized cancer treatment with greater clinical efficacy and manageable toxicity. The

success development of T-DM1 for metastatic breast cancer has done away with the view that ADCs are only useful against blood cancers (57,58). ADCs are also showing promising efficacy and limited adverse toxicity in the treatment of cancer. According to a previous study, at least 30 ADCs are now in clinical use, accounting for around 15% of the clinical-stage anticancer antibody-based pipeline and outnumbering other modified mAbs (57,59).

6. mAb-related drugs being developed for cancer therapy

Despite all the advances, there are still many questions to answer besides the identification of optimal cellular targets and antibody forms. Personalized therapies now need to identify the optimal dose, schedule, and combinations of agents for specific malignancies for specific patients (60). High specificity and high affinity are both important for antibodies developed as cancer therapies to have little impact on normal cells. The right target that is highly expressed on tumor cells but little expressed in normal cells must be chosen. To obtain a high affinity, more work has to be done to design the antigen-binding site. Dozens of MAbs are in various clinical stages, some of which are the later stages of phase II and III, indicating development of promising drugs for FDA approval (32,61).

For ADCs, MAbs that cross-react with the corresponding target antigen expressed on cells from rodents and/or non-human primates must be selected whenever possible because most target antigens used in ADCs are tumor-selective rather than tumor-specific (62,63). Thanks to the development of linker technology and utilization of sufficiently potent toxins, some promising ADCs are currently undergoing clinical trials, and ADCs to treat hematologic malignancies and solid tumors that are in phase II or III are shown in Table 2. Most ADCs in clinical development utilize humanized or fully human mAbs (63).

7. Main problems

Although there has been much progress in the development of antibody drugs with considerable specificity in patients with advanced cancer, problems and limitations still exist. mAbs are large molecules that would be expected to have limited distribution within solid tumor blood vessels, and the limited penetration of full-length antibodies into solid tumors is as an important factor restricting their efficacy (70,71). Despite the fairly mild side effects of mAbs, such as fever, chills, weakness, headaches, nausea, vomiting, diarrhea, low blood pressure, and rashes, the major drawback of mAbs is their immunogenicity, which may induce production of anti-drug antibodies that can neutralize a drug's therapeutic activity, provoke

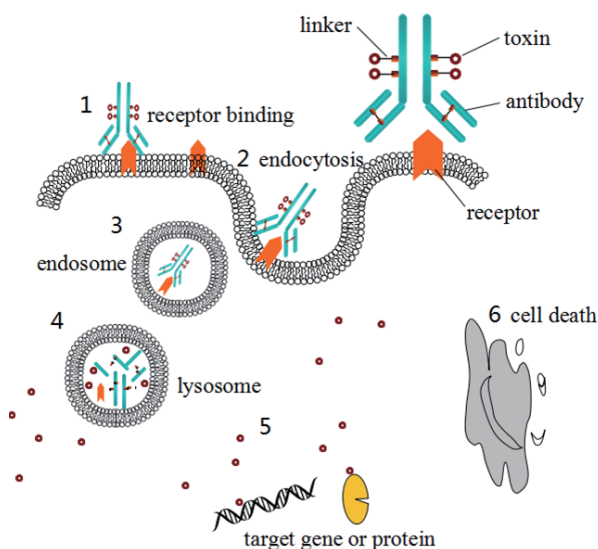


Figure 2. Mechanism of antibody-drug conjugate. An antibody-drug conjugate consists of an antibody (whole mAb or an antibody fragment) linked *via* a stable chemical linker with labile bonds to a biologically active cytotoxic anticancer toxin or drug. After binding to the targeted cell receptor, ADC is internalized and degraded, and the toxin or drug that is released ultimately induces cell death by acting on specific genes or proteins.

Table 2. Representative emerging antibody-drug conjugates in Phase 2 or Phase 3 clinical studies for cancer therapy

Agent	Company	Target	Toxin	Main indication	Highest stage (phase)	Ref.
Inotuzumab ozogamicin (CMC-544)	Pfizer	CD22	ozogamicin	relapsed/refractory acute lymphoblastic leukemia	III	63
Glembatumumab vedotin	Celldex Therapeutics	GPNMB*	MMAE	advanced GPNMB-expressing breast cancer	II	64
SAR3419	Sanofi-aventis	CD19	Maytansine DM4	Diffuse Large B-cell Lymphoma	II	60,65
BT062	Biotest	CD138	Maytansine DM4	Multiple Myeloma	II	66
Anti-PSMA ADC	Progenics	PSMA	MMAE	Prostate Cancer	II	67
Lorvotuzumab mertansine	ImmunoGen	CD56	Maytansine DM-1	Small Cell Lung Cancer	I/II	68

* glycoprotein NMB.

autoimmune symptoms, and affect the pharmacokinetic process (72-75). Although sequence humanization was believed to be sufficient to tackle these problems, multiple clinical examples now demonstrate that humanization does not suffice to avoid immune responses (76-79). Side effects due to target inhibition have also emerged. For example, bevacizumab, which targets tumor blood vessel growth (HER2), may cause side effects such as high blood pressure, bleeding, poor wound healing, blood clots, and kidney damage (45,80). Although a study suggested that brain metastases are not a risk factor for intracranial hemorrhage with bevacizumab treatment (81), bevacizumab may potentially increase the risk of bleeding.

In ADCs, the antibodies serve as a carrier to internalize the toxic component of an immunoconjugate, potentially making it more therapeutically active (82), so combining the cytotoxicity of highly potent natural or synthetic anti-neoplastic agents with mAbs conjugated by blood-stable optimized linkers is a key strategy for a new generation of ADCs (56). The first challenge is to ensure drug potency, which means to make sure that sufficient quantities of the ADC reach the target tumor cells (11,59). The second task is to design appropriate linker molecules to couple drugs to the antibody. These molecules must maintain antibody binding capacity following conjugation and also undergo selective, rather than systemic, enzymatic or chemical degradation inside the cell or on the cell surface (71).

8. Outlook and prospects for the future

After years of preclinical development, antibody drugs offer vast resources for drug discovery and new drug research. As new targets emerge, new avenues for drug design will open. Investigation of natural compounds will also offer more options for ADC drug research. Modern biological techniques have allowed the rapid production of chimeric antibodies, humanized antibodies, and totally human antibodies. Understanding of the effects and molecular mechanisms of these antibodies has improved with the development

of functional genomics, proteomics, and molecular research, and the number of clinical trials using antibody-related drugs to treat cancer has increased markedly. Some studies have found impressive clinical responses, indicating the beginning of a new and exciting phase of cancer treatment. Moreover, bispecific mAb consisting of fragments of two different mAbs have appeared. These mAbs bind to two different types of antigen, pointing the way for antibody drug development. Thus, antibody drugs have a promising future that offers better personalized therapy and combination therapy to treat malignant cancer.

References

1. A randomized clinical trial of OKT3 monoclonal antibody for acute rejection of cadaveric renal transplants. Ortho Multicenter Transplant Study Group. *N Engl J Med.* 1985; 313:337-342.
2. Alkan SS. Monoclonal antibodies: the story of a discovery that revolutionized science and medicine. *Nat Rev Immunol.* 2004; 4:153-156.
3. Holliger P, Hudson PJ. Engineered antibody fragments and the rise of single domains. *Nat Biotechnol.* 2005; 23:1126-1136.
4. MarketsandMarkets Blog. <http://www.marketsandmarketsblog.com/protein-engineering-market.html> (accessed September 1, 2013).
5. Blanco E, Kessinger CW, Sumer BD, Gao J. Multifunctional micellar nanomedicine for cancer therapy. *Exp Biol Med (Maywood).* 2009; 234:123-131.
6. Hait WN, Hambley TW. Targeted cancer therapeutics. *Cancer Res.* 2009; 69:1263-1267; discussion 1267.
7. DeVita VT, Jr, Chu E. A history of cancer chemotherapy. *Cancer Res.* 2008; 68:8643-8653.
8. Alvarez RH, Valero V, Hortobagyi GN: Emerging targeted therapies for breast cancer. *J Clin Oncol.* 2010; 28:3366-3379.
9. Stapnes C, Gjertsen BT, Reikvam H, Bruserud O. Targeted therapy in acute myeloid leukaemia: Current status and future directions. *Expert Opin Investig Drugs.* 2009; 18:433-455.
10. Christiansen J, Rajasekaran AK. Biological impediments to monoclonal antibody-based cancer immunotherapy. *Mol Cancer Ther.* 2004; 3:1493-1501.
11. Alley SC, Okeley NM, Senter PD. Antibody-drug conjugates: targeted drug delivery for cancer. *Curr Opin*

- Chem Biol. 2010; 14:529-537.
12. Schuler PJ, Hoffmann TK, Gauler TC, Bergmann C, Brandau S, Lang S. Immunotherapy of head and neck cancer: Current developments. *HNO*. 2013;61:559-572.
 13. Tazi I, Nafil H, Mahmal L. Monoclonal antibodies in hematological malignancies: Past, present and future. *J Cancer Res Ther*. 2011; 7:399-407.
 14. Harding FA, Stickler MM, Razo J, DuBridge RB. The immunogenicity of humanized and fully human antibodies: Residual immunogenicity resides in the CDR regions. *MAbs*. 2010; 2:256-265.
 15. Riechmann L, Clark M, Waldmann H, Winter G. Reshaping human antibodies for therapy. *Nature*. 1988; 332:323-327.
 16. Hoogenboom HR. Designing and optimizing library selection strategies for generating high-affinity antibodies. *Trends Biotechnol*. 1997; 15:62-70.
 17. Campoli M, Ferris R, Ferrone S, Wang X. Immunotherapy of malignant disease with tumor antigen-specific monoclonal antibodies. *Clin Cancer Res*. 2010; 16:11-20.
 18. Iannello A, Ahmad A. Role of antibody-dependent cell-mediated cytotoxicity in the efficacy of therapeutic anti-cancer monoclonal antibodies. *Cancer Metastasis Rev*. 2005; 24:487-499.
 19. Takamuku K, Akiyoshi T, Tsuji H. Antibody-dependent cell-mediated cytotoxicity using a murine monoclonal antibody against human colorectal cancer in cancer patients. *Cancer Immunol Immunother*. 1987; 25:137-140.
 20. Kaneko Y, Nimmerjahn F, Ravetch JV. Anti-inflammatory activity of immunoglobulin G resulting from Fc sialylation. *Science*. 2006; 313:670-673.
 21. Natsume A, Niwa R, Satoh M. Improving effector functions of antibodies for cancer treatment: Enhancing ADCC and CDC. *Drug Des Devel Ther*. 2009; 3:7-16.
 22. Kohrt HE, Houot R, Marabelle A, Cho HJ, Osman K, Goldstein M, Levy R, Brody J. Combination strategies to enhance antitumor ADCC. *Immunotherapy*. 2012; 4:511-527.
 23. Clynes RA, Towers TL, Presta LG, Ravetch JV. Inhibitory Fc receptors modulate *in vivo* cytotoxicity against tumor targets. *Nat Med*. 2000; 6:443-446.
 24. Hamada-Tsutsumi S, Suzuki K, Akahori Y. Antibody-dependent cell-mediated cytotoxicity is induced by a single-chain Fv-protein III fusion in the presence of a rabbit anti-protein III polyclonal antibody. *Immunol Lett*. 2011; 136:44-48.
 25. Cragg MS, French RR, Glennie MJ. Signaling antibodies in cancer therapy. *Curr Opin Immunol*. 1999; 11:541-547.
 26. Perussia B, Loza MJ. Assays for antibody-dependent cell-mediated cytotoxicity (ADCC) and reverse ADCC (redirected cytotoxicity) in human natural killer cells. *Methods Mol Biol*. 2000; 121:179-192.
 27. Hubert P, Amigorena S. Antibody-dependent cell cytotoxicity in monoclonal antibody-mediated tumor immunotherapy. *Oncimmunology*. 2012; 1:103-105.
 28. Moore GL, Chen H, Karki S, Lazar GA. Engineered Fc variant antibodies with enhanced ability to recruit complement and mediate effector functions. *MAbs*. 2010; 2:181-189.
 29. Clark MR. IgG effector mechanisms. *Chem Immunol*. 1997; 65:88-110.
 30. Nimmerjahn F, Ravetch JV. Translating basic mechanisms of IgG effector activity into next generation cancer therapies. *Cancer Immunol*. 2012; 12:13.
 31. Dangel JL, Wensel TG, Morrison SL, Stryer L, Herzenberg LA, Oi VT. Segmental flexibility and complement fixation of genetically engineered chimeric human, rabbit and mouse antibodies. *EMBO J*. 1988; 7:1989-1994.
 32. Reichert JM. Antibodies to watch in 2013: Mid-year update. *MAbs*. 2013; 5:513-517.
 33. Gajria D, Chandralapaty S. HER2-amplified breast cancer: Mechanisms of trastuzumab resistance and novel targeted therapies. *Expert Rev Anticancer Ther*. 2011; 11:263-275.
 34. Wong WM. Drug update: trastuzumab: anti-HER2 antibody for treatment of metastatic breast cancer. *Cancer Pract*. 1999; 7:48-50.
 35. Maloney DG, Grillo-Lopez AJ, Bodkin DJ, White CA, Liles TM, Royston I, Varns C, Rosenberg J, Levy R. IDEC-C2B8: Results of a phase I multiple-dose trial in patients with relapsed non-Hodgkin's lymphoma. *J Clin Oncol*. 1997; 15:3266-3274.
 36. Krasner C, Joyce RM. Zevalin. 90yttrium labeled anti-CD20 (ibritumomab tiuxetan), a new treatment for non-Hodgkin's lymphoma. *Curr Pharm Biotechnol*. 2001; 2:341-349.
 37. Press OW, Eary JF, Gooley T, *et al*. A phase I/II trial of iodine-131-tositumomab (anti-CD20), etoposide, cyclophosphamide, and autologous stem cell transplantation for relapsed B-cell lymphomas. *Blood*. 2000; 96:2934-2942.
 38. Hagenbeek A, Gadeberg O, Johnson P, *et al*. First clinical use of ofatumumab, a novel fully human anti-CD20 monoclonal antibody in relapsed or refractory follicular lymphoma: Results of a phase 1/2 trial. *Blood*. 2008; 111:5486-5495.
 39. Kluger N, Cartron G, Bessis D, Guillot B, Girard C. *Citrobacter koseri* cellulitis during anti-CD20 monoclonal antibody (ofatumumab) treatment for B-cell chronic lymphocytic leukaemia. *Acta Derm Venereol*. 2010; 90:99-100.
 40. Keating M, Hallek M. Alemtuzumab, the first monoclonal antibody (MAb) directed against CD52. *Med Oncol*. 2002; 19 (Suppl):S1-2.
 41. Humblet Y. Cetuximab, an IgG(1) monoclonal antibody for the treatment of epidermal growth factor receptor-expressing tumours. *Expert Opin Pharmacother*. 2004; 5:1621-1633.
 42. Adams CW, Allison DE, Flagella K, Presta L, Clarke J, Dybdal N, McKeever K, Sliwkowski MX. Humanization of a recombinant monoclonal antibody to produce a therapeutic HER dimerization inhibitor, pertuzumab. *Cancer Immunol Immunother*. 2006; 55:717-727.
 43. Sendur MA, Aksoy S, Altundag K. Pertuzumab in HER2-positive breast cancer. *Curr Med Res Opin*. 2012; 28:1709-1716.
 44. Bradbury J. Pertuzumab brake for prostate cancer? *Lancet Oncol*. 2007; 8:287.
 45. Schuster C, Eikesdal HP, Puntervoll H, Geisler J, Geisler S, Heinrich D, Molven A, Lonning PE, Akslen LA, Straume O. Clinical efficacy and safety of bevacizumab monotherapy in patients with metastatic melanoma: Predictive importance of induced early hypertension. *PLoS One*. 2012; 7:e38364.
 46. Majima S, Wada T, Ikeda M. Pharmacological profiles and results of clinical studies of denosumab (RANKL(R)), a human anti-RANKL antibody. *Nihon Yakurigaku Zasshi*. 2012; 140:295-302.
 47. Trinh VA, Hwu WJ. Ipilimumab in the treatment of melanoma. *Expert Opin Biol Ther*. 2012; 12:773-782.
 48. FitzGerald DJ, Wayne AS, Kreitman RJ, Pastan I. Treatment of hematologic malignancies with immunotoxins and antibody-drug conjugates. *Cancer Res*. 2011; 71:6300-

- 6309.
49. Strebhardt K, Ullrich A. Paul Ehrlich's magic bullet concept: 100 years of progress. *Nat Rev Cancer*. 2008; 8:473-480.
 50. Mathe G, Tran Ba LO, Bernard J. Effect on mouse leukemia 1210 of a combination by diazo-reaction of amethopterin and gamma-globulins from hamsters inoculated with such leukemia by heterografts. *C R Hebd Seances Acad Sci*. 1958; 246:1626-1628.
 51. Feld J, Barta SK, Schinke C, Braunschweig I, Zhou Y, Verma AK. Linked-in: Design and efficacy of antibody drug conjugates in oncology. *Oncotarget*. 2013; 4:397-412.
 52. Ducry L, Stump B. Antibody-drug conjugates: linking cytotoxic payloads to monoclonal antibodies. *Bioconjug Chem*. 2010; 21:5-13.
 53. Kovtun YV, Audette CA, Ye Y, Xie H, Ruberti MF, Phinney SJ, Leece BA, Chittenden T, Blattler WA, Goldmacher VS. Antibody-drug conjugates designed to eradicate tumors with homogeneous and heterogeneous expression of the target antigen. *Cancer Res*. 2006; 66:3214-3221.
 54. Duncan R, Gaspar R. Nanomedicine(s) under the microscope. *Mol Pharm*. 2011; 8:2101-2141.
 55. Ho M, Royston I, Beck A. 2nd PEGS Annual Symposium on Antibodies for Cancer Therapy: April 30-May 1, 2012, Boston, USA. *MAbs*. 2012; 4:562-570.
 56. Beck A, Haeuw JF, Wurch T, Goetsch L, Bailly C, Corvaia N. The next generation of antibody-drug conjugates comes of age. *Discov Med*. 2010; 10:329-339.
 57. Mullard A. Maturing antibody-drug conjugate pipeline hits 30. *Nat Rev Drug Discov*. 2013; 12:329-332.
 58. Krop IE, Beeram M, Modi S, Jones SF, Holden SN, Yu W, Girish S, Tibbitts J, Yi JH, Sliwkowski MX, Jacobson F, Lutzker SG, Burris HA. Phase I study of trastuzumab-DM1, an HER2 antibody-drug conjugate, given every 3 weeks to patients with HER2-positive metastatic breast cancer. *J Clin Oncol*. 2010; 28:2698-2704.
 59. Govindan SV, Goldenberg DM. Designing immunoconjugates for cancer therapy. *Expert Opin Biol Ther*. 2012; 12:873-890.
 60. Marshall JL. Maximum-tolerated dose, optimum biologic dose, or optimum clinical value: Dosing determination of cancer therapies. *J Clin Oncol*. 2012; 30:2815-2816.
 61. Sassoon I, Blanc V. Antibody-drug conjugate (ADC) clinical pipeline: A review. *Methods Mol Biol*. 2013; 1045:1-27.
 62. Trail PA, Bianchi AB. Monoclonal antibody drug conjugates in the treatment of cancer. *Curr Opin Immunol*. 1999; 11:584-588.
 63. Trail PA. Antibody Drug Conjugates as Cancer Therapeutics. *Antibodies*. 2013; 2:16.
 64. Thomas X. Inotuzumab ozogamicin in the treatment of B-cell acute lymphoblastic leukemia. *Expert Opin Investig Drugs*. 2012; 21:871-878.
 65. Keir CH, Vahdat LT. The use of an antibody drug conjugate, glebatumumab vedotin (CDX-011), for the treatment of breast cancer. *Expert Opin Biol Ther*. 2012; 12:259-263.
 66. Ribrag V, Dupuis J, Tilly H, Morschhauser F, Laine F, Haioun C, Copie C, Varga A, Lambert JM, Ziti-Ljajic S, Caron A, Payraud S, Coiffier B. A Phase I study of Sar3419, an anti-Cd19 antibody maytansinoid conjugate, administered once weekly in patients with relapsed/refractory B-Cell non Hodgkin's lymphoma. *Clin Cancer Res*. 2013. [Epub ahead of print]
 67. Lutz RJ, Whiteman KR. Antibody-maytansinoid conjugates for the treatment of myeloma. *MAbs*. 2009; 1:548-551.
 68. Wang X, Ma D, Olson WC, Heston WD. *In vitro* and *in vivo* responses of advanced prostate tumors to PSMA ADC, an auristatin-conjugated antibody to prostate-specific membrane antigen. *Mol Cancer Ther*. 2011; 10:1728-1739.
 69. Wood AC, Maris JM, Gorlick R, Kolb EA, Keir ST, Reynolds CP, Kang MH, Wu J, Kurmasheva RT, Whiteman K, Houghton PJ, Smith MA. Initial testing (Stage 1) of the antibody-maytansinoid conjugate, IMG901 (Lorvotuzumab mertansine), by the pediatric preclinical testing program. *Pediatr Blood Cancer*. 2013; 60:1860-1867.
 70. Lee CM, Tannock IF. The distribution of the therapeutic monoclonal antibodies cetuximab and trastuzumab within solid tumors. *BMC Cancer*. 2010; 10:255.
 71. Firer MA, Gellerman G. Targeted drug delivery for cancer therapy: the other side of antibodies. *J Hematol Oncol*. 2012; 5:70.
 72. Chirmule N, Jawa V, Meibohm B. Immunogenicity to therapeutic proteins: impact on PK/PD and efficacy. *AAPS J*. 2012; 14:296-302.
 73. Perry LC, Jones TD, Baker MP. New approaches to prediction of immune responses to therapeutic proteins during preclinical development. *Drugs R D*. 2008; 9:385-396.
 74. De Groot AS, Scott DW. Immunogenicity of protein therapeutics. *Trends Immunol*. 2007; 28:482-490.
 75. Onda M. Reducing the immunogenicity of protein therapeutics. *Curr Drug Targets*. 2009; 10:131-139.
 76. Gordon MS, Margolin K, Talpaz M, Sledge GW Jr, Holmgren E, Benjamin R, Stalter S, Shak S, Adelman D. Phase I safety and pharmacokinetic study of recombinant human anti-vascular endothelial growth factor in patients with advanced cancer. *J Clin Oncol*. 2001; 19:843-850.
 77. Maillere B, Delluc S, Ravot G. The prediction of immunogenicity of therapeutic proteins. *Med Sci (Paris)*. 2012; 28:82-88.
 78. Dore RK, Mathews S, Schechtman J, Surbeck W, Mandel D, Patel A, Zhou L, Peloso P. The immunogenicity, safety, and efficacy of etanercept liquid administered once weekly in patients with rheumatoid arthritis. *Clin Exp Rheumatol*. 2007; 25:40-46.
 79. De Groot AS, Martin W. Reducing risk, improving outcomes: Bioengineering less immunogenic protein therapeutics. *Clin Immunol*. 2009; 131:189-201.
 80. Boige V, Malka D, Bourredjem A, Dromain C, Baey C, Jacques N, Pignon JP, Vimond N, Bouvet-Forteau N, De Baere T, Ducreux M, Farace F. Efficacy, safety, and biomarkers of single-agent bevacizumab therapy in patients with advanced hepatocellular carcinoma. *Oncologist*. 2012; 17:1063-1072.
 81. Nishimura T, Furihata M, Kubo H, Tani M, Agawa S, Setoyama R, Toyoda T. Intracranial hemorrhage in patients treated with bevacizumab: report of two cases. *World J Gastroenterol*. 2011; 17:4440-4444.
 82. Oldham RK, Dillman RO. Monoclonal antibodies in cancer therapy: 25 years of progress. *J Clin Oncol* 2008; 26:1774-1777.

(Received October 7, 2013; Revised October 27, 2013; Accepted October 28, 2013)

16,17-dihydroxycyclooctatin, a new diterpene from *Streptomyces* sp. LZ35

Guishi Zhao*, Shanren Li*, Yuanyuan Wang, Huilin Hao, Yuemao Shen, Chunhua Lu**

Key Laboratory of Chemical Biology (Ministry of Education), School of Pharmaceutical Sciences, Shandong University, Ji'nan, Shandong, China.

ABSTRACT: Genome sequence analysis of *Streptomyces* sp. LZ35 has revealed a large number of secondary metabolite pathways, including a complete gene cluster for the biosynthesis of cyclooctatin. This cluster contains four genes, *cotB1–4*, located in a 5-kb region. Optimization of fermentation medium for LZ35 Δ heng (SR107) led to the identification of cyclooctatin (1) and 16,17-dihydroxycyclooctatin (2), a new diterpene. The structures of these substances were elucidated on the basis of 1D-, 2D-NMR, and HRESIMS data. Cytotoxicity against MDA-MB-231 and A549 cell lines was also evaluated. Results demonstrated that gene cluster and pathway analysis are key to guided isolation of new natural products.

Keywords: *Streptomyces* sp. LZ35, gene cluster, cyclooctatin, 16,17-dihydroxyl-cyclooctatin

1. Introduction

Cyclooctatin, a diterpene characterized by a novel 5-8-5-fused ring system, is a potent inhibitor of lysophospholipase, which was previously isolated from *Streptomyces melanosporofaciens* MI614-43F2 (1,2). The complete cyclooctatin biosynthesis gene cluster was cloned from *S. melanosporofaciens* MI614-43F2 and heterologously expressed with variations of cytochrome P450 genes in *Streptomyces albus* to produce cyclooctatin together with two new intermediates, cyclooctat-9-en-7-ol and cyclooctat-9-en-5,7-diol (3). Additionally, 17-hydroxycyclooctatin was isolated from *Streptomyces* sp. MTE4a (4). To date, only four compounds with this novel 5-8-5-fused ring backbone have been isolated thus far.

*The authors contributed equally to this work.

**Address correspondence to:

Dr. Chunhua Lu, School of Pharmaceutical Sciences of Shandong University, No. 44 West Wenhua Road, Ji'nan, Shandong 250012, China.
E-mail: ahua0966@sdu.edu.cn.

Genome sequence analysis of *Streptomyces* sp. LZ35 has revealed a complete cyclooctatin biosynthesis gene cluster containing four genes, *cotB1–4*, located in a 5-kb region (unpublished data). This cluster is highly homologous to that reported by Kim *et al.* (3). Therefore, an interesting question was whether *Streptomyces* sp. LZ35 produces cyclooctatin-type diterpenoids. To facilitate the isolation of minor components such as putative cyclooctatin derivatives, four gene clusters involved in the biosynthesis of hygrocine, elaiophylin, nigericin, and geldanamycin were deleted to afford a clean background mutant strain LZ35 Δ heng (SR107) of *Streptomyces* sp. LZ35 (Supporting Information) (5). The fermentation of LZ35 Δ heng on SSY agar medium led to the isolation of cyclooctatin (1) and 16,17-dihydroxycyclooctatin (2).

2. Materials and Methods

2.1. General experimental procedures

Mass spectra were measured using a Bruker BioTOF-Q spectrometer; NMR spectra were measured on Bruker DRX-600 MHz NMR spectrometer (Bruker Daltonics Inc., Billerica, MA, USA) with tetramethylsilane (TMS) as an internal standard. The IR spectra (KBr) were obtained on a Nicolet iN10 Micro FT-IR Microscope (Thermo Scientific). Reversed-phase (RP) C₁₈ silica gel for column chromatography (CC) was obtained from Merck (Darmstadt, Germany) and Sephadex LH-20 was obtained from GE Amersham Biosciences (Piscataway, NJ, USA). Silica gel (200–300 mesh) for CC and silica gel GF₂₅₄ for TLC were purchased from Qingdao Marine Chemical, Ltd. (Qingdao, Shandong, China).

2.2. Microorganisms

The strain *Streptomyces* sp. LZ35 was isolated from the intertidal soil collected in Ji'mei, Xia'men, China (6). The mutant strain LZ35 Δ heng (SR107) was constructed by deleting parts of *hgcA*, *elpA*, *nigA* and *gdmAI* that are the first module of PKS genes in the gene clusters for biosynthesis of hygrocine, elaiophylin, nigericin, and

geldanamycin, respectively (5).

2.3. Fermentation and isolation

The strain LZ35 Δ heng was cultured for 14 d on SSY agar media (2.5% Soluble starch, 1.5% Soybean, 0.2% Yeast extract, pH 7.2) at 28°C.

The medium (12 L) was collected and extracted three times with an equal volume of EtOAc/MeOH/AcOH 80:15:5 (v/v/v) at room temperature. The organic solutions were collected by filtration and removed under vacuum at 40°C to obtain the crude extract. This was partitioned three times between 95% MeOH and petroleum ether (1:1) to remove lipids. The 95% MeOH solution was concentrated under vacuum at 40°C to afford MeOH extract (4.5 g).

The MeOH extract (4.5 g) was subjected to column chromatography (CC) over Sephadex LH-20 (120 g) eluted with MeOH-CH₂Cl₂ (2:1, v/v) to obtain 3 fractions, Fr. A, Fr. B, and Fr. C. Fr. B was further subjected to CC over Sephadex LH-20 (120 g) eluted with MeOH to obtain 6 subfractions, Fr. B1-B6. Fr. B2 (302 mg) was subjected to MPLC over RP-18 silica gel (20 g) eluted with 15%, 40%, 60%, 80% and 100% MeOH, resp., (300 ml for each gradient) to afford 5 fractions: Fr. B2A – B2E. Fr. B2D (40 mg) obtained from 80% MeOH eluent was further purified by CC over silica gel (1.6 g) eluted with gradient CH₂Cl₂-MeOH (60:1, 50:1) to yield Fr. B2D1 (3.8 mg). Fr. B2D1 was finally purified by HPLC (Agilent 1200 equipped with a ZORBAX XDB-C18 5 μ m, column ID: 9.4 \times 250 mm, elution: 85% MeOH, flow rate: 4 mL/min, UV detection monitored at 220 and 273 nm) to afford **1** (RT 9.2 min, 3.0 mg). Fr. B2B (34 mg) obtained from 40% MeOH eluents was further purified by CC over silica gel (0.85 g) eluted with gradient CH₂Cl₂-MeOH (50:1, 30:1, 20:1) to yield **2** (2.3 mg).

2.4. Cell lines

The human breast cancer cells MDA-MB-231 and A549 were obtained directly from the American Type Culture Collection (ATCC) and maintained in DMEM containing 10% fetal bovine serum (FBS, Gibco). All cells were grown at 37°C in a humidified atmosphere of 5% CO₂.

2.5. Cell growth assay

The cytotoxicities of compounds **1** and **2** were evaluated using the sulforhodamine B (SRB) assay as described previously (7). Briefly, 3000-4000 MDA-MB-231 human breast cancer cells and A549 human lung cancer cells were seeded in 96-well plates overnight and exposed to either investigational compounds or etoposide at various concentrations for 72 h in 5% CO₂ at 37°C. After the medium was discarded, a 100 μ L solution of 10% trichloroacetic acid (TCA) was added to cell monolayers and cells were stained for

1 h at 4°C. The plates were washed five times with distilled water. Then, 100 μ L 4 mg/mL of SRB (Sigma-Aldrich) was added to each well, and cells were stained at room temperature for 10 min. The excess stain was removed by washing cells five times with 1% acetic acid. The protein-bound stain was dissolved in 200 μ L of 10 mM Tris base solution per well. The optical density was measured at 570 nm using a microplate reader (Bio-Rad, iMark680). All experiments were performed in triplicate. The rate of growth inhibition for each well was calculated as follows: Inhibition rate (%) = [A₅₇₀(control) – A₅₇₀(sample)]/[A₅₇₀(control) – A₅₇₀(blank)] \times 100.

3. Results and Discussion

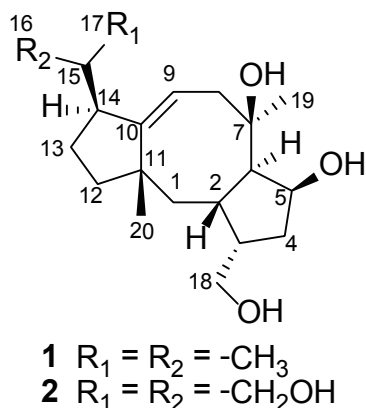
Geldanamycins and related type I polyketides, such as nigericins, elaiophylins, and hygrocins, are normally major endogenous secondary metabolites produced by wild-type *Streptomyces* sp. LZ35 (6). Biosynthesis gene clusters encoding hygrocins (*hgc*), elaiophylins (*elp*), nigericins (*nig*), and geldanamycins (*gdm*) were disrupted using a REDIRECT technique in accordance with a previously described protocol with modifications (8) (Table S1, Figures S1-4, <http://www.ddtjournal.com/docindex.php?year=2013&kanno=5>). The portion of the *gdmAI* gene was first deleted to yield the mutant LZ35 Δ *gdmAI* (SR101) (Figure S1), and double cross-over deletion mutants were obtained by screening for loss of yellow pigment production (data not shown). The *nigAI* gene was then deleted to yield the mutant LZ35 Δ *nigAI* Δ *gdmAI* (SR105) (Figure S2), and double cross-over deletion mutants were confirmed by the detection of nigericins and geldanamycins with thin-layer chromatography (TLC) (data not shown). The *elpA* gene was deleted to yield the mutant LZ35 Δ *elpA* Δ *nigAI* Δ *gdmAI* (SR106) (Figure S3). Finally, the portion of the *hgcA* gene was deleted to yield the mutant LZ35 Δ *hgcA* Δ *elpA* Δ *nigAI* Δ *gdmAI* (LZ35 Δ heng, SR107) (Figure S4). HPLC analysis of the EtOAc extract of whole broth confirmed the absence of hygrocins, elaiophylins, nigericins, and geldanamycins and revealed more absorbance peaks with similar densities (data not shown), suggesting that minor components could be readily isolated from the mutant strain LZ35 Δ heng.

Compound **1** was obtained as a colorless amorphous powder. The molecular formula of **1** was determined to be C₂₀H₃₄O₃ on the basis of HR-Q-TOF MS (*m/z* 345.4718, calcd. 345.4714 for C₂₀H₃₄O₃Na⁺) and NMR data (Table 1). Its UV spectrum revealed maximum absorption in MeOH. Its IR spectrum (KBr) revealed the presence of a hydroxyl group (3420 cm⁻¹). The ¹³C NMR spectrum revealed 20 signals, corresponding to four CH₃, six CH₂, seven CH, and three quaternary C-atoms. Complete assignment of NMR data with the aid of HMQC and HMBC experiments revealed that compound **1** was identical to cyclooctatin (Figure 1),

Table 1. The NMR data for **1** and **2**. Recorded at 600/150 MHz (δ in ppm, J in Hz)

	1 ^a		2 ^a		cyclooctatin ^c	
	¹ H	¹³ C	¹ H	¹³ C	¹ H	¹³ C
1	1.53 (m), 1.40 (m)	45.5t	1.61 (dd, 5.9, 12.6), 1.35 (m)	46.6t	1.68 (br d, 12.8), 1.20 (t, 12.8)	45.6t
2	2.56 (m)	24.6d	2.58 (m)	35.8d	2.56 (m)	35.8d
3	2.66 (m)	44.1d	2.64 (m)	44.9d	2.61 (m)	44.9d
4	1.75 (m), 1.38 (m)	38.9t	1.71 (m), 1.32 (m)	39.7t	1.71 (br dd, 12.6, 5.0), 1.38 (dt, 12.6, 3.4)	39.7t
5	4.50 (d, 3.4)	75.0d	4.45 (t, 5.0)	75.6d	4.44 (br dd, 5.0, 3.4)	75.7d
6	1.98 (t, 5.2)	58.0d	1.99 (t, 4.7)	57.9d	1.97 (t, 5.0)	58.0d
7	/	77.3s	/	78.3s	/	78.4s
8	2.69 (m), 1.96 (m)	41.7t	2.79 (t, 11.6), 1.95 (m)	42.2t	2.72 (br t, 11.6), 1.91 (dd, 12.8, 7.4)	42.2t
9	5.25 (t, 7.8)	117.8d	5.45 (t, 8.5)	118.7d	5.28 (ddd, 10.3, 7.4, 2.2)	119.1d
10	/	153.1s	/	153.9s	/	154.5s
11	/	44.7s	/	45.8s	/	45.9s
12	1.53 (m), 1.49 (m)	45.5t	1.90 (m), 1.63 (dd, 6.0, 12.0)	45.6t	1.59 (m), 1.42 (m)	46.6t
13	1.49 (m), 1.36 (m)	23.2t	1.68 (q, 5.7), 1.35 (m)	25.3t	1.56 (m), 1.38 (m)	24.3t
14	2.26 (m)	53.7d	2.68 (m)	47.1d	2.30 (m)	55.1d
15	1.79 (m)	28.9d	1.23 (t, 6.7)	45.7d	1.83 (m)	30.2d
16	0.96 (d, 6.7, 3H)	22.2q	3.85 (dd, 5.1, 8.8), 3.66 (d, 10.1)	63.7t	0.96 (d, 6.6, 3H)	22.5q
17	0.77 (d, 6.7, 3H)	17.3q	3.60 (m)	61.3t	0.79 (d, 6.6, 3H)	17.8q
18	3.77 (t, 10.2), 3.62 (dd, 7.6, 10.2)	63.3t	3.39 (t, 10.1) 3.60 (m, 2H)	63.4t	3.66 (dd, 10.8, 7.4), 3.55 (dd, 10.8, 6.8)	63.4t
19	1.33 (s, 3H)	26.3q	1.32 (s, 3H)	26.7q	1.33 (br. s, 3H)	26.7q
20	1.23 (s, 3H)	24.8q	1.27 (s, 3H)	25.4q	1.25 (s, 3H)	25.2q

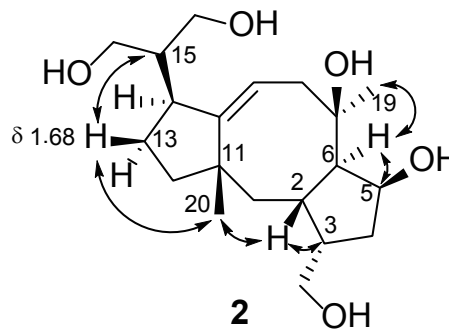
^a Measured in CDCl₃; ^b Measured in CD₃OD; ^c The NMR data listed (CD₃OD) were reported previously by Aoyama *et al.* (2).

**Figure 1.** The chemical structures of compounds **1** and **2**.

which is consistent with the literature (2).

Compound **2** was obtained as a colorless amorphous powder. The molecular formula of **2** was determined to be C₂₀H₃₄O₅ on the basis of HR-Q-TOF MS (m/z 377.4706, calcd. 377.4702 for C₂₀H₃₄O₅Na⁺) and NMR data (Table 1). Its UV spectrum revealed maximum absorption in MeOH. Its IR spectrum (KBr) revealed the presence of a hydroxyl group (3430 cm⁻¹). The ¹³C NMR spectrum revealed 20 signals, corresponding to two CH₃, eight CH₂ (three of which were oxygenated), seven CH, and three quaternary C-atoms.

The ¹H and ¹³C NMR spectra of **2** closely resembled

**Figure 2.** Selected NOE correlations for compound **2**.

those of **1** except that the isopropylidene at C-14 in **1** was replaced with a 1,3-dihydroxyisopropyl group in **2**, as indicated by the two oxygen-bearing methylenes at δ_H 3.85 (dd, 5.1, 8.8) and 3.66 (d, 10.1), δ_C 63.7 (t) and at δ_H 3.60 (m) and 3.39 (t, 10.1), δ_C 61.3 (t). Extensive analysis of HMQC and HMBC spectra indicated that **2** had a structure of 16,17-dihydroxycyclooctatin (Figure 1). The relative configuration (2*S**,3*S**,5*S**,6*R**,7*R**,11*S**,14*S**) was determined from the NOESY correlations of H-6 with H-5 and H-19, H-2 with H-3 and H-20, and H-13 β with H-15 and H-20 as those for **1** and 17-hydroxycyclooctatin (Figure 2) (4).

Cyclooctatins have a unique tricyclic diterpene skeleton (C₂₀) characterized by a 5-8-5-fused ring system. Prior to the current study, only four compounds of this type were identified, including cyclooctatin (2), cyclooctat-9-en-7-ol, cyclooctat-9-en-5,7-diol (3), and 17-hydroxycyclooctatin (4). Previous studies suggested that cyclooctatin was a potent inhibitor of lysophospholipase and exhibited no significant antimicrobial activity at 100 µg/mL (1). The current results suggested that compounds 1 and 2 showed no cytotoxicity against MDA-MB-231 and A549 cell lines at concentrations up to 50 µM.

In conclusion, the current findings have revealed important new additions to the small family of cyclooctatin diterpenoids with a novel 5-8-5-fused ring backbone. The current work has also demonstrated that gene cluster and pathway analysis are key to guided isolation of new natural products.

Acknowledgements

This work was supported by National Basic Research Programs ("973 Programs") of China (2010CB833802 and 2012CB721005), a grant for an NSFC Project (C. Lu, 81373304) and the National Science Fund for Distinguished Young Scholars (Y. Shen, 30325044).

References

1. Aoyagi T, Aoyama T, Kojima F, Hattori S, Honma Y, Hamada M, Takeuchi T. Cyclooctatin, a new inhibitor of lysophospholipase, produced by *Streptomyces melanosporofaciens* MI614-43F2. Taxonomy, production, isolation, physico-chemical properties and biological activities. *J Antibiot (Tokyo)*. 1992; 45:1587-1591.
2. Aoyama T, Naganawa H, Muraoka Y, Aoyagi T, Takeuchi T. The structure of cyclooctatin, a new inhibitor of lysophospholipase. *J Antibiot (Tokyo)*. 1992; 45:1703-1704.
3. Kim SY, Zhao P, Igarashi M, Sawa R, Tomita T, Nishiyama M, Kuzuyama T. Cloning and heterologous expression of the cyclooctatin biosynthetic gene cluster afford a diterpene cyclase and two P450 hydroxylases. *Chem Biol*. 2009; 16:736-743.
4. Kawamura A, Iacovidou M, Hirokawa E, Soll CE, Trujillo M. 17-Hydroxycyclooctatin, a fused 5-8-5 ring diterpene, from *Streptomyces* sp. MTE4a. *J Nat Prod*. 2011; 74:492-495.
5. Li SR. Activation of the silent neoansamycin biosynthesis gene cluster and hygrocinn biosynthesis in *Streptomyces* sp. LZ35. 2013; Ph D thesis of Xiamen University.
6. Shi NN, Wang HX, Lu CH, Liu Z, Shen YM. Ansamycins produced by *Streptomyces* sp. LZ35. *Chin Pharm J*. 2011; 46:1317-1320.
7. Vichai V, Kirtikara K. Sulforhodamine B colorimetric assay for cytotoxicity screening. *Nat Protoc*. 2006; 1:1112-1116.
8. Gust B, Challis GL, Fowler K, Kieser T, Chater KF. PCR-targeted *Streptomyces* gene replacement identifies a protein domain needed for biosynthesis of the sesquiterpene soil odor geosmin. *Proc Natl Acad Sci U S A*. 2003; 100:1541-1546.

(Received September 3, 2013; Revised October 25, 2013; Accepted October 27, 2013)

Anti-influenza activity of *Alchemilla mollis* extract: Possible virucidal activity against influenza virus particles

Juliann Nzembi Makau¹, Ken Watanabe¹, Nobuyuki Kobayashi^{1,2,*}

¹ Laboratory of Molecular Biology of Infectious Agents, Graduate School of Biomedical Sciences, Nagasaki University, Nagasaki, Japan;

² Central Research Center, AVSS Corporation, Nagasaki, Japan.

ABSTRACT: Influenza virus infection is a major public health problem that leads to significant morbidity and mortality. The emergence of resistance to the currently available anti-influenza agents has necessitated the development of new drugs with novel targets. Studying known ethno-medicinal plants is a promising approach for the discovery of new antiviral compounds. *Alchemilla mollis* is used in traditional medicine in Europe for different indications, including minimizing the symptoms of a sore throat. In this study, we found that *A. mollis* extract has anti-influenza activity, and investigated the mechanism underlying its inhibition of influenza virus replication. Plaque assays demonstrated that treatment of cells with *A. mollis* extract prior to infection did not inhibit influenza virus infection. However, plaque formation was markedly reduced when infected cells were overlaid with an agarose gel containing *A. mollis* extract. In addition, exposure of the virus to *A. mollis* extract prior to infection and treatment of cells during virus infection significantly suppressed plaque formation. Influenza virus-induced hemagglutination of chicken red blood cells was inhibited by *A. mollis* extract treatment. The inhibitory effect was observed against influenza A virus subtypes H1N1, H3N2, and H5N2. These findings suggest that *A. mollis* extract has virucidal or neutralizing activity against influenza virus particles. Furthermore, inhibitory effect of zanamivir synergistically increased after combination with *A. mollis* extract. Our results suggest that *A. mollis* extract has the potential to be developed as an anti-influenza agent.

Keywords: *Alchemilla mollis*, virucidal, synergistic effect, antiviral.

*Address correspondence to:

Dr. Nobuyuki Kobayashi, Laboratory of Molecular Biology of Infectious Agents, Graduate School of Biomedical Sciences, Nagasaki University, 1-14 Bunkyo-machi, Nagasaki City, Nagasaki 852-8521, Japan.
E-mail: nobnob@nagasaki-u.ac.jp

1. Introduction

Influenza viruses are enveloped, negative-strand RNA viruses with a segmented genome that belong to the Orthomyxoviridae family. Influenza pandemics or seasonal epidemics cause significant morbidity and mortality in both humans and animals. Currently, there are two main classes of anti-influenza drugs available: M2 ion channel inhibitors (amantadine and rimantadine) and neuraminidase inhibitors (zanamivir, oseltamivir, laninamivir, and peramivir). The use of M2 ion channel inhibitors is limited due to the rapid emergence of drug resistance, side effects, and the drugs' lack of effect on influenza B viruses (1), while neuraminidase inhibitor resistance in clinical isolates is also rapidly increasing (2, 3). These factors necessitate the development of novel anti-influenza drugs with reduced chances of resistance emergence.

Natural products have been in the limelight in the search for anti-viral compounds due to their abundance and the possibility for their inclusion in diet. There are numerous recent reports on plant extract constituents that possess potent antiviral activity, as reviewed by Kitazato, *et al.* (4). Several plant-derived compounds exert potent anti-influenza activity by blocking virus entry into cells, inactivating the virus, or inhibiting extracellular-signal-regulated kinase phosphorylation (5-7). We have demonstrated that valtrate and 1'-acetoxychavicol acetate derived from *Valeriana Radix* and *Alpina galanga*, respectively, inhibit influenza virus replication by preventing the nuclear export of viral ribonucleoprotein (8).

Alchemilla plants (lady's mantle) are used in traditional medicine for different indications, including minimizing the symptoms of sore throat, promoting wound healing, stopping bleeding, and alleviating nausea and vomiting. Herbal tea, Lady's Mantle Herbal Tea bags *Alchemilla* Herba *Alchemilla*, constituted from *Alchemilla* species is commercially available (9). Different studies have indicated that *A. mollis* and other *Alchemilla* species have potent free radical scavenging activity (10), attributed to the phenolic compounds, tannins, and flavonoid glycosides present in the plants

(11,12). *A. mollis* is a constituent of "Herba Alchemillae", a commercial drug with astringent, diuretic, and antispasmodic properties used in traditional medicine for the treatment of excessive menstruation and wounds (13). Despite numerous reports on the pharmacological importance of *A. mollis* and other *Alchemilla* species, their antiviral activity has not been investigated.

In this study, we investigated the anti-influenza activity of *A. mollis* extracts. We observed that *A. mollis* alkaline extract had virucidal activity against influenza virus particles and produced a synergistic effect upon co-treatment with zanamivir. This is the first report demonstrating the antiviral activity of *A. mollis* extract.

2. Materials and Methods

2.1. Cells, viruses, and chemicals

Madin-Darby Canine Kidney (MDCK) cells were grown in Minimum Essential Medium (MEM) supplemented with 5% fetal bovine serum (FBS) at 37°C in 5% CO₂. Influenza A virus strains A/WSN/33 (H1N1), A/PR/8/34 (H1N1), A/HK/8/68 (H3N2), and A/duck/Pennsylvania/84 (H5N2) were propagated in 10-day-old embryonated chicken eggs for 4 days. Allantoic fluid was then harvested and stored at -80°C. Zanamivir was purchased from GlaxoSmithKline (Middlesex, UK), dissolved in HEPES (pH 7.0) to a concentration of 10 mM, and stored at -20°C.

2.2. Extraction of *A. mollis* plant material

One gram of dried and powdered plant material was extracted in 15 mL of different solutions using the extraction methods shown in Table 1. Next, the extracts were centrifuged at 12,100 × g for 15 min and the supernatant was collected and sterilized using a 0.45-μm pore size filter.

2.3. Crystal violet assay

MDCK cells (3 × 10⁴ cells/well) were seeded in 96-well tissue culture plates and incubated at 37°C for 24 h. For cytotoxicity assays, cells were washed and treated with serial dilutions of *A. mollis* extract in MEM. Virus inocula of 25 TCID₅₀ (50% tissue culture infective dose) were added per well for the antiviral activity assay. Cells were

fixed with EtOH and stained with 0.5% crystal violet after incubation for 48 h. The optical density (OD) at 560 nm was measured with Infinite M200 Tecan plate reader (Wako Pure Chemical Industries, Osaka, Japan). The OD value of treated wells was compared with that of untreated controls, calculated as a percentage relative cell density and plotted against the concentration of *A. mollis* extract. Three independent experiments were performed. Linear regression analysis to calculate the 50% cytotoxic concentration (CC₅₀) and 50% inhibitory concentration (IC₅₀) was performed with Microsoft Excel software. The selectivity index (SI) was determined from the CC₅₀ to IC₅₀ ratio.

2.4. Plaque formation assay

Confluent MDCK cells cultured in 6-well plates were washed with serum-free medium and infected with 0.5 mL of virus solution (300 pfu/mL – A/WSN/33 virus) in serum-free MEM for 1 h at 37°C. Cells were washed with serum-free MEM and overlaid with MEM containing 0.8% agarose, 0.1% bovine serum albumin (BSA), 1% 100× MEM vitamin solution, and 0.03% glutamine. After incubation at 37°C for 72 h, plaques were visualized by fixing the cells with acetic acid:ethanol (1:1) for 1 h and staining with 0.5% amido black 10B for 3 h. Plaques were counted by visual examination. Results were represented as ratio of plaque number in the presence of extract or zanamivir to that in the absence of extract or zanamivir.

2.5. Hemmagglutination inhibition (HI) assay

HI assay was performed as previously described by Ehrhardt (14). Briefly, in 96-well micro titer plates, serial dilutions of samples (50 μL) were prepared and mixed with an equal volume of virus suspension as follows: 40 HA units - A/WSN/33 (H1N1), 256 HA units - A/HK/8/68 (H3N2), and 128 HA units - A/duck/Pennsylvania/84 (H5N2). After incubation at 4°C for 1 h, 50 μL of 5% (v/v) chicken red blood cells (RBCs) (Nippon Bio-Test Laboratories, Tokyo, Japan) in phosphate-buffered saline (PBS) (-) was added and then incubated for 1 h at room temperature (RT) to allow for hemagglutination to occur.

2.6. Heat treatment of *A. mollis* extract

Extract (400 μL) was aliquoted into 1.5-mL tubes and heated at 60°C or 100°C for 30 min. The samples were cooled at RT and stored at -30°C. The antiviral activity of the samples was determined with the crystal violet assay.

2.7. Ultra-filtration of *A. mollis* extract

Four hundred microliters of extract were added to the filter cup of 10 kDa and 30 kDa Ultrafree®-MC units (Millipore, Bedford, USA), and centrifuged at 2,500 ×

Table 1. Comparative potency of different *A. mollis* extracts

Solution	Method of extraction	^a SI
Water	Shaking at RT for 24 h	25
Water	Shaking in a 60°C hot water bath for 24 h	5
Water containing 1% (w/v) NaHCO ₃	Shaking at RT for 24 h	42
50% ethanol	Shaking at RT for 24 h	14

^a Selectivity index

g for 20 min in a fixed-angle rotor. Extract (2 mL) in 50 kDa Amicon® Ultra-4 filter devices (Millipore, Bedford, USA) was centrifuged at $2,010 \times g$ for 30 min in a swinging bucket rotor. The ultra-filtrate from each filter unit was collected and assayed for antiviral activity.

2.8. Combination treatment with *A. mollis* extract and zanamivir

Combination treatment with *A. mollis* extract and zanamivir was performed to investigate whether they have additive or synergistic effects on inhibiting influenza virus replication. MDCK cells were inoculated with A/WSN/33 virus at a multiplicity of infection (MOI) of 0.001 in the presence of mock medium or zanamivir (50 nM to 0.1 nM) mixed with 0.01%, 0.02%, 0.04%, 0.08%, 0.16%, and 0.31% of *A. mollis* extract. Cells were incubated at 37°C for 48 h and cell density was determined using the crystal violet assay. The percentage inhibitory activity of the zanamivir/*A. mollis* extract combination was calculated relative to the cell density in untreated controls. The combination treatment effect was analyzed by calculating the interaction index at 50% inhibitory activity using the isobole method as described by Tallarida (15). The following equation is used to calculate the interaction index (γ) for a combination of drugs A and B: $Ac/Ae + Bc/Be = \gamma$, where *Ac* and *Bc* correspond to the concentrations of *A* and *B* when used in combination, and *Ae* and *Be* correspond to the concentrations able to produce an effect of the same magnitude if used alone. If $\gamma < 1$, the effect of the combination is synergistic, whereas if $\gamma =$ or >1 , the effect is additive or antagonistic, respectively.

2.9. Statistical analysis

Results are represented as the mean \pm standard error of the mean from three independent experiments. The difference between test samples and untreated controls was evaluated using Student's *t* test. A *p* value < 0.05 was considered statistically significant.

3. Results

3.1. Cellular toxicity and anti-influenza activity of *A. mollis* extract

The cellular toxicity and anti-influenza activity of different *A. mollis* extracts were evaluated using the crystal violet assay after incubating MDCK cells with the extract only or the extract and virus (A/WSN/33) for 48 h. All extracts inhibited influenza virus replication and had different levels of cytotoxicity (data not shown). *A. mollis* alkaline extract showed the highest anti-influenza activity. Alkaline extraction of plant materials has been shown to improve the extraction efficiency of hydrophilic compounds (16). The selectivity index of the alkaline

extract was 42 in contrast to 25 of the water extract at RT (Table 1). The alkaline extract was not cytotoxic at concentrations of $< 2.5\%$ ($CC_{50} = 5\%$, Figure 1). Influenza virus replication was inhibited at non-cytotoxic concentrations with an IC_{50} of 0.12%. The alkaline extract of *A. mollis* was used in subsequent experiments to elucidate its inhibitory mechanism on influenza virus replication.

3.2. Sensitivity of other influenza A strains to *A. mollis* extract

The effect of *A. mollis* extract on the replication of influenza A virus strains A/WSN/33 (H1N1), A/PR/8/34 (H1N1), A/HK/8/68 (H3N2), and A/duck/Pennsylvania/84 (H5N2) was evaluated using the crystal violet assay. Infections with A/PR/8/34 (H1N1), A/HK/8/68 (H3N2), and A/Duck Pennsylvania/84 (H5N2) were performed in the presence of 2.5 $\mu\text{g/mL}$ trypsin. The extract suppressed replication of the four strains in a dose-dependent manner, although there was a slight difference in sensitivity between the strains (Table 2). These findings indicate that the antiviral activity of *A. mollis* extract is strain-independent.

3.3. Mechanism of action of *A. mollis* extract

Plaque formation assays with different cells and/or virus treatments were performed to determine the mode of action of *A. mollis* extract. Treatment of MDCK cells with either *A. mollis* extract or zanamivir (100 nM) for

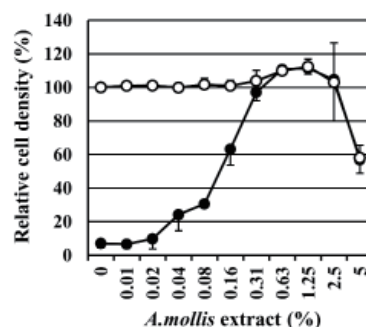


Figure 1. Cytotoxicity and anti-influenza activity of *A. mollis* alkaline extract. MDCK cells (3×10^4 cells/well) in a 96-well culture plate treated with serial dilutions of *A. mollis* extract were incubated at 37°C for 48 h in the presence (closed circles) or absence (open circles) of virus inocula. Results are represented as the mean percentage relative cell density from three independent experiments \pm SD.

Table 2. Sensitivity of different influenza A virus strains to *A. mollis* extract

Virus strain	^a IC_{50} (%)	^b SI
A/WSN/33 (H1N1)	0.12 \pm 0.02	42
A/PR/8/34 (H1N1)	0.15 \pm 0.05	33
A/HK/8/68 (H3N2)	0.08 \pm 0.02	63
A/DP/84 (H5N2)	0.10 \pm 0.03	50

^a 50% Virus growth inhibitory concentration; ^b Selectivity index.

1 h at 37°C prior to infection with influenza virus did not inhibit plaque formation (Figure 2A), suggesting that the extract does not interfere with cell receptors for influenza virus. However, plaque formation was reduced by 53% after treatment with 1.6% *A. mollis* extract when the extract or zanamivir (100 nM) and virus were added to the cells at the same time (Figure 2B). When infected cells were overlaid with MEM containing different concentrations of *A. mollis* extract or zanamivir (100 nM), plaque formation was significantly inhibited in a dose-dependent manner. Plaque formation was reduced by 32%, 51%, and 92% in the presence of 0.1%, 0.4%, and 1.6% *A. mollis* extract, respectively, suggesting that the extract inhibited influenza virus infectivity. Furthermore, no plaques were observed in the presence of zanamivir, which blocks the release of progeny virions from infected cells (Figure 2C). Next, we examined the effect of virus exposure to *A. mollis* extract prior to infection. Influenza virus particles (6×10^6 pfu) were incubated with different concentrations of the *A. mollis* extract or zanamivir (100 nM) at RT for 1 h or 3 h and then diluted (300 pfu/mL) for the plaque formation assay.

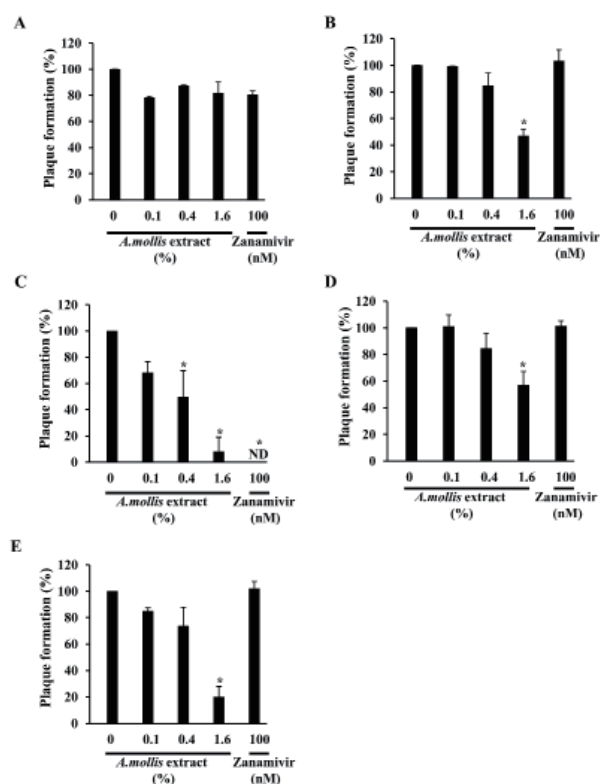


Figure 2. Effect of *A. mollis* extract and zanamivir on plaque formation. Plaque formation assays were carried out as described in the "Materials and Methods" section. (A) Treatment of cells prior to infection. (B) Treatment of cells during virus infection. (C) Treatment of cells after virus infection. (D) Treatment of virus prior to infection at RT for 1 h. (E) Treatment of virus prior to infection at RT for 3 h. The results are presented as the percentage of plaques formed in each treatment relative to the plaques formed in untreated controls, an average of 160 plaques. The results are represented as the mean \pm SD obtained from three independent experiments. * indicates statistical significance ($p < 0.05$, Student's *t* test).

A significant reduction in plaque formation was observed after incubation with 1.6% *A. mollis* extract (Figure 2D and 2E), indicating that the extract directly affects virus particles. Collectively, these results suggest that the inhibitory effect of *A. mollis* extract is due to a direct virucidal or neutralizing activity of the extract against influenza virus particles.

3.4. Inhibition of hemagglutination by *A. mollis* extract

The results of the plaque reduction assay suggest that *A. mollis* extract inhibits influenza virus particle infectivity. It is well known that influenza virus hemagglutinin (HA) plays an essential role in virus infection. Influenza A virus HA can bind to *N*-acetylneuraminic acid on the surface of RBCs, causing agglutination. Thus, to examine whether *A. mollis* extract blocks the ability of virus particles to bind to cell receptors, we performed an HI assay. Influenza A viruses A/WSN/33, A/HK/8/68, and A/duck/Pennsylvania/84 were pretreated with the extract for 1 h before the addition of RBCs and further incubation at RT for 1 h. *A. mollis* extract inhibited binding of the three strains to RBCs in a concentration-dependent manner, indicating that the extract directly acts on influenza virus particles (Figure 3A). Moreover, sodium bicarbonate solution (1%, w/v), an extraction solvent for *A. mollis*, did not inhibit the hemagglutination activity of A/WSN/33 virus particles (Figure 3B).

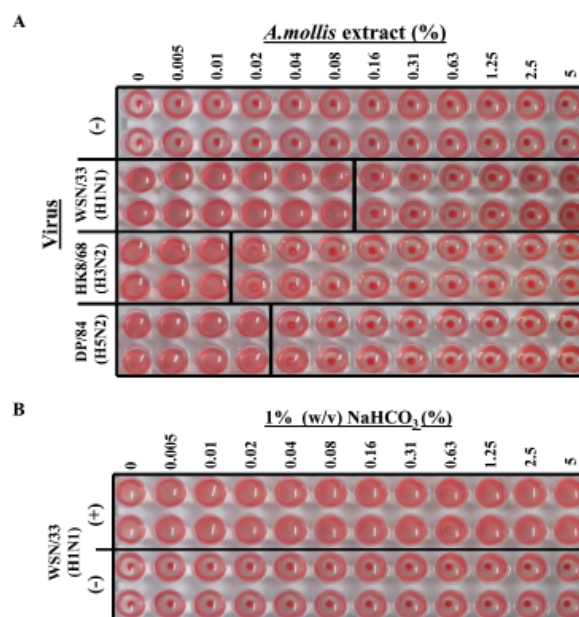


Figure 3. Hemagglutination inhibition assay. (A) *A. mollis* extract was diluted as indicated in 96-well micro titer plates using (PBS) (-). Fifty microliters of virus diluted in (PBS) (-) were added to 50 μ L of the extract dilutions and incubated for 1 h at 4°C. Chicken RBCs (5% v/v) in (PBS) (-), were mixed with the pre-treated virus and incubated again at RT for 1 h. (B) The hemagglutination inhibition activity of 1% (w/v) NaHCO₃ was tested in a similar manner.

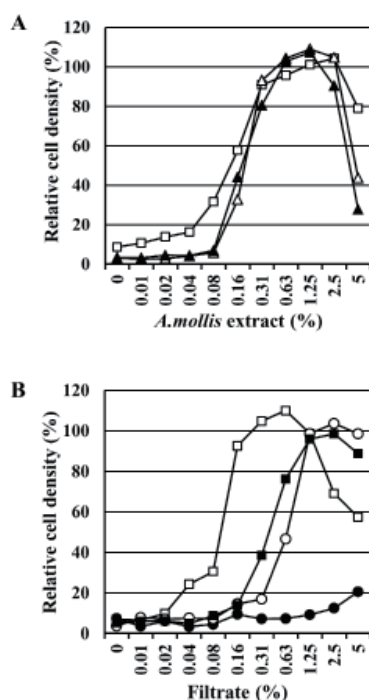


Figure 4. Heat treatment and ultra filtration of *A. mollis* extract. (A) *A. mollis* extracts heat-treated at 60°C (open triangles) or 100°C (closed triangles) and untreated control (open squares) were examined for anti-influenza activity (A/WSN/33) using the crystal violet assay. (B) Similarly, filtrates from 10 kDa (closed circles), 30 kDa (open circles), 50 kDa (closed squares) filter units and unfiltered control (open squares) were tested for antiviral activity. The percentage cell viability of infected cells was calculated relative to uninfected controls.

3.5. Thermal stability and molecular size of *A. mollis* active ingredient(s)

To determine the properties of the active ingredient(s) present in *A. mollis* extract, heat treatment and ultra-filtration of the extract were performed. Heat stability was determined by heating the extract at 60°C or 100°C for 30 min prior to testing for antiviral activity. Figure 4A shows that heat-treated and untreated extracts showed similar antiviral activities, suggesting that the active ingredient(s) of the extract are heat stable. Additionally, the molecular weight of active ingredient(s) in the extract was determined. Filtrates from 10, 30, and 50 kDa ultra-filtration columns and unfiltered control were tested for antiviral activity. The 10-kDa filtrate did not have antiviral activity, whereas the 30- and 50-kDa filtrates did, although they were less potent than the unfiltered control (Figure 4B). This can be explained by the fact that compounds with molecular weights close to the nominal molecular weight limit of the column may be partially retained. These results indicate that the active ingredient(s) in the extract have molecular weights greater than 10 kDa and less than 30 kDa.

3.6. Synergistic effect of zanamivir and *A. mollis* extract combination

Zanamivir and *A. mollis* extract have different mechanisms

Table 3. Interaction index at 50% inhibitory activity

<i>A. mollis</i> extract (%)	Zanamivir (nM)	Interaction index
0.01	2.2	0.36
0.02	2.2	0.44
0.04	1.4	0.51
0.08	0.6	0.74

of action. Zanamivir blocks the release of progeny virions from infected cells, while *A. mollis* extract inhibits the infectivity of influenza particles. Therefore, a combination study was performed to determine the effect of zanamivir and *A. mollis* extract co-treatment on influenza virus replication. The inhibitory effect of zanamivir against influenza virus increased in the presence of the extract. Using the isobole method, the interaction index at 50% inhibitory activity was calculated to determine whether the observed effect was additive or synergistic. Table 3 shows that different zanamivir and extract combinations had interaction indices of < 1, indicating synergistic effects. Increasing extract concentrations decreased synergism, and maximal synergy (interaction index = 0.36) was observed in the 0.01% *A. mollis* extract and 2.2 nM zanamivir combination.

4. Discussion

In this study, we demonstrated the anti-influenza activity of *A. mollis* extract. We found that the extract acts on influenza virus particles directly and inhibits their infectivity. Plaque assays where drugs are added to the overlay gels are one of the most reliable methods for screening compounds with antiviral activity. When infected confluent MDCK cell monolayers were overlaid with 0.8% agarose in MEM containing *A. mollis* extract, plaque formation by the A/WSN/33 virus was significantly inhibited. Exposure of the virus to the extract prior to infection and treatment of the cells during infection significantly reduced plaque formation, whereas pre-treatment of the cells did not affect plaque formation. Further, *A. mollis* extract inhibited the hemagglutination ability of influenza virus. Therefore, it is conceivable that the inhibitory effect of the extract is a result of its direct interaction with the virus. *A. mollis* extract was effective against four different strains of influenza A virus with slight differences in sensitivity, suggesting that the extract may be a wide range inhibitor against influenza virus infections. We also showed a synergistic effect on influenza virus replication when zanamivir and *A. mollis* extract were used in combination.

Alchemilla species extracts have significant radical scavenging activity because of their high levels of flavonoid glycosides and tannins. In addition to other biological activities, the flavonoid glycosides isoquercitrin, miquelianin, and hyperoside present in *A. mollis* (10) have demonstrated anti-influenza activity (17-19). However, antiviral activity of *Alchemilla*

species-derived flavonoid glycosides has not been reported. Flavonoid glycosides are soluble in water and alcohols, and if the aglycone has a free phenolic group, the compound is soluble in alkaline solutions (20), unlike most tannins, which are unstable in alkaline conditions. Since an alkaline extraction method was used to produce the *A. mollis* extract in this study, it is possible that the active ingredient(s) in the extract could be flavonoid glycosides. Moreover, most flavonoids exist as glycosides or polymers and are thermo stable (21); this is in agreement with our findings that the active ingredient(s) in *A. mollis* extract have molecular weights between 10 and 30 kDa and exhibit thermal stability.

Synergistic interactions are being widely studied in phytomedicine. The presence of many bioactive constituents and their by-products in plant extracts is claimed to be responsible for the high effectiveness of many extracts. Synergistic effects are produced when extract constituents affect different targets or interact with one another to improve the solubility and thereby increase the bioavailability of one or several substances in the extract (22). Combination therapy with a highly active antiretroviral treatment regimen has proven to be quite effective in HIV management and in drug resistance reduction (23). The combination of currently available anti-influenza drugs showed the potential for additive or synergistic antiviral activity and inhibition of drug resistance in *in vitro* and *in vivo* studies. These reports point out the benefits of combination therapy. Furthermore, a combination of drugs can also reduce side effects.

In conclusion, we have demonstrated the anti-influenza activity of *A. mollis* by direct association with influenza virus particles. In addition, the inhibitory effect of *A. mollis* was shown to be strain-independent. Because *Alchemilla* plants (lady's mantle) is available as an herbal tea (Lady's Mantle Herbal Tea bags, Alchemilka Herba Alchemillae) it could easily be used for influenza infection management together with zanamivir. Collectively, these findings indicate that *A. mollis* could be a potential anti-influenza agent, although more studies are necessary to confirm its anti-influenza effect *in vivo*.

Acknowledgements

We thank Dr. Avni Kuru (University of Istanbul) for providing us with *Alchemilla mollis* plant material. This work was partly supported by the Global Center of Excellence Program of Nagasaki University.

References

- Hayden FG. Antiviral resistance in influenza viruses - Implications for management and pandemic response. *N Engl J Med*. 2006; 354:785-788.
- Stephenson I, Democratis J, Lackenby A, McNally T, Smith J, Pareek M, Ellis J, Bermingham A, Nicholson K, Zambon M. Neuraminidase inhibitor resistance after oseltamivir treatment of acute influenza A and B in children. *Clin Infect Dis*. 2009; 48:389-396.
- Kiso M, Mitamura K, Sakai-Tagawa Y, Shiraishi K, Kawakami C, Kimura K, Hayden G, Sugaya N, Kawaoka Y. Resistant influenza A viruses in children treated with oseltamivir: descriptive study. *Lancet*. 2004; 364:759-765.
- Kitazato K, Yifei W, Kobayashi N. Viral infectious disease and natural products with antiviral activity. *Drug Discov Ther*. 2007; 1:14-22.
- Liu G, Xiang F, Guo W, Ge F, Yang R, Zhang J, Wang F, Kitazato K. Antiviral activity and possible mechanisms of action of pentagalloylglucose (PGG) against influenza A virus. *Arch virol*. 2011; 156:1359-1369.
- Haruyama T, Nagata K. Anti-influenza virus activity of *Ginkgo biloba* leaf extracts. *J Nat Med*. 2012; 67:636-642.
- Leila G, Wei Z, Zhenping C, Koji W, Mehran H. Oligonol a low molecular weight polyphenol of lychee fruit extract inhibits proliferation of influenza virus by blocking reactive oxygen species-dependent ERK phosphorylation. *Phytomedicine*. 2010; 17:1047-1056.
- Watanabe K, Takatsuki H, Sonoda M, Tamura S, Murakami N, Kobayashi N. Anti-influenza viral effects of novel nuclear export inhibitors from Valerianae Radix and *Alpinia galanga*. *Drug Discov Ther*. 2011; 5:26-31.
- Amazon.co.uk. Lady's Mantle herbal Tea bags Alchemilka Herba Alchemillae. <http://www.amazon.co.uk/Ladys-Mantle-Herbal-Alchemilka-Alchemillae/dp/B009JFOKVM> (accessed September 19, 2013).
- Trendafilova A, Todorova M, Nikolov M, Gavrilova A, Vitkova A. Flavonoid constituents and free radical scavenging activity of *Alchemilla mollis*. *Nat Prod Commun*. 2011; 6:1851-1854.
- Trendafilova A, Todorova M, Gavrilova A, Vitkova A. Flavonoid glycosides from Bulgarian endemic *Alchemilla achtarowii* Pawl. *Biochem Syst Ecol*. 2012; 43:156-158.
- Agostino M, Ramundo E, Senatore F. Flavonoid glycosides of *Alchemilla vulgaris* L. *Phytother Res*. 1998; 12:162-163.
- Bisset G. Lady's mantle in herbal drugs and phytopharmaceuticals. *Medpharm Scientific Publishers*. 1994; 52-54.
- Ehrhardt C, Korte V, Mazura I, Droebner K, Poetter A, Schmolke M, Planz O, Ludwig S. A polyphenol rich plant extract, CYSTUS052, exerts anti influenza virus activity in cell culture without toxic side effects or the tendency to induce viral resistance. *Antiviral Res*. 2007; 76:38-47.
- Tallarida RJ. The interaction index: A measure of drug synergism. *Pain*. 2002; 98:163-168.
- Nakano M, Mizuno T, Nakashima H. Polysaccharide from *Aspalathus linearis* with strong anti-HIV activity. *Biosci Biotech Biochem*. 1997; 61:267-271.
- Kim Y, Narayanan S, Chang KO. Inhibition of influenza virus replication by plant-derived isoquercetin. *Antiviral Res*. 2010; 88:227-235.
- Dongsheng F, Chao Z, Huaguo C, Yang Z, Xiaojian G. Anti-inflammatory, antiviral and quantitative study of quercetin-3-O-β-D-glucuronide in *Polygonum perfoliatum* L. *Fitoterapia*. 2011; 82:805-810.
- Assen P, Lidija S, Julia S. Biologically active constituents of a polyphenol extract from *Geranium sanguineum* L. with anti-influenza activity. *Z Naturforsch*. 2006; 61:508-516.

20. Danylo Halytskyi LVIV National Medical University. Department of Pharmacognosy and Botany. <http://vidverto.info/index.files/Page5815.htm> (accessed September 20, 2013).
21. Borghetti G, Carini P, Honorato B, Ayala A, Moreira J, Bassani L. Physicochemical properties and thermal stability of quercetin hydrates in the solid state. *Thermochim Acta.* 2012; 539:109-114.
22. Wagnera H, Ulrich G. Synergy Research: Approaching a new generation of phytopharmaceuticals. *Phytomedicine.* 2009; 16:97-110.
23. Gulick R. Combination therapy for patients with HIV-1 infection: the use of dual nucleoside analogues with protease inhibitors and other agents. *AIDS.* 1998; 12:17-22.

(Received October 7, 2013; Accepted October 19, 2013)

Effect of Celergen, a marine derivative, on *in vitro* hepatocarcinogenesis

R. Catanzaro¹, N. Zerbinati², U. Solimene³, G. Celep⁴, F. Marotta^{5,*}, A. Kushugulova⁶, M. Milazzo¹, C. Tomella⁵, G. Bertuccelli⁵, Z. Zhumadilov⁶

¹ Department of Internal Medicine, Gastroenterology Division, University of Catania, Catania, Italy;

² CMP Medical Center & Laboratories, Pavia, Italy;

³ WHO-cntr for Traditional Medicine & Biotechnology, University of Milano, Milano, Italy;

⁴ Gazi University, Faculty of Family and Consumer Sciences Department, Nutrition and Food Technology Division, Ankara, Turkey;

⁵ ReGenera Research Group for Aging-Intervention, Milano, Italy;

⁶ Center for Life Sciences, Nazarbayev University, Astana, Kazakhstan.

ABSTRACT: The aim of this study was to test for a potential anticarcinogenic effect of Celergen, a marine derivative devoid of traceable amounts of inorganic arsenic, on cell proliferation, cell cycle progression and apoptosis in the HepG2 human liver cancer cell line. Celergen significantly inhibited the proliferation of cancer cells in a dose-dependent manner while limiting the cell cycle progression at the G1 phase and significantly inducing apoptosis. Further examination showed that Celergen enhanced expression of the *p21^{CIP1/WAF1}*, *GADD153* genes and downregulated the *c-myc* gene. These results suggest that Celergen exerts promising chemopreventive properties to be further investigated.

Keywords: Antimutagenic effect, cell cycle, apoptosis, celergen, marine compound

1. Introduction

Marine derivatives, with their immense diversity and selection driven along millions of years of evolution may offer promising options for new drug discovery (1-5). In particular, several marine bioactive compounds are under study for their potential antitumor effect (6-9). Although the detailed mechanisms involved are still a matter of study, antioxidative and antimutagenic properties have been advocated for (10-12). We have recently shown that Celergen, a popular GMP-controlled marine bioceutical, could significantly inhibit ultraviolet (UV)-induced matrix-metalloproteinases (MMP) transcription and exert an antioxidant effect protecting skin fibroblasts (13). On the other hand, most recently the same food

supplement has been vaguely suggested to be implicated in a case report in which the user showed increased levels of α -fetoprotein (14). Although this report suffers some limitations and a possible major methodological flaw, the issue deserved further clarification, given that several herbal supplements, once believed as safe or even claimed to be "liver protectors" have been recently shown to be potentially hepatotoxic or even mutagenic (15-18). Thus, the aim of the present study was to test the novel biomarine derivative Celergen on *in vitro* liver carcinogenesis.

2. Materials and Methods

2.1. Chemicals

Celergen was obtained from Swisscap company (100 mg composition: DNA extract from fish milt 46 mg, fish collagen hydrolysate plus fish elastin 35 mg, whole fish protein hydrolysate 6 mg, lutein-coenzyme Q10-selenium 11 mg). As a pre-requisite, samples were blindly sent to an official Good Manufacturing Practice and Good Laboratory Practice registered toxicology laboratory which found no traceable amounts of heavy metals including organic and inorganic arsenic, having set a threshold of > 5 ppm (Redox Lab, Monza, Italy, report n. 2013001054/LAB). 7,12-Dimethylbenz[a]anthracene (DMBA) and 12-Q-tetradecanoylphorbol-13 acetate (TPA) were obtained from Sigma-Aldrich Corp. (St. Louis, MO, USA). 4-Nitroquinoline I-oxide (4NQO) was obtained from Nacalai Tesque Co. (Kyoto, Japan).

2.2. *In vitro* analysis of cell growth

Human liver cancer cell line HepG2 were cultured in DMEM supplemented with 10% fetal bovine serum and incubated at 37°C in a humidified atmosphere of 5% CO₂ in air. HepG2 cells were then seeded at a density of 4×10^4 cells/2 mL medium in 35-mm diameter

*Address correspondence to:

Dr. F. Marotta, Piazza Firenze, 12, 20154 Milano, Italy.
E-mail: fmarchimede@libero.it

dishes. Celergen were dissolved in tetrahydrofuran (THF) including 0.025% butylhydroxytoluene (BHT, as an antioxidant) and diluted to its final concentration expressed as $\mu\text{g}/\text{mL}$ in each culture dish. An equivalent volume of vehicle (THF + BHT) was added to control dishes and it showed no measurable effect on HepG2 cells. Celergen was added at graded concentrations 1 day following the inoculation. At the 72 h observation, the number of viable cells was counted using a trypan blue dye exclusion methodology.

2.3. Flow cytometry

Cells were plated at a density of 1×10^6 cells/10 mL medium in 100 mm diameter dishes. Celergen was added 1 day after the inoculation. Cells were harvested from culture dishes by trypsinization and centrifugation. After a wash with phosphate buffered solution (PBS) (-), cells were suspended in a 0.1% Triton X-100 solution. After the suspension was filtered through 50 μm nylon mesh, 0.1% RNase A and 50 $\mu\text{g}/\text{mL}$ propidium iodide were added to stain DNA. The DNA content in stained nuclei was analyzed by a flow cytometer (FACS Calibur™, Becton-Dickinson, Franklin Lakes, NJ, USA). The percentage distribution of cells in each cell cycle phase was determined using ModFit LT™ software (Becton-Dickinson) based on DNA histograms. Five separate experiments were used each time to determine the final values.

2.4. Isolation of total RNA

HepG2 cells were plated at a density of 1×10^6 cells/10 mL medium in 100 mm diameter dishes. Celergen was added 24 h after the inoculation. Total RNA was isolated from the cells at pre-fixed times in the absence or presence of Celergen using RNeasyR Kit (QIAGEN GmbH, Hilden, Germany). Briefly, total RNA was adsorbed onto a silica membrane following cell lysis. Membranes were subsequently washed and RNA was eluted with 50/11 of RNase-free water. Final RNA concentrations were assessed by spectrophotometry.

2.5. Real-time quantitative RT-PCR

Total RNA was isolated from HepG2 cells as described above. Total RNA (5 μg) was transcribed to cDNA in a 20 μL reaction volume, with Superscript II Reverse transcriptase (Invitrogen Corp., Carlsbad, CA, USA), using oligo (dT) 12-18 primers. The reaction mixture was incubated at 42°C for 50 min, then at 70°C for 15 min. An equivalent volume of cDNA solution was used for the quantification of specific cDNA by real-time quantitative RT-PCR. The primer sequences used were as follows: for the *p21^{CIP1/WAF1}* gene (318 bp), 5'-ATTAGCAGCGGAACAAGGAGTCAGACAT3' and 5'-CTGTGAAAGACACAGAACAGT

ACAGGGT-3', for *GADD153* (309 bp), 5'GAAACGGAAACAGAGTGGTCATTCCCC-3' and 5'-GTGGGATTGAGGGTCACATCATTGGCA-3', for *c-myc* (209 bp), 5'-GGCAAAGGTCAGAGTCTGG-3' and 5'-GTGCATTTTCGGTTGTTGC-3', for *glyceraldehyde 3-phosphate dehydrogenase (GAPDH)*, 181 bp), 5'-CAACTACATGGTTTACATGTTC-3' and 5'-GCCAGTGGACTCCACGAC-3'. Real-time quantitative RT-PCR was performed with the LightCycler™ system (Roche Diagnostics GmbH, Mannheim, Germany) using a SYBR Green I Kit as instructed by the manufacturer. *GAPDH*, *p21^{CIP1/WAF1}* and *GADD153* were amplified with a pre-cycling hold at 95°C for 10min, followed by 30 cycles of denaturation at 95°C for 15 s, annealing at 58°C for 5 s, and extension at 72°C for 10 s. *c-myc* was amplified with a pre-cycling hold at 95°C for 10 min, followed by 30 cycles of denaturation at 95°C for 15 s, annealing at 63°C for 5 s and extension at 72°C for 10 s. To confirm amplification specificity, the PCR products were subjected to a melting curve analysis. Quantification data were analyzed using LightCycler analysis software. The expression levels of *p21^{CIP1/WAF1}*, *GADD153*, and *c-myc* were normalized to the level of GAPDH mRNA of the same sample.

2.6. Statistical analysis

For statistical analysis "One Way" variance analysis was employed and significance between the experimental and control groups was determined by Bonferroni's method. A difference of $p < 0.05$ was considered significant. Results were expressed as mean \pm S.D.

3. Results

3.1. HepG2 cell proliferation: in vitro effects of Celergen

Treatment of HepG2 cells with Celergen brought about a significant inhibition of human liver cancer cell proliferation in a dose-dependent manner. Three days after the incubation with 25 μM , 50 μM , 100 μM and 200 μM Celergen, HepG2 cell growth decreased to 63, 52, 38 and 27% of the control, respectively. The concentration of Celergen with 50% growth inhibition was calculated as 50 μM (Figure 1).

3.2. Effect of Celergen on G1 arrest and apoptosis in HepG2 cells

The DNA content of HepG2 cells was calculated by flow cytometry analysis to identify whether the growth inhibitory effect of Celergen was determined by specific actions on cell cycle-related events. From DNA histograms it appeared that Celergen enabled a not significant trend increase of the ratio of G1 cells, but most significantly it increased pre-G1 apoptotic cells at

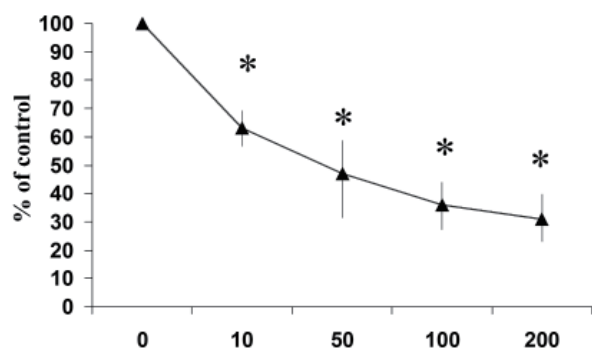


Figure 1. Growth inhibitory effect of Celergen on HepG2 cells. Cells were cultured for 72 h with or without Celergen at concentrations ranging from 25 to 200 μ M. On day 3, the number of viable cells was determined. Data are expressed as means \pm S.D. of three separate experiments.

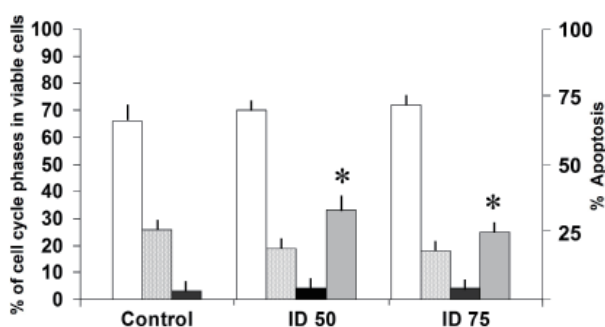


Figure 2. Effect of Celergen on cell cycle and apoptosis in HepG2 cells. HepG2 cells were treated with Celergen at ID 50 or ID 75 for 72 h and stained with propidium iodide to assess DNA content. The percentage of cells in each phase of the cell cycle was assessed by flow cytometric analysis. Data are expressed as means \pm S.D. of five separate experiments. Left vertical line indicates the ratio of each phase in viable cells. Right vertical line indicates the percentage of apoptotic cells. White bars: G1; dotted bars: S; black bars: G2/M and grey bars: apoptosis. * $p < 0.01$ compared with control.

the 72h observation ($p < 0.005$, Figure 2). On the other hand, the effect of Celergen on the cell cycle on days 1 and 2 was not significant (not shown)..

3.3. Gene expression of $p21^{CIP1/WAF1}$, $GADD153$ and $c-myc$ expression: effect of Celergen regulation

The effects of Celergen on the expression of cell cycle and apoptosis-related genes were examined using real-time quantitative RT-PCR. Significant induction of $p21^{CIP1/WAF1}$ and $GADD153$ was clearly observed at 48 h following treatment with Celergen and it was maintained throughout the observation period (72 h) while a significant late downregulation of $c-myc$ occurred as well ($p < 0.01$, Figure 3).

4. Discussion

Celergen is a popular marine derivative containing DNA, collagen elastin and protein extracts and we

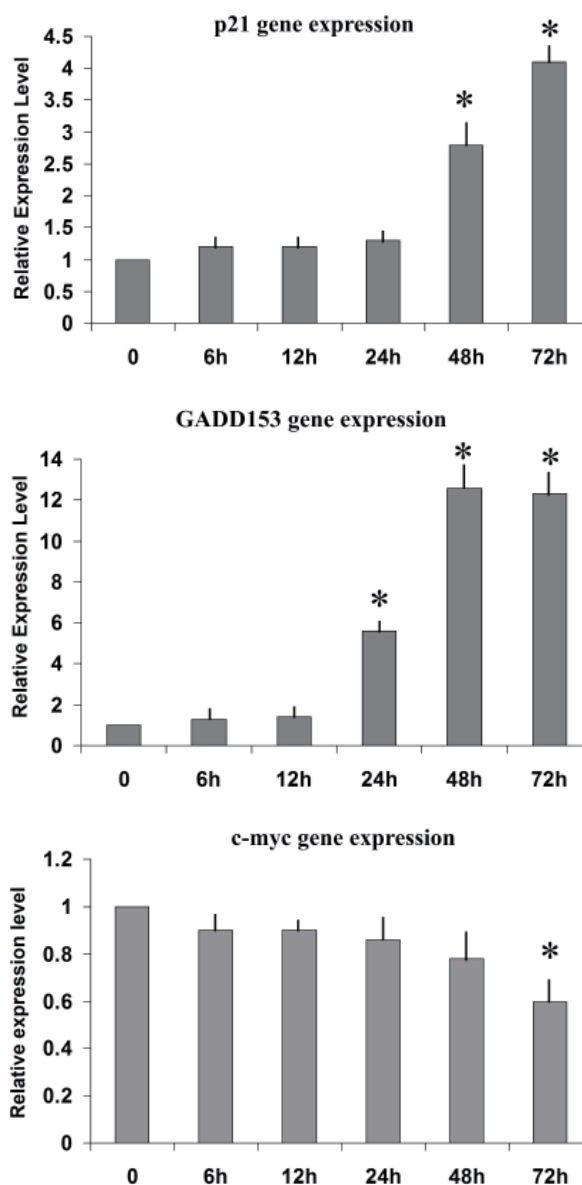


Figure 3. Effect of Celergen on $p21^{CIP1/WAF1}$, $GADD153$, and $c-myc$ mRNA expression. Real-time quantitative RT-PCR was performed with 5 μ g of total RNA from HepG2 cells treated with 50 μ M Celergen or vehicle alone (control) for the test periods indicated. Values are means \pm S.D. of five separate tests. All values were normalized to the GAPDH expression level. * $p < 0.05$ compared with control.

have been recently shown that it exhibits a strong skin fibroblast protecting effect against UV irradiation (13).

In the present study, Celergen was shown to significantly inhibit cell growth *via* induction of G1 arrest of the cell cycle and apoptosis in HepG2 cells. To explore the action mechanism of cell cycle inhibition by Celergen, we assessed the expression of cell cycle and apoptosis related genes and found that the expression of $p21^{CIP1/WAF1}$ and $GADD153$ was significantly induced by Celergen. It is known that $p21^{CIP1/WAF1}$ is significantly induced by DNA damage and regulates the G1 and G2/M checkpoints (19,20) and that the induction of $p21^{CIP1/WAF1}$ usually follows a

p53 dependent mechanism (21). Moreover, *GADD153* and *c-myc* are known to be involved in apoptosis progression. *GADD153* is a member of the CCAAT/enhancer-binding protein family of transcription factors and its expression is markedly enhanced by various cellular stresses (22,23). On the other hand, *c-myc* is a proto-oncogene and is implicated in various processes including cell growth, proliferation and cell death (24). In particular, the overexpression of *c-myc* represents a genetic abnormality frequently found in hepatocellular carcinoma (HCC) (25). Indeed, the relevance of *c-myc* expression in HCC has been confirmed in transgenic mice studies (26) and in clinics where overexpression of this gene is detected in most HCC patients while correlating also with poor prognosis (27). In our study, the induction of p21^{CIP1/WAF1} and *GADD153* occurred significantly at 48 h after treatment with Celergen and subsequently, an increase in G1 phase and apoptotic pre-G1 cells was observed at 72 h. However, *c-myc* showed a late but significant downregulation. Since p53 is known to be functional in HepG2 cells, p21^{CIP1/WAF1} is likely to have been induced by a mechanism which depends on p53 and may be implicated in G1 arrest exerted by Celergen. Nonetheless, the induction of apoptosis by Celergen may be caused by *GADD153* and has to be considered as well.

In summary, our data suggest that Celergen inhibits the proliferation of HepG2 cells and induces G1 arrest and apoptosis. The induction was associated with enhanced expression of p21^{CIP1/WAF1}, *GADD153* but suppression of *c-myc*. These results suggest that such marine compounds may have anticarcinogenic properties while more finely-detailed proteomic studies are awaited. This data is in contrast with the albeit isolated clinical report of Chua *et al.* (14) suggesting an arsenic-related hepatocarcinogenesis effect of the same compound. However, that study bears the main methodological bias in that the authors measured the whole arsenic content, while the literature has clearly demonstrated that only the inorganic component is the one with the noxious effect (28) and the only one deserving monitoring from major epidemiological studies (29,30). On the contrary, the organic one is regarded as safe (31) and its concentration may also vary (32) as probably occurred in their study. For instance, seafood and seaweeds generally contain almost completely nontoxic organic arsenic such as arsenosugars (33). Thus, their suggestion cannot be supported and their observed abnormality of α -fetoprotein observed in their case report has to be correlated to other factors (episodic aflatoxin exposure, either environmental or food-borne *etc.*) which have not been analyzed in their report together with the lack of a separate measurement of organic and inorganic arsenic content. From the above, the study of Chua *et al.* has to be disregarded similarly because of what happened

with a similar case of a different seafood compound after review by a number of experts in the field (34-36). While our study needs further research and *in vivo* follow up, our general conclusion is that marine derivatives, if properly farmed, collected and processed maintain a promising potential as a safe source of beneficial treatment.

References

- Lorenzetti A, Marotta F, Yadav H, Celep G, Minelli E, Carrera-Bastos P, Jain S, Polimeni A, Solimene U. Improving sperm quality and spermatogenesis through a bioactive marine compound: An experimental study. *Acta Biomed.* 2012; 83:108-113.
- Catanzaro R, Marotta F, Jain S, Rastmanesh R, Allegrì F, Celep G, Lorenzetti A, Polimeni A, Yadav H. Beneficial effect of a sturgeon-based bioactive compound on gene expression of tumor necrosis factor- α , matrix metalloproteinases and type-10 collagen in human chondrocytes. *J Biol Regul Homeost Agents.* 2012; 26:337-345.
- Newman DJ, Cragg GM. Marine natural products and related compounds in clinical and advanced preclinical trials. *J Nat Prod.* 2004; 67:1216-1238.
- Cabrita MT, Vale C, Rauter AP. Halogenated compounds from marine algae. *Mar Drugs.* 2010; 8:2301-2317.
- Newman DJ, Cragg GM. Advanced preclinical and clinical trials of natural products and related compounds from marine sources. *Curr Med Chem.* 2004; 11:1693-1713.
- Simmons TL, Andrianasolo E, McPhail K, Flatt P, Gerwick WH. Marine natural products as anticancer drugs. *Mol Cancer Ther.* 2005; 4:333-342.
- Singh R, Sharma M, Joshi P, Rawat DS. Clinical status of anti-cancer agents derived from marine sources. *Anticancer Agents Med Chem.* 2008; 8:603-617.
- Provencio M, Sánchez A, Gasent J, Gómez P, Rosell R. Cancer treatments: Can we find treasures at the bottom of the sea? *Clin Lung Cancer.* 2009; 10:295-300.
- Jimeno J, López-Martín JA, Ruiz-Casado A, Izquierdo MA, Scheuer PJ, Rinehart K. Progress in the clinical development of new marine-derived anticancer compounds. *Anticancer Drugs.* 2004; 15:321-329.
- Tang HG, Wu TX, Zhao ZY, Pan XD. Effects of fish protein hydrolysate on growth performance and humoral immune response in large yellow croaker (*Pseudosciaena crocea* R.). *J Zhejiang Univ Sci B.* 2008; 9:684-690.
- Theodore AE, Raghavan S, Kristinsson HG. Antioxidative activity of protein hydrolysates prepared from alkaline-aided channel catfish protein isolates. *J Agric Food Chem.* 2008; 56:7459-7466.
- Yang Y, Zhang Z, Pe, X, Han H, Wang J, Wang L, Long Z, Shen X, Li Y. Immunomodulatory effects of marine oligopeptide preparation from Chum Salmon (*Oncorhynchus keta*) in mice. *Food Chem.* 2009; 113:464-470.
- Marotta F, Kumari A, Yadav H, Polimeni A, Soresi V, Lorenzetti A, Naito Y, Jain S. Biomarine extracts significantly protect from ultraviolet A-induced skin photoaging: An *ex vivo* study. *Rejuvenation Res.* 2012; 15:157-160.
- Chua C, Tan IB, Choo SP, Toh HC. Increased

- α -fetoprotein likely induced by complementary health products. *J Clin Oncol.* 2013; 31:e80-82.
15. Navarro VJ, Bonkovsky HL, Hwang SI, Vega M, Barnhart H, Serrano J. Catechins in dietary supplements and hepatotoxicity. *Dig Dis Sci.* 2013; 58:2682-2690.
 16. Teschke R, Schwarzenboeck A, Eickhoff A, Frenzel C, Wolff A, Schulze J. Clinical and causality assessment in herbal hepatotoxicity. *Expert Opin Drug Saf.* 2013; 12:339-366.
 17. Brandon-Warner E, Eheim AL, Foureau DM, Walling TL, Schrum LW, McKillop IH. Silibinin (Milk Thistle) potentiates ethanol-dependent hepatocellular carcinoma progression in male mice. *Cancer Lett.* 2012; 326:88-95.
 18. McCormick DL, Hollister JL, Bagg BJ, Long RE. Enhancement of murine hepatocarcinogenesis by all-trans-retinoic acid and two synthetic retinamides. *Carcinogenesis.* 1990; 11:1605-1609.
 19. Dang CV. *c-Myc* target genes involved in cell growth, apoptosis, and metabolism. *Mol Cell Biol.* 1999; 19:1-11.
 20. Kurland JF, Tansey WP. Myc-mediated transcriptional repression by recruitment of histone deacetylase. *Cancer Res.* 2008; 68:3624-3629.
 21. Dang CV, O'Donnell KA, Zeller KI, Nguyen T, Osthus RC, Li F. The *c-Myc* target gene network. *Semin Cancer Biol.* 2006; 16:253-264.
 22. Liao Y, Fung TS, Huang M, Fang SG, Zhong Y, Liu DX. Up-regulation of CHOP/GADD153 during coronavirus infectious bronchitis virus infection modulates apoptosis by restricting activation of the extracellular signal-regulated kinase pathway. *J Virol.* 2013; 87:8124-8134.
 23. De Luca P, Moiola CP, Zalazar F, Gardner K, Vazquez ES, De Siervi A. BRCA1 and p53 regulate critical prostate cancer pathways. *Prostate Cancer Prostatic Dis.* 2013; 16:233-238.
 24. Zhao Y, Jian W, Gao W, Zheng YX, Wang YK, Zhou ZQ, Zhang H, Wang CJ. RNAi silencing of *c-Myc* inhibits cell migration, invasion, and proliferation in HepG2 human hepatocellular carcinoma cell line: *c-Myc* silencing in hepatocellular carcinoma cell. *Cancer Cell Int.* 2013; 13:23-28.
 25. Lin CP, Liu CR, Lee CN, Chan TS, Liu HE. Targeting *c-Myc* as a novel approach for hepatocellular carcinoma. *World J Hepatol.* 2010; 2:16-20
 26. Cao Z, Fan-Minogue H, Bellovin DI, Yevtodiyanenko A, Arzeno J, Yang Q, Gambhir SS, Felsher DW. MYC phosphorylation, activation, and tumorigenic potential in hepatocellular carcinoma are regulated by HMG-CoA reductase. *Cancer Res.* 2011; 71:2286-2297.
 27. Peng S, Lai P, Hsu H. Amplification of the *c-myc* gene in human hepatocellular carcinoma: biologic significance. *J Formos Med Assoc.* 1993; 92:866.
 28. Huang CY, Su CT, Chung CJ, Pu YS, Chu JS, Yang HY, Wu CC, Hsueh YM. Urinary total arsenic and 8-hydroxydeoxyguanosine are associated with renal cell carcinoma in an area without obvious arsenic exposure. *Toxicol Appl Pharmacol.* 2012; 262:349-354.
 29. Calderon RL, Hudgens EE, Carty C, He B, Le XC, Rogers J, Thomas DJ. Biological and behavioral factors modify biomarkers of arsenic exposure in a U.S. population. *Environ Res.* 2013; 126:134-144.
 30. Osorio-Yáñez C, Ayllon-Vergara JC, Aguilar-Madrid G, Arreola-Mendoza L, Hernández-Castellanos E, Barrera-Hernández A, De Vizcaya-Ruiz A, Del Razo LM. Carotid intima-media thickness and plasma asymmetric dimethylarginine in mexican children exposed to inorganic arsenic. *Environ Health Perspect.* 2013; 121:1090-1096.
 31. Francesconi KA, Edmonds JS. Arsenic and marine organisms. In: *Advances in Inorganic Chemistry*, Vol. 44. 1997; 44:147.
 32. Taylor VF, Jackson BP, Siegfried M, Navratilova J, Francesconi KA, Kirshtein J, Voytek M. Arsenic speciation in food chains from mid-Atlantic hydrothermal vents. *Environ Chem.* 2012; 9:130-138.
 33. Kaise TOY, Ochi T, Okubo T, Hanaoka K, Irgolic KJ, Sakurai T, Matsubara C. Toxicological study of organic arsenic compound in marine algae using mammalian cell culture technique. *J Food Hyg Soc Jpn.* 1996; 37:135-141.
 34. Fabricant D. Arsenic in herbal kelp supplements: concentration, regulations, and labeling. *Environ Health Perspect.* 2007; 115:A574.
 35. Lewis AS. Organic versus inorganic arsenic in herbal kelp supplements. *Environ Health Perspect.* 2007; 115:A575.
 36. McGuffin M, Dentali S. Safe use of herbal kelp supplements. *Environ Health Perspect.* 2007; 115:A575-576.

(Received September 6, 2013; Revised October 10, 2013, Re-revised October 26, 2013; Accepted October 28, 2013)

Preclinical anticancer effects and toxicologic assessment of hepatic artery infusion of fine-powder cisplatin with lipiodol *in vivo*

Toshiya Yamaguchi^{1,*}, Naoko Nakajima¹, Iwao Nakamura¹, Hiroko Mashiba¹, Takashi Kawashiro¹, Keiko Ebara¹, Eiji Ichimura¹, Chihiro Nishimura¹, Kazuya Okamoto¹, Yuh-ichiro Ichikawa¹, Takafumi Ichida²

¹ Pharmaceutical Research Laboratories, Nippon Kayaku Co., Ltd., Tokyo, Japan;

² Department of Gastroenterology and Hepatology, Juntendo University Shizuoka Hospital, Shizuoka, Japan.

ABSTRACT: We conducted an *in vivo* study to evaluate the anticancer effect and toxicity of fine-powder cisplatin suspended in lipiodol (fCDDP/LPD suspension) after a single administration of three different doses to rats *via* the intrahepatic artery after transplantation of rat ascites hepatoma cells. The toxicity of the fCDDP/LPD suspension was also assessed in the same protocol in noncancer-bearing rats and the observed toxicologic changes were compared among groups administered saline (Sal), an aqueous solution of fCDDP (fCDDP/Sal solution), and LPD alone. In parallel with the toxicity test, plasma CDDP concentrations were compared between the fCDDP/LPD suspension and fCDDP/Sal solution. The mean weight of the tumors in the fCDDP/LPD suspension groups was significantly less than in the LPD-alone group. The pathologic changes in the liver observed in the fCDDP/LPD suspension group increased with dose, were more marked compared with those in the fCDDP/Sal solution and LPD-alone groups, and were reversible. No other toxicologic effects were observed. The concentration of CDDP in the plasma in the fCDDP/LPD suspension group was slightly lower than that in the fCDDP/Sal solution group. In conclusion, the results indicate that the fCDDP/LPD suspension has sufficient anticancer efficacy and tolerability for use in the clinical treatment of hepatocellular carcinoma.

Keywords: Hepatocellular carcinoma, fine-powder cisplatin, lipiodol, transcatheter arterial chemoembolization, rats

*Address correspondence to:

Dr. Toshiya Yamaguchi, Pharmaceutical Research Laboratories, Nippon Kayaku Co., Ltd., 31-12, Shimo 3-chome, Kita-ku, Tokyo 115-8588, Japan.

E-mail: toshiya.yamaguchi@nipponkayaku.co.jp

1. Introduction

At present, patients with unresectable or postoperatively recurrent hepatocellular carcinoma are generally treated with transcatheter arterial embolization (TAE) or transcatheter arterial infusion (TAI) of anticancer drugs. There have been numerous reports of excellent therapeutic results when hepatocellular carcinoma patients were administered a suspension of cisplatin (CDDP) in lipiodol (LPD) (1), an oil-soluble iodinated contrast medium that accumulates in liver cancer lesions in proportion to their vascularity (2,3). In the case of TAI, a high drug concentration at the tumor site is essential, requiring administration as close as possible to the tumor. In that context, a fine-powder formulation of CDDP (fCDDP; mean particle diameter: 20-30 μ m) was developed to yield a solution with a high drug concentration. fCDDP was approved for the treatment of hepatocellular carcinoma in Japan in 2004 (4). Subsequently, fCDDP/LPD suspension has been used as a TAI (Lip-TAI) and transcatheter arterial chemoembolization (TACE) agent (5,6). However, no basic studies have been conducted to evaluate the efficacy and safety of Lip-TAI and TACE employing an fCDDP/LPD suspension, and the detailed mechanism of action of this combination therapy is not fully understood. This study was designed to clarify the mechanism as well as to evaluate the degree of fCDDP/LPD and CDDP bulk substance/LPD suspendability.

2. Materials and Methods

2.1. Anticancer effects of fCDDP suspension

2.1.1. Experimental animals

Fifty-seven male Donryu rats at 14 weeks of age (Charles River Japan Co., Ltd., Yokohama, Japan) were used for the study of anticancer efficacy. At 17 to 18 weeks of age, they underwent tumor cell transplantation with AH109A, a rat ascites hepatoma cell line obtained from the

Tohoku University Cell Resource Center for Biomedical Research Institute of Development, Aging and Cancer, Sendai, Japan. The cells were suspended in Matrigel at a concentration of 5×10^6 cells/mL. Transplantation of the AH109 cells was performed by infusing 20 μ L of cell suspension into the parenchyma of the left lateral lobe of the liver of anesthetized (mixed anesthesia using ketamine 37.5 mg/kg and xylazine 5 mg/kg) rats.

Rats with confirmed tumor engraftment without ascites were selected on day 10 following transplantation and then administered the test samples. Handling of the rats and ethical considerations for all experiments were in accordance with the Regulations for Animal Experiments issued by the Committee on Animal Experiments of the Nippon Kayaku Co., Ltd. Pharmaceutical Research Laboratory.

2.1.2. Preparation of test samples

fCDDP (IA-call) was obtained from Nippon Kayaku Co., Ltd. (Tokyo, Japan). The fCDDP/LPD suspensions were prepared by mixing LPD (Lipiodol Ultra-Fluide, Laboratoire Guerbet, Aulnay-sous-Bois, France) with weighed amounts of fCDDP to yield CDDP concentrations of 5, 10, and 20 mg/mL and then suspensions were created in a vortex mixer.

2.1.3. Treatment groups

Three groups of rats ($n = 8$ in each group) received 20 μ L of the fCDDP/LPD suspension with a fCDDP dose of 0.1, 0.2, and 0.4 mg, respectively. Two control groups received LPD alone or saline (Sal). The maximum fCDDP dosage in the fCDDP/LPD suspension groups was 20 mg/mL, corresponding to that used in clinical practice.

2.1.4. Test sample administration

Administration of test samples was performed under the same anesthesia used for tumor transplantation described above. A midline abdominal incision was performed to expose the injection site, the gastroduodenal artery. The test sample was drawn into a microsyringe attached to a polyethylene tube (PE-10, Becton Dickinson & Company, Franklin Lakes, NJ, USA). Then the polyethylene tube was inserted against the blood flow from the gastroduodenal artery, and the test sample was slowly administered so that it would flow into the hepatic artery with the blood.

2.1.5. Observations, measurements, and assessments

The tumors were enucleated carefully from the liver lobe using forceps on day 8 following test sample administration and weighed. The mean tumor weight was calculated for each treatment group, and the results

are shown as mean \pm SD. The tumor weight in each group was analyzed using a nonparametric method. The Dunnett test was used to analyze the anticancer effects in each fCDDP/LPD suspension group versus the LPD-alone group and in the Sal group versus the LPD-alone group. Statistical analyses were performed using the SAS system preclinical package, ver. 5.0.

2.2. Toxicity study of fCDDP/LPD suspension

2.2.1. Experimental animals

Thirty-two male Donryu rats at 10 weeks of age (Charles River Japan Co., Ltd., Yokohama Japan) were used for the study of fCDDP/LPD suspension toxicity. They were quarantined, acclimatized, and used in the experiments at 19 weeks of age, as in the anticancer experiments.

2.2.2. Preparation of test samples

fCDDP/LPD suspensions for use in the toxicity study were prepared at a concentration of 10 mg/mL, as in the anticancer experiments. In addition, fCDDP/Sal solution was prepared at a concentration of 1.43 mg/mL to reflect the dose used in clinical practice.

2.2.3. Treatment groups

The rats were divided into the Sal, fCDDP/Sal solution, LPD-alone, and fCDDP/LPD suspension groups. The fCDDP dosage for the fCDDP/LPD suspension group was 0.2 mg, because the results of the anticancer experiments showed efficacy at this dose. The same dosage was also used in the fCDDP/Sal solution group. The volume administered was 140 μ L for the Sal and fCDDP/Sal solution, reflecting that used in clinical practice (1.43 mg/mL), and 20 μ L (fCDDP concentration: 10 mg/mL) for the LPD-alone and fCDDP/LPD suspension groups. Each group consisted of 8 rats. Four rats were killed and autopsied on days 7 and 28 after the administration of the test samples.

2.2.4. Test sample administration

The test samples were administered to the rats in each group as in the anticancer experiments.

2.2.5. Observations, measurements, and assessments

The general condition including survival was confirmed in the rats in each group for 28 days after the administration of the test samples. Their body weight and food consumption were measured using an electrobalance scale (model PB8001, Mettler, Tokyo, Japan) at baseline and on days 2, 4, 6, 10, 14, 21, and 27 after test sample administration.

After fasting for approximately 16 h on days 7

and 28, the rats were anesthetized with diethyl ether, and blood was drawn from the abdominal aorta into a syringe. Ethylenediaminetetraacetic acid-2K was then added to the collected blood samples. A blood cell analyzer (XT-2000iV, Sysmex Corporation, Kobe, Japan) was used to analyze the following parameters for each specimen: red blood cell count; hemoglobin; hematocrit; white blood cell count, platelet count, reticulocyte count, and differential leukocyte count; corpuscular volume average; corpuscular hemoglobin; and mean corpuscular hemoglobin concentration. In addition, for blood biochemical assessment, heparin was added to blood samples in the same manner as for the hematology analyses. The specimens were then centrifuged (4°C, 1,600 × g, 10 min) to obtain the plasma, which was analyzed for the following using a Hitachi model 7180 autoanalyzer (Hitachi High-Technologies Corporation, Tokyo, Japan): aspartate aminotransferase; alanine aminotransferase; alkaline phosphatase; lactate dehydrogenase; creatine phosphokinase; total bilirubin; direct bilirubin; total cholesterol; triglycerides; phospholipids; total protein; albumin; albumin/globulin ratio; urea nitrogen; creatinine; calcium; glucose; sodium; potassium; and chloride.

After blood sampling for the hematology and blood biochemistry studies on days 7 and 28, the rats were euthanized by exsanguination from the abdominal aorta, and the injection site, heart, lungs, liver, spleen, kidneys, adrenal glands, thymus, testes, pituitary, brain, prostate, submaxillary glands, thyroid, pancreas, esophagus, stomach, duodenum, jejunum, ileum, colon, urinary bladder, epididymis, seminal vesicles, sternum, femur (including bone marrow), spinal cord, mesenteric lymph nodes, mandibular lymph nodes, thigh muscle, sciatic nerve, eyes, hardierian glands, skin, mammary glands, aorta, trachea, and tongue were isolated and inspected macroscopically. Specimens of all organs were prepared to assess histopathologic changes by fixation in 10% phosphate-buffered formalin solution (for the eyes, a mixture of equal volumes of 3% glutaraldehyde and 10% phosphate-buffered formalin solution) and were stained with hematoxylin-eosin.

2.3. Determination of CDDP concentrations in plasma

2.3.1. Experimental animals

Eighteen of the 57 male Donryu rats used for the toxicologic assessment were quarantined, acclimatized, and then used for the determination of CDDP plasma concentration

2.3.2. Preparation of test samples

The fCDDP/LPD suspension and the fCDDP/Sal solution prepared for the toxicologic assessment were used to determine plasma CDDP concentrations.

2.3.3. Treatment groups

Nine rats each from the fCDDP/LPD suspension group and fCDDP/Sal solution group in the toxicologic assessment were used in this study, and the CDDP plasma concentration was measured 5 min, 6 h, and 24 h after test sample administration in 3 rats in each group.

2.3.4. Test sample administration

The test samples were administered to rats in the 4 groups as in the anticancer experiments.

2.3.5. Measurement of CDDP concentration in plasma

The plasma concentrations of total CDDP and protein-unbound (free) CDDP were analyzed. The same rats as used in the toxicokinetic (TK) studies in the fCDDP/Sal and fCDDP/LPD groups were anesthetized with diethyl ether 5 min, 6 h, and 24 h after test sample administration. Blood was collected from the abdominal aorta using a heparin-treated syringe. The blood was centrifuged (4°C, 1,800 × g, 10 min) to separate plasma, and the plasma was chilled on ice. Inductively coupled plasma mass spectrometry was used to measure the total platinum (total Pt) concentration. The protein-unbound platinum (free Pt) concentration in the plasma was analyzed with 1 ml of the plasma ultrafiltered through a Centrifree membrane filter (Millipore, Billerica, MA, USA) (4°C, 1,800 × g, 30 min). The results were converted to the CDDP concentration. The TK parameters ($C_{5\text{min}}$, $AUC_{0-24\text{h}}$) were calculated based on the CDDP concentration using WinNonlin software, ver. 5.2.1 (Pharsight, Mountain View, CA, USA).

2.4. Comparison of suspendability of fCDDP and CDDP bulk substance in LPD

For comparisons of suspendability, CDDP bulk substance was obtained from Nippon Kayaku Co., Ltd. (mean particle diameter: approximately 100 μm). One hundred milligrams of fCDDP and CDDP bulk substance in LPD was weighed and placed in vials, and then 5 mL of LPD was added to each. After vortex mixing, the 5-mL LPD suspensions were drawn into syringes. The syringes were placed in a horizontal position to observe the sedimentation visually over a 10-min period.

2.5. Statistical analyses

The body weight, food consumption, hematologic parameters, and blood biochemical parameters (mean ± SD) were calculated for the LPD-alone, fCDDP/Sal solution, and fCDDP/LPD suspension groups and compared with the Sal control group. The data were first tested for homogeneity of variance using the *F* test, after which a Student's *t*-test (two-sided) was employed in the

case of equal variance, while a Aspin-Welch *t*-test was applied in the absence of unequal variance. Statistical analyses were performed using the Toxi-Win system (SAS statistical package, Sumisho Computer Systems Corporation, Tokyo, Japan). A two-tailed *p* value of less than 0.05 and a *p* value of less than 0.01 were considered to represent statistically significant differences.

3. Results

3.1. Anticancer effects of fCDDP suspension

In the study of anticancer effects, the mean weight of tumors in the LPD group was 0.854 ± 0.875 g, whereas those in the 0.4-, 0.2-, and 0.1-mg fCDDP/LPD suspension groups were 0.198 ± 0.311 g, 0.190 ± 0.263 g, and 0.226 ± 0.134 g, respectively (Figure 1). All tumor

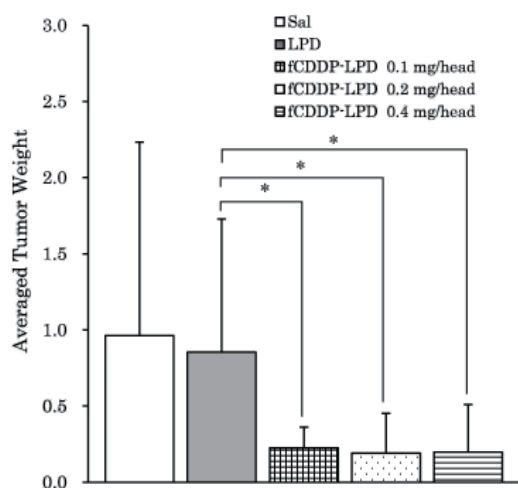


Figure 1. Antitumor activity of fCDDP suspended in LPD against orthotopically allografted rat ascites hepatoma AH109A. Mean tumor weights are shown by each bar. * *p* < 0.05, fCDDP suspended in LPD vs. LPD.

weights in the fCDDP/LPD suspension groups were significantly lower than that in the LPD-alone group, indicating the efficacy of the fCDDP/LPD suspension dosages. There was no difference in tumor weight between the Sal and LPD-alone groups (0.963 ± 1.269 g).

Five deaths occurred during the study of one rat each time, on day 4 in the LPD group, on day 6 in both the Sal and fCDDP/LPD 0.4-mg groups, on day 7 in the fCDDP/LPD 0.4-mg group, and on day 8 in the fCDDP/LPD 0.1-mg group.

3.2. Toxicity study of fCDDP/LPD suspension

In the study examining the toxicity of the fCDDP/LPD suspension, there were no treatment-related deaths or abnormalities among the experimental rats in the Sal, fCDDP/Sal solution, LPD-alone, or fCDDP/LPD suspension groups. Although body weight and food consumption decreased from the day after the test sample administration, both improved several days later. Compared with the Sal group, there were no statistically significant differences between the fCDDP/Sal solution, LPD-alone, and fCDDP/LPD suspension groups. The hematologic assessments performed on days 7 and 28 after test sample administration did not show any statistically significant changes in any experimental group. In addition, the blood biochemistry tests showed no significant changes in any value examined and no liver or kidney damage was observed (Figure 2).

The pathology studies found adhesion of cavity organs in all groups on days 7 and 28. In the histopathologic studies, single-cell necrosis of cholangiocytes and periportal hepatocytes was observed on day 7 in the fCDDP/Sal solution and fCDDP/LPD suspension groups, while cholangiocyte hypertrophy and vacuolation in the interlobular artery were observed in the fCDDP/LPD suspension and LPD-alone groups. Moreover, in

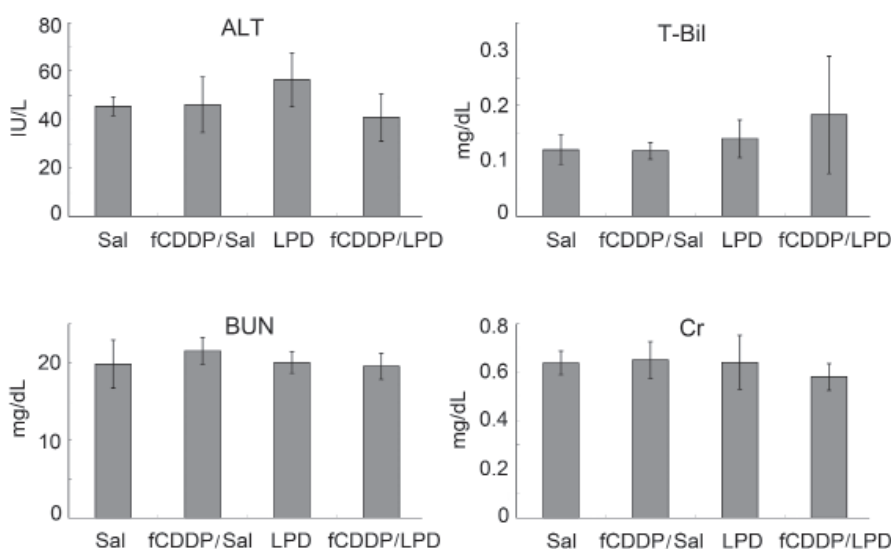


Figure 2. Serum chemistry in male rats after a single intrahepatic artery administration of each test sample.

the fCDDP/LPD group, microgranulomas around the interlobular arteries were also observed (Figure 3).

Granulomas of the gastroduodenal artery injection site and of the hepatic artery were also seen in all experimental groups. On day 28, interlobular artery vacuolation was observed in the fCDDP/LPD suspension and LPD-alone groups, and vacuolar degeneration of hepatocytes was seen in the fCDDP/LPD suspension and fCDDP/Sal solution groups. Microgranulomas were observed around the interlobular arteries except in the Sal group, while granulomas were seen in the gastroduodenal artery injection site and hepatic artery in all groups. In the kidney, regeneration of the tubular epithelium was observed on day 7 in more rats in the fCDDP/Sal solution, LPD-alone, and fCDDP/

LPD suspension groups compared with the Sal group. However, no enhanced effects on the renal tubules in the fCDDP/LPD suspension group were noted. In addition, fewer rats in the fCDDP/Sal solution, LPD-alone, and fCDDP/LPD suspension groups showed abnormal changes on day 28 (Tables 1 and 2). Changes were also observed in the heart, lungs, spleen, pituitary, small intestine, and other organs of these three groups, although they were also seen to some extent in the Sal group. The changes were not considered to be caused by test sample administration.

3.3. Determination of CDDP concentrations in plasma

The results of the study measuring the CDDP plasma

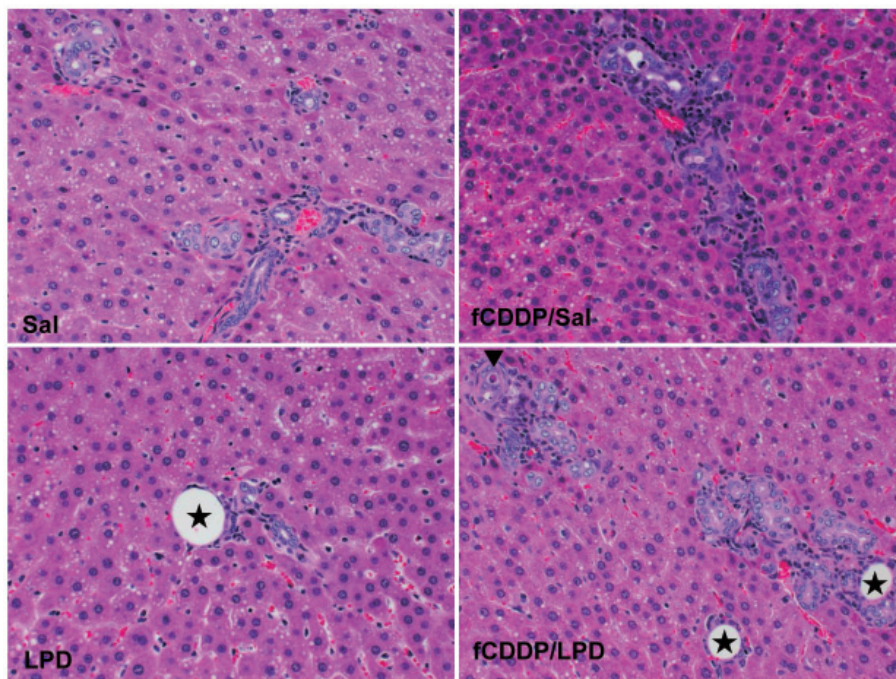


Figure 3. Single-cell necrosis of cholangiocytes (▼) and vacuolation in the interlobular artery (★) in the liver of rats treated with fCDDP/LPD suspension and LPD alone. Original magnification, ×20.

Table 1. Histopathologic findings on day 7

Object of observation	Grade	Number of rats with pathological changes			
		Sal	fCDDP/Sal	LPD	fCDDP/LPD
Liver					
Hypertrophy of cholangiocytes	1+	0	0	4	2
Vacuolation in interlobular artery	1+	0	0	3	4
Microgranuloma around interlobular artery	1+	0	0	0	3
Single-cell necrosis of hepatocytes, periportal	1+	0	0	0	1
Single-cell necrosis of cholangiocytes	1+	0	1	0	2
Microgranuloma in capsule	1+	0	2	2	2
Injection site (hepatic & gastroduodenal arteries)					
Granuloma	1+	2/3	2/3	3	1
Kidney					
Regeneration of tubular epithelium	1+	1	3	4	4
Hyaline casts	1+	0	3	3	3

Grade: 0, none; 1+, mild; 2+, moderate; 3+, severe. The fCDDP dosage for the fCDDP/Sal and fCDDP/LPD suspension group was 0.2 mg, respectively. Four rats were sacrificed and examined in each group.

Table 2. Histopathologic findings on day 28

Object of observation	Grade	Number of rats with pathological changes			
		Sal	fCDDP/Sal	LPD	fCDDP/LPD
Liver					
Microgranuloma around interlobular artery	1+	0	2	2	2
Degeneration of interlobular artery	1+	0	2	0	2
Vacuolation in interlobular artery	1+	0	0	4	4
Microgranuloma in capsule	1+	4	3	4	1
Injection site (hepatic & gastroduodenal arteries)					
Granuloma	2+	3/3	1/3	0	3
	1+	0/3	0/3	1	1
Kidney					
Regeneration of tubular epithelium	1+	0	2	1	3
Hyaline casts	1+	0	0	2	1

Grade: 0, none; 1+, mild; 2+, moderate; 3+, severe. The fCDDP dosage for the fCDDP/Sal and fCDDP/LPD suspension group was 0.2 mg, respectively. Four rats were sacrificed and examined in each group.

concentrations in the four experimental groups showed that the mean concentrations in the fCDDP/Sal solution group were 1,290 ng/mL at C_{5min} , which decreased to 114 ng/mL 6 h and to 101 ng/mL 24 h after administration. In the fCDDP/LPD suspension group, the corresponding values were 942 ng/mL, 99.9 ng/mL, and 67.8 ng/mL, respectively. In addition, the AUC_{0-24h} value was 6,200 $ng^{-1} h/mL$ in the fCDDP/Sal solution group and 4,670 $ng^{-1} h/mL$ in the fCDDP/LPD suspension group. Therefore these two groups had similar TK parameters.

On the other hand, the mean CDDP concentrations in the ultrafiltered plasma (free CDDP concentrations) were 729 ng/mL at C_{5min} and 2.22 ng/mL at 24 h, with an AUC_{0-24h} value of 2,300 $ng^{-1} h/mL$ in the fCDDP/Sal solution group. In the fCDDP/LPD suspension group, the respective values were 649 ng/mL, 1.21 ng/mL, and 2,030 $ng^{-1} h/mL$, which were similar to those in the fCDDP/Sal group (Figure 4). However, all TK parameters in the fCDDP/LPD suspension group were lower than those in the fCDDP/Sal solution group at each time point measured (Table 3).

3.4. Comparison of suspendability of fCDDP and CDDP bulk substance in LPD

When the sedimentation rate of the fCDDP and CDDP bulk substance in LPD in syringes was examined, it was found that the CDDP bulk substance rapidly began to sink to the bottom of the horizontal syringe, and nearly complete sedimentation occurred within 3 min. In contrast, the sedimentation rate of fCDDP was slower (Figure 5).

4. Discussion

Under the experimental conditions in this study, the fCDDP/LPD suspension showed anticancer effects against orthotopically transplanted AH109A hepatoma cells even at a dose of 0.1 mg of fCDDP, corresponding to the minimum fCDDP concentration administered in

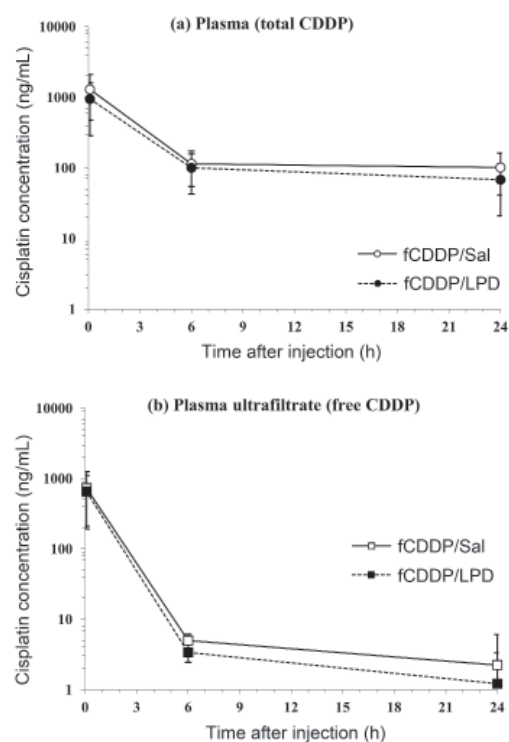
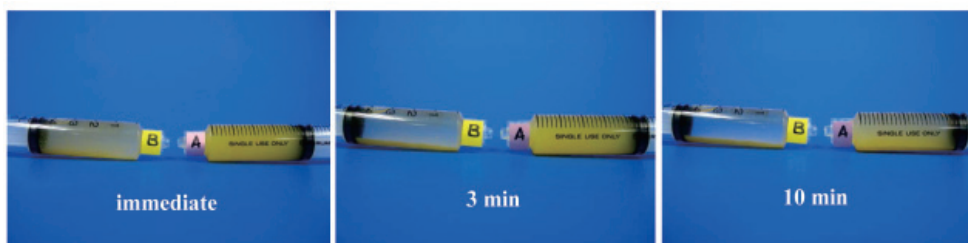


Figure 4. Plasma and ultrafiltered plasma concentration-time profiles of cisplatin in rats after a single intrahepatic artery injection of fCDDP/Sal or fCDDP/LPD (0.2 mg/rat).

clinical practice. The mean tumor weight in the LPD-alone group was almost the same as that in the Sal group. This means that the tumor growth-inhibitory effects of the fCDDP/LPD suspension were likely due to the activity of fCDDP. Because an fCDDP/Sal solution group was not used in this study, we could not compare the tumor growth inhibition between the fCDDP/LPD suspension and fCDDP/Sal solution. Sonoda et al., however, performed this comparison in VX2 tumor-bearing rabbits and found that the fCDDP/LPD suspension group showed greater tumor growth inhibition than the fCDDP/Sal solution group (7). In addition, Morimoto *et al.* (8) administered fCDDP/LPD

Table 3. Toxicokinetic parameters of CDDP (0.2 mg/rat)

Test sample	Toxicokinetic parameter	Plasma (total CDDP)	Ultrafiltered plasma (free CDDP)
fCDDP/Sal	C _{5min} (ng/mL)	1,290 ± 816	729 ± 520
	AUC _{0-24h} (ng•h/mL)	6,200	2,300
fCDDP/LPD	C _{5min} (ng/mL)	942 ± 659	649 ± 457
	AUC _{0-24h} (ng•h/mL)	4,670	2,030

**Figure 5. Comparison of time-courses of sedimentation of fCDDP and CDDP bulk substance following suspension in LPD. A: fCDDP/LPD suspension; B: CDDP bulk substance/LPD suspension.**

suspension *via* the intrahepatic artery to VX2 tumor-bearing rabbits and compared the Pt concentrations in the tumors and normal liver tissue after TACE with fCDDP/LPD suspension and TACE with fCDDP/Sal solution. They found that the Pt concentration in normal tissues did not differ between the two treatments, whereas its concentration in tumors was 10-fold higher when fCDDP/Sal solution was used in combination with LPD (8). Based on that report and the results of the present study, it appears that the combined use of LPD with fCDDP in TAI and TACE for the treatment of liver carcinoma may have greater efficacy than fCDDP/Sal solution monotherapy.

The toxicologic effects of fCDDP 0.2 mg were investigated, a dosage that had shown marked effects in the anticancer activity experiments. In nontumor-bearing rats, histopathologic changes in the liver and interlobular artery vacuolation in the 0.2-mg fCDDP/LPD suspension group were caused by LPD emboli, and degeneration and single-cell necrosis were seen in the periportal hepatocytes, around the interlobular artery, and in cholangiocytes. However, the same changes were also observed in the fCDDP/Sal solution and LPD-alone groups. The changes that appeared in the fCDDP/LPD suspension group appeared to be simply extra effects. Findings that were associated with the pathologic changes observed in the liver were concluded to be mild reactions because there were no changes in other liver function markers and the pathologic changes reversed after day 28. In addition, granulomas were observed from the gastroduodenal artery (the injection site) to the hepatic artery. However, they were observed in all experimental groups, were not especially more marked in the drug-treated groups, and were considered to be caused by the administration technique.

The results indicate that the administration of fCDDP suspended in LPD does not induce a strong

inflammatory reaction or other changes at the blood vessel injection site. In the combined administration of fCDDP with LPD in TAI and TACE, fCDDP is retained in the blood vessel for a long time because of the efficacy of LPD. Long-term exposure to fCDDP was expected to damage blood vessels. However, our histopathologic studies of blood vessel injection sites and the interlobular arteries of the liver did not reveal any evidence of such damage. Histopathologic examinations of the kidney showed that regeneration rates of the tubular epithelium were higher in the fCDDP/Sal, LPD-alone, and fCDDP/LPD groups than in the Sal group. However, those changes were mild in each drug-treatment group, and there were no abnormal changes in the levels of plasma urea nitrogen or creatinine. Therefore, we conclude that the administration of fCDDP suspended in LPD does not adversely affect kidney function.

When the CDDP concentrations in plasma and ultrafiltered plasma were compared, little difference was found between the fCDDP/Sal solution and fCDDP/LPD suspension groups in terms of the TK parameters. Therefore, we believe that the administration of fCDDP/Sal solution formulated as a suspension in LPD has almost no effect on the systemic exposure to CDDP. Morimoto *et al.* found that the Pt concentrations in both plasma and ultrafiltered plasma were lower in TACE performed using fCDDP combined with LPD than in TACE using an fCDDP aqueous solution without LPD (8). Compared with the results after the administration of fCDDP without LPD, the LPD suspension may alleviate the adverse reactions associated with CDDP, *i.e.*, kidney damage, nausea and vomiting, *etc.* Moriguchi *et al.* (9) also found that the total Pt concentration in plasma after intrahepatic artery administration of an LPD suspension of the clinically recommended dosage of fCDDP, 65 mg/m², to patients with unresectable hepatocellular carcinoma was lower

than when fCDDP was not suspended in LPD for 1 h following administration, and it increased thereafter. Therefore, the results from this study showing that the CDDP values in the fCDDP/LPD suspension group were lower than those in the fCDDP/Sal solution group at all measurement times is similar to the results from the previous two reports (8,9).

In summary, we found that a single intrahepatic artery administration of fCDDP/LPD suspension to rats with orthotopically transplanted hepatoma showed striking anticancer efficacy attributed to CDDP. In the toxicology study, the toxicity of the treatment with the suspension at a dosage that had shown anticancer efficacy was similar to that of fCDDP/Sal solution and LPD alone. The main toxicity was liver dysfunction and was reversible. The side effects caused by systemic exposure to CDDP were milder when it was combined in the LPD suspension.

Based on the present results, we conclude that the fCDDP/LPD suspension has sufficient anticancer efficacy and is well tolerated in the treatment of hepatocellular carcinoma. In addition, our results and those of previous studies (8,9) indicate that fCDDP has more potent efficacy in combination with LPD than when combined with Sal solution when treating hepatic cancer *via* TAI or TACE. Regarding the suspendability of fCDDP and CDDP bulk substance in LPD at a CDDP concentration of 20 mg/mL, the concentration used in clinical practice, the sedimentation of fCDDP was much slower than that of CDDP bulk substance. Future studies should be conducted to determine CDDP tumor concentrations in both fCDDP/LPD and fCDDP/Sal solution groups.

References

1. Nakakuma K, Tashiro S, Hiraoka T, Uemura K, Konno T, Miyauchi Y, Yokoyama I. Studies on anticancer treatment with an oily anticancer drug injected into the ligated feeding hepatic artery for liver cancer. *Cancer*. 1983; 52:2193-2200.
2. Shibata J, Fujiyama S, Sato T, Kishimoto S, Fukushima S, Nakano M. Hepatic arterial injection chemotherapy with cisplatin suspended in an oily lymphographic agent for hepatocellular carcinoma. *Cancer*. 1989; 64:1586-1594.
3. Maeda S, Shibata J, Fujiyama S, Tanaka M, Moumaru S, Sato K, Tomita K. Long-term follow-up of hepatic arterial chemoembolization with cisplatin suspended in iodized oil for hepatocellular carcinoma. *Hepato-Gastroenterology*. 2003; 50:809-813.
4. Yoshikawa M, Ono N, Yodono H, Ichida T, Nakamura H. Phase II study of hepatic arterial infusion of a fine-powder formulation of cisplatin for advanced hepatocellular carcinoma. *Hepatol Res*. 2008; 38:474-483.
5. Yodono H, Matsuo K, Shinohara A. A retrospective comparative study of epirubicin-lipiodol emulsion and cisplatin-lipiodol suspension for use with transcatheter arterial chemoembolization for treatment of hepatocellular carcinoma. *Anti-cancer Drugs*. 2011; 3:277-282.
6. Kasai K, Ushio A, Sawara K, Miyamoto Y, Kasai Y, Oikawa K, Kuroda H, Takikawa Y, Suzuki K. Transcatheter arterial chemoembolization with a fine-powder formulation of cisplatin for hepatocellular carcinoma. *World J Gastroenterol*. 2010; 27:3437-3444.
7. Sonoda A, Nitta N, Ohta S, Itoh R, Takahashi M, Murata K, Morikawa S, Inubushi T, Miyagawa Y, Takamori M, Oonaka Y. Plasma platinum concentration and anti-tumor effects after intra-arterial infusion of lipiodol-CDDP suspension evaluation with VX2 rabbit liver cancer model and 7.0 tesla MRI system. *Jpn J Cancer Chemother*. 2006; 33:951-957.
8. Morimoto K, Sakaguchi H, Tanaka T, Yamamoto K, Anai H, Hayashi T, Satake M, Kichikawa K. Transarterial chemoembolization using cisplatin powder in a rabbit model of liver cancer. *Cardiovasc Intervent Radiol*. 2008; 31:981-985.
9. Moriguchi M, Takayama T, Nakamura M, Aramaki O, Higaki T, Nakayama H, Ohkubo Y, Fujii M. Phase I/II study of a fine-powder formulation of cisplatin for transcatheter arterial chemoembolization in hepatocellular carcinoma. *Hepatol Res*. 2010; 40:369-375.

(Received September 9, 2013; Revised October 25, 2013; Accepted October 26, 2013)

Standardized clinical pathways may potentially help to reduce the opacity of medical treatment in China – Reflections on the murder of a doctor in Wenling, Zhejiang

Lin Mei, Lingzhong Xu*

Department of Health Care Management and Maternal and Child Health, Shandong University, Ji'nan, Shandong, China.

ABSTRACT: A doctor was murdered at Wenling First People's Hospital in Zhejiang, China on October 25, 2013. During the incident, a patient assaulted three doctors, resulting in the death of one of the doctors. This incident has led to a heated discussion about the unhealthy doctor-patient relationship in China. There are complex reasons for the strained doctor-patient relationship in China, but one aspect that helped lead to this situation is the opacity of medical treatment. Research has shown that implementation of clinical pathways reduces the variability of clinical practice and improves outcomes. Standardized clinical pathways can provide a standard for evaluation of the rationality of treatment and also suggest a recommended treatment, potentially reducing the opacity of medical treatment in China. However, the standardized clinical pathways that are currently in use in China still need to be improved. The implementation of clinical pathways needs to be increased, those pathways need to be formulated in detail, a supervisory body needs to be established, and the public needs to be better informed. These aspects should be studied further.

Keywords: Doctor-patient relationship, doctor-patient contradiction, standardized clinical pathway

1. Introduction

A doctor was murdered at Wenling First People's Hospital in Zhejiang, China on October 25, 2013. A male patient assaulted 3 doctors, resulting in the death of one of the doctors. According to reports, the murderer was a patient at the hospital who underwent minimally invasive surgery on his nose on March 20, 2012. After

the surgery, patient repeatedly indicated that his nose was blocked and that he had difficulty breathing. After the patient complained to the hospital, the hospital arranged several meetings in an attempt to identify the problem but concluded that the surgery was successful. The hospital tried to explain to the patient that the surgery was successful but the patient disagreed (1,2). After a prolonged period of filing complaints, the patient attacked hospital staff and ultimately caused the death of a doctor.

After this incident, the unhealthy doctor-patient relationship in China was reexamined again and a heated discussion ensued. In 1994, the Chinese Government began to reform the medical system. However, the doctor-patient relationship improved little, and this relationship is more strained now than it ever was in China's history. There are complex reasons for the strained doctor-patient relationship, but one aspect that helped lead to this situation is the opacity of medical treatment.

A standardized clinical pathway consists of "systematically developed statements to assist practitioner and patient decisions about appropriate health care for specific clinical circumstances" (3). Clinical pathways have been viewed as formal procedures for care and disease management (4) as well as a way to potentially reduce the opacity of medical treatment. After the first standardized clinical pathway was adopted by the New England Medical Center in Boston in 1985, the concept of clinical pathway has spread around the world.

2. The role of standardized clinical pathways in a medical dispute

A clinical pathway is expected to play 3 roles: *i*) assisting practitioners in appropriate clinical decision-making; *ii*) improving the quality of healthcare and outcomes for patients; and *iii*) supporting and influencing regional or national policies for efficient resource allocation and better delivery systems (5-7). In more specific terms, a clinical pathway can help to formalize the treatment process, help explain treatment and increase transparency, and help optimize health resources and

*Address correspondence to:

Dr. Lingzhong Xu, Department of Health Care Management and Maternal and Child Health, NO.110 mailbox, Shandong University, 44 Wenhua Road, 250012 Ji'nan, Shandong, China.
E-mail: lzxu@sdu.edu.cn

facilitate rational decisions such as revision of essential drug lists and improvement of health insurance.

Research has shown that the implementation of clinical pathways reduces the variability of clinical practice and improves outcomes (8-11). With a standardized clinical pathway, the patient can easily distinguish between treatment that is rational and treatment that is not, and the doctor is given better tools to explain the outcomes of that treatment. Thus, a standardized clinical pathway provides a standard for evaluation of the rationality of treatment. For example, a series of guidelines regarding the diagnosis and treatment of hepatocellular carcinoma (HCC) has been adopted in Japan with the support of Japanese Ministry of Health, Labor, and Welfare (5,12). These guidelines determine the appropriate treatment for each situation by recommending a preferred treatment and special treatment in specific circumstances, and these guidelines also indicate the possible outcomes of each treatment as a reference. Based on these guidelines, doctors and patients can easily identify which type of treatment is necessary or recommended and what type of results may occur, thus helping to reduce treatment disputes between the doctor and patient. In other words, these guidelines not only provide a way to reduce treatment disputes between patients and doctors but also offer a way to potentially reduce the opacity of medical treatment by providing a standardized treatment process.

3. Standardized clinical pathways in China

Standardized clinical pathways are a relatively new concept in China, but the Chinese Government has emphasized research on standardized clinical pathways. As an example, the Chinese Government implemented a series of standardized clinical pathways for diagnosis and treatment of liver cancer. The most recent pathways were determined in 2011 and include the detection and screening of high-risk groups, clinical manifestations, diagnostic criteria (clinical and pathological), staging, criteria for selection of different treatments, and follow-up visits (13). Similar standardized clinical pathways have also been adopted at different medical facilities (14-16).

The implementation of clinical pathways Few Chinese hospitals have currently implemented standardized clinical pathways. One study found that only 0.82% of hospitals nationwide had implemented such pathways and that those pathways had only been implemented for an average of 2.02 years. Of the hospitals that had implemented clinical pathways, 82.7% had pathways for fewer than 10 diseases while only 4.8% had pathways for more than 50 diseases (14). In relative terms, developed countries have more extensive implementation of clinical pathways (17). As an example, a Swedish study indicated that clinical pathways were in use at 20% of Swedish intensive care units (ICUs) and a total of 56 clinical pathways were reported within a range of

fields and areas (18). A study of clinical pathways in 17 member states of the European Union found that the United Kingdom had the highest estimated level of pathway use, with a level reaching almost 45% in 2004. Countries with lower levels of pathway use such as Slovenia, the Netherlands, Belgium, and Austria had a level reaching almost 10% (19). Given these findings, the clinical pathways currently in use in China are unlikely to provide a complete standard or a way to reduce the opacity of medical treatment. Therefore, further research into increasing the implementation of clinical pathways needs to be conducted.

Formulation of clinical pathways in detail The standardized clinical pathways currently in use in China tend to contain general information about disease but still lack information about standards for specific treatments. As an example, the standardized clinical pathway for diagnosis and treatment of liver cancer in China include information about when a hepatectomy is indicated but lack information about how that hepatectomy should be performed, such as preoperative preparations, preoperative fasting, and preoperative assessment (13). Thus, clinical pathways do not provide a reliable standard when there is a disagreement about a hepatectomy. Further study of clinical pathways in detail would be of use.

Establishment of a supervisory body China lacks an official supervisory body to oversee the implementation of standardized clinical pathways. The few local supervisory bodies that do exist have little authority to ensure pathways are followed. Doctors have little fear of repercussions should they fail to follow clinical pathways, making them more likely to ignore those pathways. The lack of a supervisory body also leads to distrust on the part of the patient. Thus, the lack of a supervisory body has possibly hampered the implementation and use of clinical pathways.

Better public education about standardized clinical pathways There is little recognition of the usefulness of clinical pathways in China, both among doctors and patients. Although a number of hospitals have adopted the concept of clinical pathways, the idea of using those pathways to explain treatment and to reduce treatment disputes is relatively new. No studies in China have examined patient education about clinical pathways. Better public education about standardized clinical pathways can help to increase both doctor and patient awareness of the usefulness of clinical pathways and help to potentially reduce the opacity of medical treatment.

4. Prospects for standardized clinical pathways to reduce the opacity of medical treatment in China

A strained doctor-patient relationship is particular to China. There are complex reasons for this situation, but the opacity of medical treatment is one contributing factor. A system of standardized clinical pathways including complete clinical pathways, a powerful

supervisory body, and better education of the public may provide a way to increase the level of standardized medical treatment and to reduce the opacity of that treatment. Therefore, further research into increasing the implementation of clinical pathways, formulation of clinical pathways in detail, establishment of a supervisory body, and better education of the public may offer better chances of increasing the level of standardized treatment, reducing the opacity of that treatment, and improving the doctor-patient relationship.

References

- Xinhuanet, Xinhua News Agency. How did a minimally invasive surgery lead to a murder? http://news.xinhuanet.com/legal/2013-10/27/c_117889203.htm (accessed October 27, 2013). (in Chinese).
- Beijing Youth Daily. Three questions about the murder of a doctor in Wenling. http://epaper.yynet.com/html/2013-10/27/content_19198.htm?div=-1 (accessed October 27, 2013). (in Chinese)
- Pavlidis N. Evidence-based medicine: Development and implementation of guidelines in oncology. *Eur J Cancer*. 2009; 45 (Suppl 1):468-470.
- Karen Z. Integrated care pathways: Eleven international trends. *J Integrated Care Pathways*. 2002; 6:101-107.
- Song P, Tobe RG, Inagaki Y, Kokudo N, Hasegawa K, Sugawara Y, Tang W. The management of hepatocellular carcinoma around the world: A comparison of guidelines from 2001 to 2011. *Liver Int*. 2012; 32:1053-1063.
- Wolf SH, Grol R, Hutchinson A, Eccles M, Grimshaw J. Clinical guidelines: Potential benefits, limitations, and harms of clinical guidelines. *BMJ*. 1999; 318:527-530.
- Eisenberg JM, Power EJ. Transforming insurance coverage into quality health care: Voltage drops from potential to delivered quality. *JAMA*. 2000; 284:2100-2107.
- Preston SR, Markar SR, Baker CR, Soon Y, Singh S, Low DE. Impact of a multidisciplinary standardized clinical pathway on perioperative outcomes in patients with oesophageal cancer. *Br J Surg*. 2013; 100:105-112.
- Seo HS, Song KY, Jeon HM, Park CH. The impact of an increased application of critical pathway for gastrectomy on the length of stay and cost. *J Gastric Cancer*. 2012; 12:126-131.
- Panella M, Marchisio S, Brambilla R, Vanhaecht K, Di Stanislao F. A cluster randomized trial to assess the effect of clinical pathways for patients with stroke: Results of the clinical pathways for effective and appropriate care study. *BMC Med*. 2012; 10:71.
- Song PP, Gao JJ, Kokudo N, Dong JH, Tang W. "Knowledge into action" Exploration of an appropriate approach for constructing evidence-based clinical practice guidelines for hepatocellular carcinoma. *Biosci Trends*. 2012; 6:147-152.
- Song P, Tang W, Tamura S, Hasegawa K, Sugawara Y, Dong J, Kokudo N. The management of hepatocellular carcinoma in Asia: A guideline combining quantitative and qualitative evaluation. *Biosci Trends*. 2010; 4:283-287.
- Guangxi Health Information Network. Guidelines on diagnosis and treatment of primary liver cancer (2011 edition) of the National Health and Family Planning Commission of the People's Republic of China. <http://www.gxws.gov.cn/uploads/soft/120229/8-120229154457.doc> (accessed October 28, 2013).
- Tao, H, Liu P, Liang, J, Ke X, Guo S, Qu H. Survey of hospitals implementing clinical pathways and analysis of relevant factors. *Chinese Hospital Management*. 2010; 2:28-31. (in Chinese)
- Huo T, Jin F, Han J, Jiang F, Li N, Guo S, Sun X, Yan Y. Analysis of the status of a pilot program to manage clinical pathways. *Chinese Hospitals*. 2011; 15:2-6. (in Chinese)
- Zhao X, Yu L. The effects of and issues with clinical pathways. *Chinese Hospital Management*. 2010; 2:31-33. (in Chinese)
- Kris V, Massimiliano P, Ruben Z, Walter S. An overview on the history and concept of care pathways as complex interventions. *Intl J Care Pathways*. 2011; 15:49-52.
- Bjurling-Sjöberg P, Jansson I, Wadensten B, Engström G, Pöder U. Prevalence and quality of clinical pathways in Swedish intensive care units: A national survey. *J Eval Clin Pract*. 2013.
- Don H, Anne-Marie Y. Clinical pathways in 17 European Union countries: A purposive survey. *Austral Health Rev*. 2005; 29:94-104.

(Received October 29, 2013; Accepted October 30, 2013)

Guide for Authors

1. Scope of Articles

Drug Discoveries & Therapeutics welcomes contributions in all fields of pharmaceutical and therapeutic research such as medicinal chemistry, pharmacology, pharmaceutical analysis, pharmaceuticals, pharmaceutical administration, and experimental and clinical studies of effects, mechanisms, or uses of various treatments. Studies in drug-related fields such as biology, biochemistry, physiology, microbiology, and immunology are also within the scope of this journal.

2. Submission Types

Original Articles should be well-documented, novel, and significant to the field as a whole. An Original Article should be arranged into the following sections: Title page, Abstract, Introduction, Materials and Methods, Results, Discussion, Acknowledgments, and References. Original articles should not exceed 5,000 words in length (excluding references) and should be limited to a maximum of 50 references. Articles may contain a maximum of 10 figures and/or tables.

Brief Reports definitively documenting either experimental results or informative clinical observations will be considered for publication in this category. Brief Reports are not intended for publication of incomplete or preliminary findings. Brief Reports should not exceed 3,000 words in length (excluding references) and should be limited to a maximum of 4 figures and/or tables and 30 references. A Brief Report contains the same sections as an Original Article, but the Results and Discussion sections should be combined.

Reviews should present a full and up-to-date account of recent developments within an area of research. Normally, reviews should not exceed 8,000 words in length (excluding references) and should be limited to a maximum of 100 references. Mini reviews are also accepted.

Policy Forum articles discuss research and policy issues in areas related to life science such as public health, the medical care system, and social science and may address governmental issues at district, national, and international levels of discourse. Policy Forum articles should not exceed 2,000 words in length (excluding references).

Case Reports should be detailed reports of the symptoms, signs, diagnosis, treatment, and follow-up of an individual patient. Case reports may contain a demographic profile of the patient but usually describe an unusual or novel occurrence. Unreported or unusual side effects or adverse interactions involving medications will also be considered. Case

Reports should not exceed 3,000 words in length (excluding references).

News articles should report the latest events in health sciences and medical research from around the world. News should not exceed 500 words in length.

Letters should present considered opinions in response to articles published in Drug Discoveries & Therapeutics in the last 6 months or issues of general interest. Letters should not exceed 800 words in length and may contain a maximum of 10 references.

3. Editorial Policies

Ethics: Drug Discoveries & Therapeutics requires that authors of reports of investigations in humans or animals indicate that those studies were formally approved by a relevant ethics committee or review board.

Conflict of Interest: All authors are required to disclose any actual or potential conflict of interest including financial interests or relationships with other people or organizations that might raise questions of bias in the work reported. If no conflict of interest exists for each author, please state "There is no conflict of interest to disclose".

Submission Declaration: When a manuscript is considered for submission to Drug Discoveries & Therapeutics, the authors should confirm that 1) no part of this manuscript is currently under consideration for publication elsewhere; 2) this manuscript does not contain the same information in whole or in part as manuscripts that have been published, accepted, or are under review elsewhere, except in the form of an abstract, a letter to the editor, or part of a published lecture or academic thesis; 3) authorization for publication has been obtained from the authors' employer or institution; and 4) all contributing authors have agreed to submit this manuscript.

Cover Letter: The manuscript must be accompanied by a cover letter signed by the corresponding author on behalf of all authors. The letter should indicate the basic findings of the work and their significance. The letter should also include a statement affirming that all authors concur with the submission and that the material submitted for publication has not been published previously or is not under consideration for publication elsewhere. The cover letter should be submitted in PDF format. For example of Cover Letter, please visit <http://www.ddtjournal.com/downloadcentre.php> (Download Centre).

Copyright: A signed JOURNAL PUBLISHING AGREEMENT (JPA) must be provided by post, fax, or as a scanned file before acceptance of the article. Only forms with a hand-written signature are accepted. This copyright will ensure the widest possible dissemination of information. A form facilitating transfer of copyright can be downloaded by clicking the appropriate link and can be returned to the e-mail address or fax number noted on the form (Please visit

Download Centre). Please note that your manuscript will not proceed to the next step in publication until the JPA form is received. In addition, if excerpts from other copyrighted works are included, the author(s) must obtain written permission from the copyright owners and credit the source(s) in the article.

Suggested Reviewers: A list of up to 3 reviewers who are qualified to assess the scientific merit of the study is welcomed. Reviewer information including names, affiliations, addresses, and e-mail should be provided at the same time the manuscript is submitted online. Please do not suggest reviewers with known conflicts of interest, including participants or anyone with a stake in the proposed research; anyone from the same institution; former students, advisors, or research collaborators (within the last three years); or close personal contacts. Please note that the Editor-in-Chief may accept one or more of the proposed reviewers or may request a review by other qualified persons.

Language Editing: Manuscripts prepared by authors whose native language is not English should have their work proofread by a native English speaker before submission. If not, this might delay the publication of your manuscript in Drug Discoveries & Therapeutics.

The Editing Support Organization can provide English proofreading, Japanese-English translation, and Chinese-English translation services to authors who want to publish in Drug Discoveries & Therapeutics and need assistance before submitting a manuscript. Authors can visit this organization directly at <http://www.iacmhr.com/iac-eso/support.php?lang=en>. IAC-ESO was established to facilitate manuscript preparation by researchers whose native language is not English and to help edit works intended for international academic journals.

4. Manuscript Preparation

Manuscripts should be written in clear, grammatically correct English and submitted as a Microsoft Word file in a single-column format. Manuscripts must be paginated and typed in 12-point Times New Roman font with 24-point line spacing. Please do not embed figures in the text. Abbreviations should be used as little as possible and should be explained at first mention unless the term is a well-known abbreviation (e.g. DNA). Single words should not be abbreviated.

Title page: The title page must include 1) the title of the paper (Please note the title should be short, informative, and contain the major key words); 2) full name(s) and affiliation(s) of the author(s), 3) abbreviated names of the author(s), 4) full name, mailing address, telephone/fax numbers, and e-mail address of the corresponding author; and 5) conflicts of interest (if you have an actual or potential conflict of interest to disclose, it must be included as a footnote on the title page of the manuscript; if no conflict of interest exists for each author, please state "There is no conflict of interest to disclose"). Please visit [Download Centre](#) and refer to the title page of the manuscript sample.

Abstract: The abstract should briefly state the purpose of the study, methods, main findings, and conclusions. For article types including Original Article, Brief Report, Review, Policy Forum, and Case Report, a one-paragraph abstract consisting of no more than 250 words must be included in the manuscript. For News and Letters, a brief summary of main content in 150 words or fewer should be included in the manuscript. Abbreviations must be kept to a minimum and non-standard abbreviations explained in brackets at first mention. References should be avoided in the abstract. Key words or phrases that do not occur in the title should be included in the Abstract page.

Introduction: The introduction should be a concise statement of the basis for the study and its scientific context.

Materials and Methods: The description should be brief but with sufficient detail to enable others to reproduce the experiments. Procedures that have been published previously should not be described in detail but appropriate references should simply be cited. Only new and significant modifications of previously published procedures require complete description. Names of products and manufacturers with their locations (city and state/country) should be given and sources of animals and cell lines should always be indicated. All clinical investigations must have been conducted in accordance with Declaration of Helsinki principles. All human and animal studies must have been approved by the appropriate institutional review board(s) and a specific declaration of approval must be made within this section.

Results: The description of the experimental results should be succinct but in sufficient detail to allow the experiments to be analyzed and interpreted by an independent reader. If necessary, subheadings may be used for an orderly presentation. All figures and tables must be referred to in the text.

Discussion: The data should be interpreted concisely without repeating material already presented in the Results section. Speculation is permissible, but it must be well-founded, and discussion of the wider implications of the findings is encouraged. Conclusions derived from the study should be included in this section.

Acknowledgments: All funding sources should be credited in the Acknowledgments section. In addition, people who contributed to the work but who do not meet the criteria for authors should be listed along with their contributions.

References: References should be numbered in the order in which they appear in the text. Citing of unpublished results, personal communications, conference abstracts, and theses in the reference list is not recommended but these sources may be mentioned in the text. In the reference list, cite the names of all authors when there are fifteen or fewer authors; if there are sixteen or more authors, list the first three followed by *et al.* Names of journals should

be abbreviated in the style used in PubMed. Authors are responsible for the accuracy of the references. Examples are given below:

Example 1 (Sample journal reference):
Nakata M, Tang W. Japan-China Joint Medical Workshop on Drug Discoveries and Therapeutics 2008: The need of Asian pharmaceutical researchers' cooperation. *Drug Discov Ther.* 2008; 2:262-263.

Example 2 (Sample journal reference with more than 15 authors):
Darby S, Hill D, Auvinen A, *et al.* Radon in homes and risk of lung cancer: Collaborative analysis of individual data from 13 European case-control studies. *BMJ.* 2005; 330:223.

Example 3 (Sample book reference):
Shalev AY. Post-traumatic stress disorder: Diagnosis, history and life course. In: *Post-traumatic Stress Disorder, Diagnosis, Management and Treatment* (Nutt DJ, Davidson JR, Zohar J, eds.). Martin Dunitz, London, UK, 2000; pp. 1-15.

Example 4 (Sample web page reference):
World Health Organization. The World Health Report 2008 – primary health care: Now more than ever. http://www.who.int/whr/2008/whr08_en.pdf (accessed September 23, 2010).

Tables: All tables should be prepared in Microsoft Word or Excel and should be arranged at the end of the manuscript after the References section. Please note that tables should not in image format. All tables should have a concise title and should be numbered consecutively with Arabic numerals. If necessary, additional information should be given below the table.

Figure Legend: The figure legend should be typed on a separate page of the main manuscript and should include a short title and explanation. The legend should be concise but comprehensive and should be understood without referring to the text. Symbols used in figures must be explained.

Figure Preparation: All figures should be clear and cited in numerical order in the text. Figures must fit a one- or two-column format on the journal page: 8.3 cm (3.3 in.) wide for a single column, 17.3 cm (6.8 in.) wide for a double column; maximum height: 24.0 cm (9.5 in.). Please make sure that artwork files are in an acceptable format (TIFF or JPEG) at minimum resolution (600 dpi for illustrations, graphs, and annotated artwork, and 300 dpi for micrographs and photographs). Please provide all figures as separate files. Please note that low-resolution images are one of the leading causes of article resubmission and schedule delays. All color figures will be reproduced in full color in the online edition of the journal at no cost to authors.

Units and Symbols: Units and symbols conforming to the International System of Units (SI) should be used for physicochemical quantities. Solidus notation (*e.g.* mg/kg, mg/mL, mol/mm²/min) should be used. Please refer to the SI Guide www.bipm.org/en/si/ for standard units.

Supplemental data: Supplemental data might be useful for supporting and enhancing your scientific research and Drug Discoveries & Therapeutics accepts the submission of these materials which will be only published online alongside the electronic version of your article. Supplemental files (figures, tables, and other text materials) should be prepared according to the above guidelines, numbered in Arabic numerals (*e.g.*, Figure S1, Figure S2, and Table S1, Table S2) and referred to in the text. All figures and tables should have titles and legends. All figure legends, tables and supplemental text materials should be placed at the end of the paper. Please note all of these supplemental data should be provided at the time of initial submission and note that the editors reserve the right to limit the size and length of Supplemental Data.

5. Submission Checklist

The Submission Checklist will be useful during the final checking of a manuscript prior to sending it to Drug Discoveries & Therapeutics for review. Please visit [Download Centre](#) and download the Submission Checklist file.

6. Online submission

Manuscripts should be submitted to Drug Discoveries & Therapeutics online at <http://www.ddtjournal.com>. The manuscript file should be smaller than 5 MB in size. If for any reason you are unable to submit a file online, please contact the Editorial Office by e-mail at office@ddtjournal.com

7. Accepted manuscripts

Proofs: Galley proofs in PDF format will be sent to the corresponding author *via* e-mail. Corrections must be returned to the editor (proof-editing@ddtjournal.com) within 3 working days.

Offprints: Authors will be provided with electronic offprints of their article. Paper offprints can be ordered at prices quoted on the order form that accompanies the proofs.

Page Charge: A page charge of \$140 will be assessed for each printed page of an accepted manuscript. The charge for printing color figures is \$340 for each page. Under exceptional circumstances, the author(s) may apply to the editorial office for a waiver of the publication charges at the time of submission.

(Revised February 2013)

Editorial and Head Office:

Pearl City Koishikawa 603
2-4-5 Kasuga, Bunkyo-ku
Tokyo 112-0003
Japan
Tel: +81-3-5840-9697
Fax: +81-3-5840-9698
E-mail: office@ddtjournal.com

JOURNAL PUBLISHING AGREEMENT (JPA)

Manuscript No.:

Title:

Corresponding author:

The International Advancement Center for Medicine & Health Research Co., Ltd. (IACMHR Co., Ltd.) is pleased to accept the above article for publication in Drug Discoveries & Therapeutics. The International Research and Cooperation Association for Bio & Socio-Sciences Advancement (IRCA-BSSA) reserves all rights to the published article. Your written acceptance of this JOURNAL PUBLISHING AGREEMENT is required before the article can be published. Please read this form carefully and sign it if you agree to its terms. The signed JOURNAL PUBLISHING AGREEMENT should be sent to the Drug Discoveries & Therapeutics office (Pearl City Koishikawa 603, 2-4-5 Kasuga, Bunkyo-ku, Tokyo 112-0003, Japan; E-mail: office@ddtjournal.com; Tel: +81-3-5840-9697; Fax: +81-3-5840-9698).

1. Authorship Criteria

As the corresponding author, I certify on behalf of all of the authors that:

- 1) The article is an original work and does not involve fraud, fabrication, or plagiarism.
- 2) The article has not been published previously and is not currently under consideration for publication elsewhere. If accepted by Drug Discoveries & Therapeutics, the article will not be submitted for publication to any other journal.
- 3) The article contains no libelous or other unlawful statements and does not contain any materials that infringes upon individual privacy or proprietary rights or any statutory copyright.
- 4) I have obtained written permission from copyright owners for any excerpts from copyrighted works that are included and have credited the sources in my article.
- 5) All authors have made significant contributions to the study including the conception and design of this work, the analysis of the data, and the writing of the manuscript.
- 6) All authors have reviewed this manuscript and take responsibility for its content and approve its publication.
- 7) I have informed all of the authors of the terms of this publishing agreement and I am signing on their behalf as their agent.

2. Copyright Transfer Agreement

I hereby assign and transfer to IACMHR Co., Ltd. all exclusive rights of copyright ownership to the above work in the journal Drug Discoveries & Therapeutics, including but not limited to the right 1) to publish, republish, derivate, distribute, transmit, sell, and otherwise use the work and other related material worldwide, in whole or in part, in all languages, in electronic, printed, or any other forms of media now known or hereafter developed and the right 2) to authorize or license third parties to do any of the above.

I understand that these exclusive rights will become the property of IACMHR Co., Ltd., from the date the article is accepted for publication in the journal Drug Discoveries & Therapeutics. I also understand that IACMHR Co., Ltd. as a copyright owner has sole authority to license and permit reproductions of the article.

I understand that except for copyright, other proprietary rights related to the Work (e.g. patent or other rights to any process or procedure) shall be retained by the authors. To reproduce any text, figures, tables, or illustrations from this Work in future works of their own, the authors must obtain written permission from IACMHR Co., Ltd.; such permission cannot be unreasonably withheld by IACMHR Co., Ltd.

3. Conflict of Interest Disclosure

I confirm that all funding sources supporting the work and all institutions or people who contributed to the work but who do not meet the criteria for authors are acknowledged. I also confirm that all commercial affiliations, stock ownership, equity interests, or patent-licensing arrangements that could be considered to pose a financial conflict of interest in connection with the article have been disclosed.

Corresponding Author's Name (Signature):

Date:

